

## Structural inheritance in the North Atlantic

Christian Schiffer<sup>1,2</sup>, Anthony G. Doré<sup>3</sup>, Gillian R. Foulger<sup>2</sup>, Dieter Franke<sup>4</sup>, Laurent Geoffroy<sup>5</sup>, Laurent Gernigon<sup>6</sup>, Bob Holdsworth<sup>2</sup>, Nick Kuszniir<sup>7</sup>, Erik Lundin<sup>8</sup>, Ken McCaffrey<sup>2</sup>, Alex Peace<sup>9,10</sup>, Kenni D. Petersen<sup>11</sup>, Thomas Phillips<sup>2</sup>, Randell Stephenson<sup>12</sup>, Martyn S. Stoker<sup>13</sup>, Kim Welford<sup>9</sup>

<sup>1</sup> *Department of Earth Sciences, Uppsala University, Villavägen 16, 75236 Uppsala, Sweden*

<sup>2</sup> *Department of Earth Sciences, Durham University, Science Laboratories, South Rd. DH1 3LE, UK*

<sup>3</sup> *Energy & Geoscience Institute (EGI, University of Utah), London W5 2SE.*

<sup>4</sup> *Bundesanstalt für Geowissenschaften und Rohstoffe (Federal Institute for Geosciences and Natural Resources), Germany*

<sup>5</sup> *Université de Bretagne Occidentale, Brest, 29238 Brest, CNRS, UMR 6538, Laboratoire Domaines Océaniques, 29280 Plouzané, France*

<sup>6</sup> *Norges Geologiske Undersøkelse (NGU), Geological Survey of Norway, Leiv Erikssons vei 39, N-7491 Trondheim, Norway*

<sup>7</sup> *University of Liverpool, School of Environmental Sciences, Liverpool L69 3GP, United Kingdom;*

<sup>8</sup> *Equinor, Research Centre, Arkitekt Ebbels vei 10, 7053 Trondheim, Norway*

<sup>9</sup> *Department of Earth Sciences, Memorial University of Newfoundland, St. Johns, Newfoundland, Canada, A1B 3X5*

<sup>10</sup> *now at: School of Geography and Earth Sciences, McMaster University, Hamilton, Ontario, Canada, L8S 4L8*

<sup>11</sup> *Department of Geoscience, Aarhus University, Høegh-Guldbergs Gade 2, DK-8000 Aarhus C., Denmark*

<sup>12</sup> *School of Geosciences, University of Aberdeen, King's College, Aberdeen AB24 3UE, UK*

<sup>13</sup> *Australian School of Petroleum, University of Adelaide, Adelaide, SA 5005, Australia*

38 **Abstract**

39 The North Atlantic, extending from the Charlie Gibbs Fracture Zone to the north Norway-  
40 Greenland-Svalbard margins, is regarded as both a classic case of structural inheritance and an  
41 exemplar for the Wilson-cycle concept. This paper examines different aspects of structural  
42 inheritance in the Circum-North Atlantic region: 1) as a function of rejuvenation from  
43 lithospheric to crustal scales, and 2) in terms of sequential rifting and opening of the ocean and  
44 its margins, including a series of failed rift systems. We summarise and evaluate the role of  
45 fundamental lithospheric structures such as mantle fabric and composition, lower crustal  
46 inhomogeneities, orogenic belts, and major strike-slip faults during breakup. We relate these  
47 to the development and shaping of the NE Atlantic rifted margins, localisation of magmatism,  
48 and microcontinent release. We show that, although inheritance is common on multiple scales,  
49 the Wilson Cycle is at best an imperfect model for the Circum-North Atlantic region.  
50 Observations from the NE Atlantic suggest depth dependency in inheritance (surface, crust,  
51 mantle) with selective rejuvenation depending on time-scales, stress field orientations and  
52 thermal regime. Specifically, post-Caledonian reactivation to form the North Atlantic rift  
53 systems essentially followed pre-existing orogenic crustal structures, while eventual breakup  
54 reflected a change in stress field and exploitation of a deeper-seated, lithospheric-scale shear  
55 fabrics. We infer that, although collapse of an orogenic belt and eventual transition to a new  
56 ocean does occur, it is by no means inevitable.

57

58 **Keywords:** North Atlantic; Wilson Cycle; plate tectonics; structural inheritance; reactivation;  
59 rifting; continental breakup; magmatism; lithosphere;

60

61

62

63

64

65

66

67

68

69

70

71

72

73

74

75

76

77

78	<b>Contents</b>	
79	<b>1</b>	Introduction ..... 5
80	<b>2</b>	The Wilson Cycle and the North Atlantic ..... 6
81	<b>3</b>	What is structural inheritance? ..... 7
82	<b>4</b>	Structural inheritance and rejuvenation at different scales ..... 8
83	4.1	Bulk lithosphere structure, composition and thermal history..... 8
84	4.2	Discrete lithospheric structures ..... 9
85	4.3	Pervasive lithospheric fabric ..... 10
86	4.4	Crustal-basin scale concepts ..... 11
87	<b>5</b>	Pre-rift structural framework of the Circum-North Atlantic region ..... 12
88	5.1	Archaean-Proterozoic cratons ..... 12
89	5.2	The Grenville-Sveconorwegian Orogeny ..... 13
90	5.3	The Timanian Orogeny..... 13
91	5.4	The Caledonian Orogeny..... 13
92	5.5	The Variscan Orogeny ..... 14
93	<b>6</b>	Structural segmentation and inheritance in the CNAR..... 15
94		<i>Segment 1 – Norway-Greenland margins</i> ..... 16
95		<i>Segment 2 – SE Greenland-Rockall-Hatton margins</i> ..... 17
96		<i>Segment 3 – The Greenland-Iceland-Faroe Ridge and adjacent margins</i> ..... 18
97		<i>Segment 4 – North Sea &amp; Tornquist Zone</i> ..... 19
98		<b>Segment 5 – Labrador Sea, Baffin Bay &amp; Davis Strait</b> ..... 20
99	<b>7</b>	Discussion..... 22
100	7.1	Rifting, segmentation and breakup in the CNAR ..... 22
101	7.2	Magmatism, rifting and breakup ..... 24
102	7.3	Role of strike-slip faults..... 25
103	7.4	Microcontinent formation ..... 27
104	7.5	The Wilson Cycle revisited ..... 28
105	<b>8</b>	<b>Conclusions</b> ..... 29
106	<b>9</b>	<b>Figures</b> ..... 31
107	<b>10</b>	<b>References</b> ..... 45
108		
109		
110		
111		
112		
113		

- 114 List of abbreviations
- 115 CNAR – Circum-North Atlantic Region
- 116 COB – Continent Ocean Boundary
- 117 COT – Continent Ocean Transition
- 118 GGF – Great Glen Fault
- 119 GIFR – Greenland-Iceland-Faroe Ridge
- 120 GIR – Greenland-Iceland Ridge
- 121 HBF – Highland Boundary Fault
- 122 HFZ – Hardangerfjord Fault Zone
- 123 HVLC/HVLCB – High velocity lower crust/ High velocity lower crustal body
- 124 IFR – Iceland-Faroe Ridge
- 125 JMMC – Jan Mayen Microplate Complex
- 126 Moho – Mohorovičić Discontinuity/Crust-Mantle boundary
- 127 MTTC – Møre-Trøndelag Fault Complex
- 128 NAIP – North Atlantic Igneous Province
- 129 SDR – Seaward Dipping Reflector
- 130 TZ – Tornquist Zone
- 131 TIB – Trans-Scandinavian Igneous Belt
- 132 WBF – Walls Boundary Fault

133

134

135

136

137

138

139

140

141

142

143

144

145

146

147

148

149 **1 Introduction**

150 Structural inheritance has been invoked as an important influence on plate-tectonic processes  
151 including rifting, and rifted-margin end-member style (i.e., magma-rich or magma-poor) (e.g.  
152 Vauchez et al. 1997; Bowling and Harry 2001; Manatschal et al. 2015; Chenin et al. 2015;  
153 Schiffer et al. 2015b; Svartman Dias et al. 2015; Petersen and Schiffer 2016; Duretz et al.  
154 2016), the formation of oceanic fracture zones, transform faults, and transform margins  
155 (Bellahsen et al. 2006; Gerya 2012; Doré et al. 2015; Peace et al. 2018b), magmatism (Hansen  
156 et al. 2009; Whalen et al. 2015), and intraplate deformation (Stephenson et al. this volume;  
157 Sutherland et al. 2000; Gorczyk and Vogt 2015; Audet et al. 2016; Heron et al. 2016; Tarayoun  
158 et al. 2018; Heron 2018).

159 The inspiration for major concepts of large-scale structural inheritance, such as the “Wilson  
160 Cycle” lies in the Circum-North Atlantic region (CNAR) (Wilson 1966; see review by Wilson  
161 et al. 2019), where at least two oceans have opened and closed along broadly similar trends  
162 (Cawood et al. 2007; Bingen et al. 2008a; Li et al. 2008; Lorenz et al. 2012; Thomas 2018).

163 The CNAR comprises the North Atlantic Ocean, Labrador Sea-Baffin Bay, Iceland and the  
164 surrounding continental landmasses, including Greenland, Scandinavia, the British Isles and  
165 northeastern Canada. The lithosphere comprises stable Precambrian continental cores in the  
166 interior of Greenland, North America and Scandinavia, while the geology along the continental  
167 margins and northern Europe was mainly reshaped in the Phanerozoic (e.g. Peace et al. this  
168 volume; Cocks and Torsvik 2006, 2011; St-Onge et al. 2009). The continental margins host a  
169 number of failed rift systems, such as the North Sea, the Rockall-Hatton Basins and the Møre-  
170 Vøring Basins (Figure 1) (Péron-Pinvidic and Manatschal 2010; Peace et al. 2019). In detail,  
171 continental breakup did not always follow earlier rift systems or known orogenic structures and  
172 has in some cases broken through seemingly undisturbed cratonic lithosphere. Several aspects  
173 of North Atlantic geology remain enigmatic, such as the nature and significance of the North  
174 Atlantic Igneous Province (NAIP) and the Greenland-Iceland-Faroes Ridge (GIFR) (Vink  
175 1984; White and McKenzie 1989; Foulger and Anderson 2005; Meyer et al. 2007; Foulger et  
176 al. 2019), the development of a spectrum of rifted continental margins (Geoffroy 2005; Franke  
177 2013; Clerc et al. 2018), and the development of the Jan Mayen Microplate Complex (JMMC)  
178 (Foulger et al. 2003; Gaina et al. 2009; Gernigon et al. 2015; Blischke et al. 2017, 2019;  
179 Schiffer et al. 2018).

180 Whether rifting, continental breakup and associated magmatism were related to deep, active  
181 mantle upwelling (White and McKenzie 1989; Hill 1991) or plate tectonic processes (Nielsen  
182 et al. 2007; Ellis and Stoker 2014; Foulger et al. 2019) (the bottom-up and top-down views) is  
183 still under debate (Peace et al. this volume; van Wijk et al. 2001; Foulger et al. 2005, 2019;  
184 Lundin and Doré 2005). Despite the often-proposed deep, active, buoyant upwellings beneath  
185 the CNAR, factors like the thermal state and composition of the crust and mantle, small-scale  
186 convection, upwelling, volatile content, and general, pre-existing (inherited) lithospheric and  
187 crustal structure may play major roles in the magmatic and tectonic evolution (e.g. King and  
188 Anderson 1998; Asimow and Langmuir 2003; Korenaga 2004; Foulger et al. 2005, 2019;  
189 Meyer et al. 2007; Simon et al. 2009; Hole and Millett 2016; Petersen et al. 2018; Hole and  
190 Natland 2019).

191 In this contribution, we aim at defining the most important concepts of structural inheritance  
192 and review how they may have influenced the structural evolution of the CNAR as a whole.  
193 We then take five segments of the CNAR that differ markedly in structural style as examples  
194 (Fig. 1) and describe and discuss these further: namely, the Norwegian-Greenland Sea (*segment*  
195 *1*), where early rifting followed Caledonian crustal trends, but breakup occurred obliquely, is  
196 in contrast to the SE Greenland-Rockall-Hatton margins (*segment 2*), where rifting and breakup

197 occurred through seemingly undisturbed cratonic lithosphere, but parallel to the Caledonian  
198 trends in the British and Irish Isles, some 500 km to the east. The enigmatic GIFR, a large  
199 physiographic high crossing the North Atlantic (*segment 3*) forms a buffer between *segments*  
200 *1* and *2*. The North Sea (*segment 4*) forms a major failed intracontinental rift system influenced  
201 by Variscan, Caledonian and Precambrian inheritance, but never developed into a new ocean.  
202 Lastly, in the Labrador Sea and Baffin Bay rifting broke through cratonic lithosphere but  
203 seafloor-spreading was abandoned after ~30 Ma (*segment 5*).

204

## 205 **2 The Wilson Cycle and the North Atlantic**

206 Tuzo Wilson's famous question of 1966, "Did the Atlantic close and then re-open?" gave rise  
207 to the "Wilson Cycle" concept (Wilson 1966; Dewey and Spall 1975; see review by Wilson et  
208 al. 2019). In its simplest form, this hypothesis envisages closure and reopening of oceans along  
209 former orogens that represent the weakest zones in a disintegrating continent. Applied stresses  
210 exploit inherited weaknesses during later rifting events, rather than breaking up continents  
211 through their stronger, stable interiors.

212 This paradigm works well in the Central Atlantic, where the new ocean closely tracks the  
213 parallel Appalachians (Thomas 2018). Similarly, breakup between Scandinavia and Greenland  
214 generally follows the Caledonian Orogen, but farther south the Iapetus suture is preserved and  
215 runs through northern England and central Ireland (McKerrow and Soper 1989; Soper et al.  
216 1992). The rifting thus left significant pieces of Laurentian cratonic crust on Europe's  
217 northwestern seaboard including the Rockall-Hatton margin. The Labrador Sea and Baffin Bay  
218 cut through pre-existing cratons (the Archaean North Atlantic and Rae cratons) and almost  
219 orthogonally across Precambrian orogenic belts (Buchan et al. 2000; Bowling and Harry 2001;  
220 St-Onge et al. 2009; Peace et al. 2018b).

221 It is becoming increasingly clear that the age of inherited structures prone to rejuvenation  
222 extends much further back in time than simply the most recent Wilson Cycle. Accordingly,  
223 Archaean-to-Palaeoproterozoic structures also guided fragmentation and segmentation of  
224 onshore and offshore areas during rifting and continental breakup in the NE Atlantic  
225 (Gabrielsen et al. 2018; Rotevatn et al. 2018; Schiffer et al. 2018) and Labrador Sea-Baffin  
226 Bay (Peace et al. 2018a; Heron et al. 2019). Recent attempts to formally extend the Wilson  
227 Cycle concept have been made, for example by including reactivation of long-lived intraplate  
228 inheritance (Heron et al. 2016), by systemising the role of mantle plumes in the Wilson Cycle  
229 (Heron, 2018), or by adding systematic "short-cuts" through the Wilson Cycles, such as the  
230 closure of failed rift basins (Chenin et al. 2018).

231 Current understanding of the precise mechanisms that govern rifting and breakup is hindered  
232 by ambiguous observations, interpretations, concepts and definitions. The exact location and  
233 definition of the continent-ocean "boundary" is often not known due to the presence of  
234 magmatic or sedimentary cover and, in many cases, continental margins have wide transition  
235 zones (Eagles et al. 2015). High velocity lower crust (HVLC, see Foulger et al., this volume,  
236 and Gernigon et al., this volume for discussion) underlying continental margins can have  
237 different pre-, syn-, and post-rift/breakup origins, knowledge of which is crucial to  
238 understanding thinning, magmatism and the role of structural inheritance during rifting. Local  
239 mantle upwellings associated with small-scale convection or diapirism and magmatic  
240 intrusions prior and during continental extension and breakup may have a crucial role in  
241 changing the lithospheric rheology and localising strain (e.g. Gernigon et al. this volume;  
242 Geoffroy 1998; Geoffroy et al. 2007; Gac and Geoffroy 2009; Ebinger et al. 2013). The nature  
243 of the crust can be ambiguous in highly thinned areas of "transitional" crust that appears to

244 show neither classic oceanic or continental crustal properties. Finally, terms such as  
245 ‘continental suture’ are difficult to define and can have complex, three-dimensional geometries  
246 and do not represent a simple lineament. Such a suture zone could reactivate, not where it  
247 appears at the surface, but where it is weakest at depth.  
248 The imperfect fit of the Wilson Cycle concept to observations (e.g. Krabbendam 2001; Buitter  
249 and Torsvik 2014; Dalziel and Dewey 2018) shows that the process of opening an ocean is  
250 more complex than a simple 2D-unzipping of continental sutures.

### 251 3 What is structural inheritance?

252 Continents contain broad zones of active deformation that extend deep into their interiors  
253 (Gordon 1998; Nielsen et al. 2007, 2014; Şengör et al. 2018). Such non-rigid behaviour departs  
254 significantly from the original paradigm of rigid plate tectonics. It results from the presence,  
255 preservation and repeated deformation of crustal and mantle-lithospheric mechanical  
256 weaknesses (Thatcher 1995; Holdsworth et al. 2001). The buoyancy of continental crust means  
257 that it, and its underlying lithospheric mantle, are not subducted in the same way as oceanic  
258 crust. As a result, zones of pre-existing weakness are preserved in the continental lithosphere  
259 and can be rejuvenated many times during successive phases of deformation over geologic time  
260 (Sutton and Watson 1986). *Structural inheritance* is a property of the continental lithosphere  
261 that guides deformation along pre-existing rheological heterogeneities at all scales. When this  
262 occurs under a given stress regime, the resulting process is known as (structural) *rejuvenation*.

263 Rejuvenation (Figure 5a) includes (i) *reactivation*, the repeated focussing of deformation along  
264 discrete pre-existing structures, e.g., faults, shear zones or lithological contacts and (ii)  
265 *reworking*, the repeated focussing of metamorphism, ductile deformation, recrystallisation,  
266 metasomatism and magmatism into the same lithospheric volume. Reactivation is primarily  
267 controlled by the compositional and mechanical properties of pre-existing structures, whilst  
268 reworking is primarily influenced by the thermal history of the lithosphere (Holdsworth et al.  
269 2001).

270 At shallow depths, brittle fracturing or frictional sliding occurs, with slip facilitated by low-  
271 friction minerals such as talc, serpentinite and smectite (e.g., Escartín et al. 2003; Moore et al.  
272 2004; Schroeder and John 2004). The transition between brittle and ductile deformation in  
273 crystalline rocks is dependent on temperature, composition and strain-rate and typically occurs  
274 at crustal depths of 10-15 km (Figure 5b; Sibson 1977; Gueydan et al. 2014). Movement along  
275 deformation zones is characterised by diffusion-accommodated viscous creep in phyllosilicate-  
276 rich rocks in this depth range. In the viscous regime, deformation is typically plastic and  
277 distributed over broader, more diffuse zones (Holdsworth 2004; Jefferies et al. 2006; Imber et  
278 al. 2008) (Figure 5b), but strain localisation here is still widespread at different scales (Braun  
279 et al. 1999; Precigout et al. 2007).

280 It is important to emphasise that, although reactivation controlled by structural inheritance is  
281 widely recognised along the NE Atlantic margin, this process should not always be assumed to  
282 be the primary control on lithosphere-scale rifting. A coincidence in rift-related structural  
283 trends with those of older basement structures may be a good indicator for reactivation, but is  
284 not in itself actual proof (see discussions in Holdsworth et al. 1997; Roberts and Holdsworth  
285 1999), especially when structures are mapped at depth in the offshore. The most conclusive  
286 test for inheritance in offshore rift systems is the recognition of reactivation in correlative  
287 onshore regions (e.g. Wilson et al. 2006; Peace et al. 2018b).

288

291 The lithospheric and basin evolution of the CNAR was likely governed by a complex  
292 combination of rejuvenation of different inherited structures and fabrics with different scales  
293 and orientations, alongside other processes such as magmatism. Lithosphere-scale rejuvenation  
294 includes almost every conceivable process that affects lithospheric rheology, locally or as a  
295 whole. These include changes in crustal and lithospheric thickness, thermal state and  
296 composition, sedimentary basin processes (faulting, sedimentation) and the mechanical  
297 heterogeneities of metamorphic and intrusive fabrics (Dunbar and Sawyer 1989a; Krabbendam  
298 and Barr 2000; Nagel and Buck 2004; Yamasaki and Gernigon 2009; Tommasi et al. 2009;  
299 Huismans and Beaumont 2011; Brune et al. 2014; Manatschal et al. 2015; Tommasi and  
300 Vauchez 2015; Petersen and Schiffer 2016; Duretz et al. 2016).

#### 301 4.1 Bulk lithosphere structure, composition and thermal history

302 Post-Archaean orogenic processes generally led to lithospheric volumes that are weaker and  
303 warmer compared to stable cratonic lithosphere (Cloetingh et al. 1995; Krabbendam and Barr  
304 2000; Rey et al. 2001; Corti et al. 2007). This may not always be the case, as, Krabbendam  
305 (2001) hypothesise that orogens with low heat flow (and “cold” crustal geotherms) have strong  
306 lithosphere, impeding reactivation. Nevertheless, the alignment of new structures with old  
307 weaknesses is persuasive, and has historically led many authors to postulate that reactivation  
308 is a major factor in breakup (e.g. Dunbar and Sawyer 1989a).

309 Numerical modelling suggests that discrete pre-existing lithospheric heterogeneities localise  
310 strain and control rift distribution (Dunbar and Sawyer 1989b) and asymmetric conjugate  
311 margin geometries (Yamasaki and Gernigon 2009; Petersen and Schiffer 2016; Beniest et al.  
312 2018). Therefore, rifts generally localise at the boundaries of lithospheric blocks of varying  
313 rheology (Pascal and Cloetingh 2002; Beniest et al. 2018). The relative strength between crust  
314 and mantle lithosphere is strongly influenced by crustal thickness and this also governs depth-  
315 dependent extension and thinning (Huismans and Beaumont 2011; Petersen and Schiffer 2016)  
316 (Figure 6). Thickened, warm and weak crust can undergo delocalised thinning, whilst the  
317 mantle lithosphere is more abruptly thinned (Buck 1991; Huismans and Beaumont 2011).  
318 Preferential thinning of mantle lithosphere leads to decompression melting of the  
319 asthenosphere which can occur while the crust remains intact (Petersen and Schiffer 2016)  
320 (Figure 6). Increasing obliquity to the extension direction and curvature of the zone of  
321 thickened crust produce more asymmetric and segmented rift zones (Van Wijk 2005; Corti et  
322 al. 2007). In contrast, a thinned crust with a shallow Moho prior to extension and/or longer  
323 periods of thermal relaxation (>30-50 Ma) can produce a cold and strong lithosphere, impeding  
324 rift localisation (Harry and Bowling 1999; van Wijk and Cloetingh 2002; Guan et al., 2019). If  
325 the mantle is weaker than the crust, it flows laterally whilst the crust is locally thinned, forming  
326 narrow necking zones and impeding pre-breakup melt generation (Petersen and Schiffer 2016)  
327 (Figure 6).

328 The lithosphere beneath stagnated rifts may cool and harden, leading to rift jumps away from  
329 the stronger lithosphere of the old rift, producing asymmetric continental margins (van Wijk  
330 and Cloetingh 2002; Naliboff and Buitter 2015). Such a process has been proposed to explain  
331 the formation of the volcanic margins in the NE Atlantic off-axis from previously thinned crust  
332 and failed rifts hosting Palaeozoic and Jurassic sedimentary basins (Gernigon et al. this volume;  
333 Guan et al. 2019). The zone of rheological contrast of such cooled/re-equilibrated rift zones  
334 and associated sedimentary infill may be reactivated during later episodes of extension, or may  
335 partition deformation (Odinsen et al. 2000; Frederiksen et al. 2001; Brune et al. 2017).

336 Armitage et al. (2010) demonstrated that thinned lithosphere from prior rift phases can enhance  
337 melt productivity in a subsequent rift phase.

338 Lithospheric delamination has been suggested to have a major impact on rift evolution and  
339 magmatism (Bird 1979; Kay and Kay 1993; Meissner and Mooney 1998; Elkins-Tanton 2005;  
340 Meier et al. 2016; Petersen et al. 2018). Şengör et al. (2018) suggested that rejuvenation of pre-  
341 existing structures may be linked to removal of the lithospheric mantle, which would weaken  
342 the entire remaining lithospheric column. Subsequently, extensive magmatism would inhibit  
343 thermal re-equilibration of the lithosphere and allow rejuvenation to continue for a long time.  
344 Liu et al. (2018) and Wang et al. (2018) propose models where a “Mid-Lithospheric  
345 Discontinuity” or the lower crust can act as a sub-horizontal weakness zone along which the  
346 lithosphere may delaminate.

347

#### 348 **4.2 Discrete lithospheric structures**

349 Discrete structures include regional-scale features such as sutures, shear zones, igneous bodies  
350 and other large features found at depth within the lithosphere.

351 Pre-existing rheological heterogeneities such as suture, fault and shear zones, possibly  
352 incorporating preserved eclogite and hydrated peridotite within the continental lithosphere may  
353 influence rifting, location of breakup and margin architecture (e.g. Petersen and Schiffer 2016).

354 Pre-existing mafic or ultramafic magmatic rocks are known to increase crustal strength and  
355 viscosity (Burov 2011). For example, the development of continent-dipping bounding faults of  
356 SDRs at magma-rich passive margins requires increased lower crustal viscosities (Geoffroy et  
357 al. 2015). Syn-rift magmatic systems such as crustal intrusions (Ebinger and Casey 2001; Keir  
358 et al. 2006), crustal magma chambers (Geoffroy 1998; Doubre and Geoffroy 2003) or  
359 instabilities at the lithospheric thermal boundary layer (Geoffroy et al., 2007; Gac and  
360 Geoffroy, 2009) weaken the lithosphere and can accommodate and localise deformation (Buck  
361 and Karner 2004) at different lithospheric levels during the rifting process.

362 In the North Atlantic rifting and breakup-related magmatism was typically focussed in igneous  
363 centres. Some of those igneous centres are located along pre-existing inherited fault and shear  
364 zones (e.g., the Great Glen Fault) (Bott and Tuson 1973; Geoffroy et al. 2007; Gueydan et al.  
365 2014). The spacing, location, size and magmatic budget of these igneous centres are governed  
366 by complex interactions between pre-existing discrete structures, pre-existing lithospheric  
367 thickness variations and mantle composition, as well as the timing and degree of melting  
368 (Gernigon et al. this volume; Gouiza and Paton 2019).

369 High-velocity lower crustal bodies (HVLCBs) are observed along most continental margins of  
370 the CNAR (Mjelde et al. 2008; Lundin and Doré 2011; Funck et al. 2016a) (Figure 7).  
371 Identifying the origin of HVLCBs is essential to understand extension and magmatism in rifts  
372 and passive margins. Many are associated with magmatic underplating or intrusions added to  
373 the lower continental crust during extension (Olafsson et al. 1992; Eldholm and Grue 1994;  
374 Ren et al. 1998; Mjelde et al. 2007b; White et al. 2008; Thybo and Artemieva 2013; Wrona et  
375 al. 2019). However, it is unclear to what extent such features are emplaced during rifting related  
376 to breakup. Some HVLCBs in the CNAR have been interpreted as metasomatised,  
377 metamorphosed or intruded mafic rocks in the uppermost mantle originating from Caledonian  
378 or older subduction and collision zones (Abramovitz and Thybo 2000; Christiansson et al.  
379 2000; Gernigon et al. 2004, 2006; Ebbing et al. 2006; Wangen et al. 2011; Fichler et al. 2011;  
380 Mjelde et al. 2013; Nirrengarten et al. 2014; Schiffer et al. 2015a, 2016; Abdelmalak et al.  
381 2017; Slagstad et al. 2018) (Figure 7). If the HVLCBs are deformed, pre-existing structures,

382 they will likely have influenced and localised the rifting before breakup-related magmatism  
383 (Gernigon et al. 2004; Petersen and Schiffer 2016).

384 Salazar-Mora et al. (2018) showed that during rifting of an orogenic belt, initial reactivation  
385 usually occurs along pre-existing lithospheric-scale suture zones, whilst the amount of previous  
386 contraction governs the width of the reactivated crustal segment and its offset from the suture.  
387 Thus, pre-existing contractional shear zones are reactivated first and new shear zones form  
388 later. Intrusions in the upper crust may weaken the surrounding rock and control breakup  
389 localisation (Geoffroy et al. 1998). Increasing obliquity of crustal weak zones encourages  
390 increasingly diffuse rift zones, delaying lithospheric breakup (Brune et al. 2014). Heron et al.  
391 (2016; 2018) showed that reactivation of long-lasting intraplate “mantle scars” may lead to  
392 substantial intraplate deformation. Like many of the above studies, they also emphasised that  
393 mantle heterogeneities are usually favourably reactivated in comparison to crustal structures.  
394 This is because these are the load-bearing layers of the lithosphere (e.g. Holdsworth et al.,  
395 2001).

396

### 397 **4.3 Pervasive lithospheric fabric**

398 Small-scale compositional and rheological variations form fabrics in the crust and mantle and  
399 localise strain, forming complex patterns of crustal-scale, anastomosing shear bands,  
400 lithospheric boudinage structures, crustal rafts or continental ribbons in continental margins  
401 (Lister et al. 1986; Clerc et al. 2015; Jammes and Lavier 2016). Similarly, extension of a  
402 chemically heterogeneous, finely layered lithosphere leads to boudinage/necking of relatively  
403 strong layers causing intense structural softening as weaker layers become mechanically  
404 interconnected (Duretz et al. 2016).

405 Rifting and continental breakup may exploit anisotropies formed during previous phases of  
406 deformation in the lithospheric mantle (Vauchez and Nicolas 1991; Tommasi and Vauchez  
407 2001; Misra 2016). Seismic anisotropy of the lithosphere may reflect mechanical anisotropy  
408 and is often, but not always, parallel to mountain/deformation belts (e.g. Vauchez et al. 1997;  
409 Tommasi and Vauchez 2001; Huang et al. 2006; Barruol et al. 2011). With some exceptions,  
410 the general trend of the fast direction of shear wave splitting along the North Atlantic margins  
411 is aligned with that of Caledonian-Variscan structures and deformation (e.g. Helffrich 1995;  
412 Barruol et al. 1997; Kreemer 2009; Wüstefeld et al. 2009; Darbyshire et al. 2015; Wang and  
413 Becker 2019).

414 Regional seismic tomography shows that present-day mantle anisotropy is generally aligned  
415 with late-Caledonian shear zones in the British Isles, the North Sea and southern Norway  
416 (GGF, WBF, HBF, MTFC, HFZ, Fig. 2,4), but oblique to those farther north (north of the Jan  
417 Mayen microplate complex) (Zhu and Tromp 2013). While breakup in the southern NE  
418 Atlantic followed the general Caledonian orogenic trends, breakup in the northern NE Atlantic  
419 (NE Greenland-NW Norway) followed an oblique, more easterly trend relative to the main  
420 Caledonian axis (defined as the central/median line between the orogenic fronts). This trend  
421 follows the late orogenic sinistral shear fabric of the NE Atlantic (Soper et al. 1992; Dewey  
422 and Strachan 2003), a fabric that was likely also reactivated during Late Caledonian extension  
423 (Figure 4) (Andersen et al. 1991; Dewey et al. 1993; Fossen 2010). This suggests that the  
424 mantle fabric and line of breakup in the north are to some extent related, while crustal fabric  
425 and breakup can be oblique.

426 A critical observation is that most of the rift systems that predated breakup (e.g. SW Barents  
427 Sea Basins, Danmarkshavn Basin, the Lofoten, Vøring, Møre basins, Faroe-Shetland basins,  
428 Hatton and Rockall basins (Tsikalas et al. 2012; Gaina et al. 2017; Stoker et al. 2017) largely

429 followed the major orogenic NE-SW crustal trends (Figure 8). In Section 7.1 we propose that  
430 pre-breakup continental rift systems inherited the shallower, crustal fabric mainly, whilst the  
431 later breakup dominantly exploited the oblique, deeper, pervasive, mantle fabrics, controlled  
432 by a major change in stress field.

433

#### 434 **4.4 Crustal-basin scale concepts**

435 At crustal-basin scale, deformation typically localises along weak zones such as pre-existing  
436 faults or shear zones. The size, geometry and interconnectivity of the discrete structures control  
437 the amount and magnitude of reactivation (Holdsworth 2004). Basin-scale structures exert a  
438 range of influences over later tectonic events, including strain localisation to control rift and  
439 fault nucleation, and also partitioning strain to potentially segment and block the propagation  
440 of rift related structures. But whether, and how, rifting is influenced depends on the type and  
441 geometry of the pre-existing structure and its relation to the imposed stress field. The  
442 orientation of the extensional stress field controls which older crustal structures reactivate at a  
443 given time, resulting eventually in co-linear/sub-parallel alignments between basins and older  
444 orogenic structural trends (Shannon 1991; Bartholomew et al. 1993; Doré et al. 1997; Roberts  
445 et al. 1999).

446 Pre-existing faults undergo varying degrees and styles of reactivation during later rift events  
447 (Bell et al. 2014; Whipp et al. 2014; Henstra et al. 2015; Deng et al. 2017b). The presence and  
448 reactivation of pre-existing basement structures, such as pervasive fabrics or discrete structures,  
449 can produce fault and rift geometries that depart from idealised geometries for orthogonal rift  
450 systems (Morley et al. 2004; Paton and Underhill 2004; Whipp et al. 2014). These effects may  
451 manifest as fault patterns oriented oblique to the regional stress field, and may also display  
452 complex internal transfer and linkage patterns (Morley et al. 2004; Bird et al. 2015; Bladon et  
453 al. 2015; Mortimer et al. 2016). In some instances, pre-existing structures may transfer strain  
454 across a rift from margin to axis as extension progresses (Morley et al. 2004; Bladon et al.  
455 2015; Mortimer et al. 2016). Pre-existing structures can also act as stress guides that locally  
456 rotate the maximum horizontal stress in the overlying basin, controlling the trends of newly  
457 forming structures (Morley 2010; Whipp et al. 2014; Duffy et al. 2015; Reeve et al. 2015;  
458 Phillips et al. 2016). Oblique extension or transtension in the presence of pre-existing weak  
459 zones commonly leads to partitioning displacement into strike-slip and dip-slip fault  
460 components (De Paola et al. 2006; Wilson et al. 2006; Philippon et al. 2015; Kristensen et al.  
461 2018).

462 Steeper dipping structures are preferentially reactivated under extensional stress compared to  
463 shallowly dipping structures (Bird et al. 2015; Phillips et al. 2016; Fazlikhani et al. 2017). Daly  
464 et al. (1989) show that gently dipping shear zones may be reactivated in a dip-slip manner  
465 whereas steeply dipping structures tend to display strike-slip reactivation. Structures at high  
466 angles to the regional stress direction (typically  $> 45^\circ$ ) are typically not reactivated (Henstra et  
467 al. 2015; Deng et al. 2017b; Henstra et al. 2017; Deng et al. 2018) and may be cross-cut by  
468 later faults (Duffy et al. 2015; Henstra et al. 2015; Phillips et al. 2016; Fazlikhani et al. 2017).  
469 Alternatively, they may inhibit fault propagation and segment rift basins (Doré et al. 1997;  
470 Fossen et al. 2014; Nixon et al. 2014).

471 During multiple phases of extension, pre-existing fault networks influence the development of  
472 later faults. Faults that reactivate pre-existing structures often quickly attain the length of the  
473 reactivated structure before undergoing displacement-dominated growth (Walsh et al. 2002;  
474 Whipp et al. 2014; Childs et al. 2017). The influence of pre-existing faults may be complicated  
475 by healing during burial following earlier rift phases, the combination of pre-existing fault

476 orientations and the applied stress orientation, as well as lithospheric properties (Cowie et al.  
477 2005; Baudon and Cartwright 2008; Henza et al. 2011; Bell et al. 2014; Whipp et al. 2014;  
478 Henstra et al. 2015, 2017; Claringbould et al. 2017). Complex fault geometries from multi-  
479 phase rifts have been documented in natural examples (Nixon et al. 2014; Duffy et al. 2015;  
480 Reeve et al. 2015; Rotevatn et al. 2018) and simulated in analogue models (Keep and McClay  
481 1997; Corti et al. 2007; Henza et al. 2010, 2011; Henstra et al. 2015; Duffy et al. 2017)  
482 although in some instances complex, non-colinear fault networks may also arise in single-phase  
483 rifts due to a 3D stress field (Healy et al. 2015; Collanega et al. 2017; Gernigon et al. 2018).

484 The emplacement of igneous rocks may be controlled by pre-existing structures at the crustal  
485 (Peace et al. 2017) and intrusion scale (Peace et al. 2018c). Igneous complexes may  
486 subsequently favour the nucleation and formation of new shear zones (Neves et al. 1996) and  
487 can lead to spatial variations in deformation patterns within rift systems and basins (Woodcock  
488 and Underhill 1987; Buck 2006; Dineva et al. 2007; Magee et al. 2014, 2017; Phillips et al.  
489 2017). Steeply dipping intrusions, such as dyke systems, may promote strain localisation in a  
490 similar way to basement faults and fabrics during rifting, introduce anisotropy and controlling  
491 the geometry and evolution of faults (Buck 2006; Ruch et al. 2016; Phillips et al. 2017). In  
492 contrast, sub-horizontal intrusions such as sills and laccoliths may produce more distributed  
493 strain patterns caused by uplift and outer arc extension in forced folds at sub-basin scales  
494 (Wilson et al. 2016; Magee et al. 2017).

495 Compression of previously formed rift basins typically leads to basin inversion (Stephenson et  
496 al. this volume; Buchanan and Buchanan 1995; Lowell 1995). During basin inversion, the  
497 geometry of the extensional faults, which may themselves be influenced by basement fabric,  
498 affects the style of inversion produced when reactivated under oblique convergence (Withjack  
499 et al. 2010; Kley 2018). On the NE Atlantic margins, the widespread Cenozoic inversion  
500 structures (Stephenson et al. this volume; Johnson et al. 2005; Doré et al. 2008; Pascal and  
501 Cloetingh 2009) also seem to track underlying extensional basin and lithospheric structure  
502 (Nielsen et al. 2014). This, in turn, was probably inherited indirectly from basement fabric  
503 (Kimbell et al. 2017; Reilly et al. 2017).

504

## 505 **5** Pre-rift structural framework of the Circum-North Atlantic region

506

507 The main accretionary events predating CNAR breakup were the mid-Neoproterozoic  
508 Sveconorwegian-Grenvillian (Bingen et al. 2008b; Roberts and Slagstad 2015), the  
509 Neoproterozoic Timanian (Roberts and Siedlecka 2002; Gee and Pease 2004) and the  
510 Phanerozoic Caledonian (Roberts 2003; Gee et al. 2008) and Variscan orogenies (Matte 2001;  
511 Winchester et al. 2002; Franke 2006). These orogenies were in essence the expressions of two  
512 Wilson cycles: (i) the assembly and dispersal of the supercontinent Rodinia in the  
513 Neoproterozoic leading to the formation of the Iapetus Ocean, followed by (ii) the renewed  
514 assembly and dispersal of Pangaea in the Phanerozoic and formation of the North Atlantic in  
515 the Cenozoic (Stampfli et al. 2013).

### 516 **5.1** Archaeo-Proterozoic cratons

517 The North American and East European cratons, the respective cores of the palaeocontinents  
518 Laurentia and Baltica (prior to their Caledonian suturing to become Laurussia (Roberts et al.  
519 1999; Ziegler 2012), were formed from the Archaean through to the Proterozoic and consist of  
520 terranes of different age separated by networks of mobile belts. In Baltica, the main tectonic  
521 episodes were the Archaean Karelian and Lapland-Kola events in northern Scandinavia, the  
522 Palaeoproterozoic Svecofennian orogeny in central Scandinavia, and formation of the Trans-

523 Scandinavian Igneous Belt (TIB) in the late Palaeoproterozoic from southern Sweden to NW  
524 Norway (Gorbatshev and Bogdanova 1993; Balling 2000). Similarly, Laurentia depicts  
525 differently aged cratonic terranes and mobile belts (St-Onge et al. 2009). In the CNAR, these  
526 include the North Atlantic Craton, the Rae Craton and the Superior Craton, conjoined by the  
527 Palaeoproterozoic Nagsuqqotidian, Makkovik-Ketilidian, Rinkian and other orogens (St-Onge  
528 et al. 2009) (Fig. 2, 3).

529

### 530 **5.2 The Grenville-Sveconorwegian Orogeny**

531 The Grenville-Sveconorwegian fold belt evolved during the assembly of Rodinia in the late  
532 Mesoproterozoic (Li et al. 2008). The Grenville Orogen in NE North America includes the  
533 collision between Laurentia and Amazonia (1.09-1.02 Ga), marked by high-grade  
534 metamorphism (Hynes and Rivers 2010; Rivers 2015). The basement of southern Scandinavia  
535 was assembled by several events prior to the Sveconorwegian orogeny: the Gothian (1.64-1.52  
536 Ga), Telemarkian (1.52-1.48 Ga) and Hallandian events (1.47-1.42) (Bingen et al. 2008a). The  
537 actual Sveconorwegian Orogen is characterised by terrane accretion events between 1.14 and  
538 0.97 Ga arising from collision between Baltica and other continental fragments, followed by  
539 orogenic collapse at 0.9 Ga (Bingen et al. 2008a). Although the Sveconorwegian orogeny was  
540 largely coeval, and likely also spatially related to the Grenville Orogen, the precise connection  
541 between these orogens is unclear, as well as the regional configuration, especially of Baltica at  
542 this time (Bingen et al. 2008b; Slagstad et al. 2013, 2019; Cawood and Pisarevsky 2017).  
543 Sveconorwegian-aged deformation is also reported in the Arctic but any relationship to the  
544 main fold-belt is unclear (Lorenz et al. 2012). The latest Neoproterozoic Valhalla Orogeny has  
545 been proposed as an accretionary orogen along Laurentia's free margin (East Greenland)  
546 (Cawood et al. 2010; Spencer and Kirkland 2016).

### 547 **5.3 The Timanian Orogeny**

548 The Timanian fold-and-thrust belt records ocean-continent collisions along the northern margin  
549 of Baltica and the accretion of island arc complexes, terranes and microcontinents at ~0.62-  
550 0.55 Ga stretching from the Scandinavian Arctic to the Arctic Urals (Roberts and Siedlecka  
551 2002; Gee and Pease 2004; Gee et al. 2006, 2008). The Trollfjorden-Komagelva Fault Zone is  
552 a major Timanian structure extending from the Urals across the Timan Range to northernmost  
553 Norway, where it was later reworked by the Caledonides (Gernigon and Brönnner 2012;  
554 Gernigon et al. 2014, 2018; Klitzke et al. 2019). Neoproterozoic Timanian basement terranes,  
555 metasediments and volcanic sequences were drilled in the Pechora Basin (Roberts and  
556 Siedlecka 2002; Dovzhikova et al. 2004). The Timanian suture may be deeply buried in the  
557 central Barents Sea (Gernigon et al. 2018) possibly associated with high velocity-high density  
558 lower crustal rocks (Shulgin et al. 2018). Basement structures in the eastern and central Barents  
559 Sea show a persistent NW-SE oriented Timanian fabric throughout the region (Gee et al. 2006,  
560 2008; Pease 2011; Klitzke et al. 2019). The Torellian orogeny on Svalbard may be a Timanian  
561 equivalent or prolongation (Majka et al. 2008).

### 562 **5.4 The Caledonian Orogeny**

563 Prior to opening of the North Atlantic Ocean, Europe, North America and Greenland comprised  
564 part of the most recent continental amalgamation, Laurasia, the northern constituent of Pangaea  
565 (reconstructions in Figure 3,4) (Cocks and Torsvik 2006, 2011; Lawver et al. 2011; Stampfli  
566 et al. 2013). As part of Laurasia, Laurussia was formed by closure of the Iapetus Ocean and  
567 Tornquist seaway, and collision of three palaeocontinents – Laurentia, Baltica and Avalonia –  
568 as well as smaller terranes, culminating in the Scandian phase of the Caledonian orogeny at  
569 425-400 Ma (Soper and Woodcock 1990; Pharaoh 1999; McKerrow et al. 2000; Roberts 2003;  
570 Gee et al. 2008; Leslie et al. 2008). This was preceded by phases of arc-accretion in Norwegian,  
571 British and North American Caledonides in the late Cambrian-early Ordovician, i.e. the

572 Finnmarkian/Jämtlandian (Brueckner and Van Roermund 2007), Grampian (Dewey 2005) and  
573 Taconian stages (Karabinos et al. 1998), respectively. Laurasia's assembly was completed by  
574 accretion of the Siberian and Kazakhstan continental plates during the Uralian and Mongol-  
575 Okhotsk orogenies (Blakey 2008). Avalonia was the first of several large terranes released from  
576 Gondwana to dock against Baltica and Laurentia, opening the Rheic Ocean in the mid-  
577 Ordovician (Matte 2001). the docking of the peri-Gondwana terranes Armorica and Megumia  
578 to the south of Avalonia in the British Isles and Appalachians defines the Early Devonian  
579 Acadian stage after the complete closure of the Iapetus Ocean and docking of Avalonia  
580 (Murphy and Keppie 2005; Woodcock et al. 2007; Mendum 2012; Woodcock and Strachan  
581 2012). In case of the Appalachians, other authors have proposed that the Acadian represents  
582 the actual docking of Avalonia during the closure of the Iapetus Ocean (Hatcher et al. 2010;  
583 Hibbard et al. 2010). In the Barents Sea the observed trends and seismic evidence suggest two  
584 branches of the Caledonian suture (Doré 1991; Gudlaugsson et al. 1998; Breivik et al. 2005;  
585 Gee et al. 2008; Gernigon et al. 2014), an NE-SW oriented branch and an N-S oriented branch  
586 parallel to the present-day western Barents margin towards Svalbard (Gudlaugsson et al. 1998;  
587 Breivik et al. 2002; Aarseth et al. 2017). Shortening in the Palaeozoic Ellesmerian fold belt in  
588 Svalbard, North Greenland and Arctic Canada was broadly contemporaneous with Caledonian  
589 deformation (Ziegler 1988; Gasser 2013; Gee 2015).

590 While the fundamental tectonic elements of the Caledonian orogeny are reasonably well  
591 understood, significant aspects of timing, deformation, polarity and number of subduction  
592 events are not resolved. Structural and tectonic relationships are complicated due to overlap  
593 and interaction of Caledonian structures with earlier structures (Roffeis and Corfu 2014). Ages  
594 of Caledonian metamorphism and intrusions in East Greenland and Scandinavia range from  
595 500 to 360 Ma with early age populations (~500-422; Kalsbeek et al. 2008; Corfu et al. 2014),  
596 the main Scandian phase (~425 Ma; Dobrzhinetskaya et al. 1995; van Roermund and Drury  
597 1998; Hacker et al. 2010) in Scandinavia and East Greenland, as well as young ages in NE  
598 Greenland (~360 Ma, Gilotti et al. 2014), indicating complex and prolonged evolution (Gasser  
599 2013; Corfu et al. 2014). These observations have led to departures from a simple model of  
600 only west-dipping Scandian subduction and collision. Other suggested models include  
601 additional early west-dipping (Brueckner and van Roermund 2004; Brueckner 2006) or east-  
602 dipping subduction events (Yoshinobu et al. 2002; Andréasson et al. 2003; Roberts 2003; Gee  
603 et al. 2008; Schiffer et al. 2014), possibly as a northward equivalent of the Grampian  
604 (Karabinos et al. 1998; van Staal et al. 2009) or Taconian phases (van Staal et al. 1998; Dewey  
605 2005), and late intracratonic eastward underthrusting (Gilotti and McClelland 2011). Although  
606 the Caledonian orogeny between Greenland and Scandinavia can be approximated as a linear,  
607 "two-dimensional" orogen, complexities of Caledonian fabrics can be observed along the  
608 length of the orogen indicating a composite, non-orthogonal collision and subduction system  
609 (Fossen et al. 2008). The late Caledonian phases were dominated by the gravitational collapse  
610 of high, unstable topography, accompanied by lithospheric extension and possibly lithospheric  
611 delamination (Seranne 1992; Fossen et al. 2014; Gabrielsen et al. 2015) with major sinistral  
612 strike-slip along the Baltic and Laurentian margins (Harland 1969, 1971; Roberts 1983; Soper  
613 et al. 1992).

614

## 615 **5.5 The Variscan Orogeny**

616 Following consolidation of Laurasia in the Late Silurian-Early Devonian, the basement  
617 substructure of the southern CNAR was modified by the Variscan-Appalachian Orogeny, a  
618 major continent-continent collision to the south with Gondwana and peri-Gondwanan terranes  
619 and microcontinents (McKerrow et al. 2000; Franke 2006; Winchester et al. 2006; Kroner and  
620 Romer 2013). The episodic release of peri-Gondwana terranes was probably driven by back-

621 arc spreading on the Gondwana margin (Stampfli and Borel 2002). These terranes successively  
622 docked against Laurasia to the north, each generating individual compressional pulses. While  
623 the orogenic evolution of the Appalachians is relatively well-defined (Hatcher et al. 2010), the  
624 situation is more complicated in the European Variscides, due to a more complex subduction  
625 history (Matte 2001). The Variscan Orogeny ended with collision between Gondwana and  
626 Laurasia in Late Carboniferous-Permian time (McKerrow et al. 2000; Matte 2001), forming a  
627 major fold belt, running E-W through southern Europe and NE-SW between eastern North  
628 America and NW Africa.

629 This collision involved dextral transpression and likely resulted in major orogen-parallel  
630 transform faults in the Appalachians (Hatcher 2002). Similarly, the Variscides of the Iberian  
631 Peninsula were bounded by the NW-trending Coimbra-Cordoba and Ossa-Morena shear zones  
632 in the south, likely connected to the North Iberia Fault. The Coimbra-Cordoba shear zone  
633 experienced at least 72 km of sinistral motion (Burg et al. 1981). A transform system may have  
634 continued from the North Iberia Fault along the proto-Flemish Cap and Goban Spur margins,  
635 through the proto-Labrador Sea, connecting with the Hudson Strait-Foxe Channel fault system  
636 (Lundin and Doré 2018).

## 637 **6** Structural segmentation and inheritance in the CNAR

638 The CNAR margins are segmented in terms of crustal thickness, width, basin thickness,  
639 magmatism and presence of HVLCBs (Skogseid et al. 2000; Lundin and Doré 2011; Peron-  
640 Pinvidic et al. 2013; Funck et al. 2016b; Ady and Whittaker 2018; Lundin et al. 2018). A  
641 number of failed rift systems are present, including the North Sea Central and Viking grabens,  
642 the conjoined Møre and Vøring basins, the parallel Rockall and Hatton basins, plus the  
643 Porcupine, Orphan, Danmarkshaven and Bjørnøya basins (Ziegler 1992; Péron-Pinvidic and  
644 Manatschal 2010; Lundin and Doré 2011; Gernigon et al. 2014). This rift network on the  
645 continental shelves may be linked to pre-existing lithospheric-scale structures, lineaments and  
646 terranes (Doré et al. 1997; Chenin et al. 2015; Gaina et al. 2017; Schiffer et al. 2018).

647 A key observation in the northern NE Atlantic is that in some areas, the late Caledonian shear  
648 zones, primarily recognised in the onshore, are largely parallel to the breakup trend, while in  
649 other areas there is a distinct obliquity of the breakup axis with earlier rift basins that follow  
650 Caledonian trends (Fig. 8). This obliquity likely relates to interaction between different sets  
651 and depths of pre-existing structures and varying extensional stress-fields.

652 The relationship between the Caledonian Orogen and the CNAR can be described in the context  
653 of five primary segments (Fig. 1):

654 (1) In the northern section between East Greenland and Norway, many of the late Palaeozoic-  
655 Early Cretaceous rift basins (Møre, Vøring, Lofoten-Vesterålen, Danmarkshavn basins, and  
656 possibly the Thetis Basin) follow the mapped NE-SW Caledonian trends, while latest  
657 Cretaceous- earliest Cenozoic rifting and breakup is clockwise oblique by ~20-30° (Figures  
658 4,8). North-south Mid-Late Jurassic faulting, as expressed in the Halten Terrace, appears to be  
659 strongly discordant to this pattern, although a link to duplex systems between Caledonian  
660 shears was suggested by Doré et al., (1997).

661 (2) In the southern NE Atlantic, between SE Greenland and the British Isles, the Cretaceous-  
662 Jurassic Rockall and Hatton basins and the axis of breakup all follow the general Caledonian  
663 trend. However, breakup produced highly asymmetric margins lying 500 km or more west of  
664 the Caledonian front, and cutting through cratonic lithosphere (Figures 3, 4, 8).

665 (3) The Greenland-Iceland-Faroe Ridge (GIFR) separates segments 1 and 2. Formation of this  
666 ridge is discussed in detail by Foulger et al. (this volume). Relative movements between the  
667 Reykjanes Ridge to the south and the abandoned Aegir Ridge, and active Kolbeinsey Ridge to

668 the north must have been accommodated along the GIFR. Additionally, the GIFR formed  
669 where the North Atlantic rift crosscut the western Caledonian front and along the southern  
670 margin of the Rae Craton.

671 (4) The North Sea experienced rift phases in the Permian-Triassic, Late Jurassic and Early  
672 Cretaceous in the area of the Iapetus-Thor Suture triple junction and the Danish-German-Polish  
673 Caledonides. The physiography of the later rift is dominated by the northern Viking Graben,  
674 the western Moray Firth Graben and the Central Graben (Færseth et al. 1995). As indicated in  
675 point (1), the dominant N-S faulting of the northern North Sea, generally discordant to the  
676 Caledonian trends, is probably attributable to rift propagation from the SE (e.g. Figs. 4 and 8).

677 (5) The Labrador Sea and Baffin Bay are two ocean basins formed during the Palaeogene by a  
678 now-extinct spreading system, with the Davis Strait separating and accommodating relative  
679 motions between them. Rifting and continental breakup both cross-cut and ran sub-parallel to  
680 crustal terrane boundaries (Figs. 2,3).

681 The principal rift architectures and possible relations to inherited fabrics in these segments are  
682 as follows:

683

#### 684 *Segment 1 – Norway-Greenland margins*

685 North of the GIFR, the conjugate margins of Norway and Greenland are asymmetric, with  
686 structural variations along strike, as a result of the oblique breakup axis (Fig. 8) (Gernigon et  
687 al. this volume). The narrow continental shelf in central East Greenland contrasts strongly with  
688 the wide conjugate Vøring margin. Further north, the NE Greenland shelf is much wider than  
689 its conjugate Lofoten margin.

690 The Mid-Norwegian margin is magma-rich with thick NE-SW trending sedimentary basins and  
691 highs. This NE-SW trend is attributed to Caledonian and Precambrian inheritance (Bergh et al.  
692 2007; Maystrenko et al. 2017). The margin is divided into the Møre, Vøring and Lofoten-  
693 Vesterålen margins from south to north (Gernigon et al. this volume; Lundin and Doré 1997;  
694 Brekke 2000; Mosar 2003). This segmentation is related to margin-perpendicular transfer  
695 zones, the Jan Mayen Lineament/Corridor between the Møre and Vøring margins (Eldholm et  
696 al. 2002) and the Bivrost Lineament separating the Vøring from the Lofoten-Versterålen  
697 margin (Blystad 1995). These lineaments are expressed through offsets in basin axes, inferred  
698 by some authors to reflect Caledonian or Precambrian basement fabrics (Doré et al. 1997, 1999)  
699 or Late Jurassic–Early Cretaceous extensional structures (Eldholm et al. 2002).

700 As indicated earlier, Jurassic faulting, as expressed in the Halten Terrace (e.g. Blystad et al.,  
701 1995), is approximately N-S and strongly discordant to both the Caledonian trends, later (Early  
702 Cretaceous) basin formation and Cenozoic breakup (Fig. 8). The N-S faulting here and in the  
703 North Sea may represent an attempt by Tethys, the dominant oceanic domain at the time, to  
704 propagate through the North Sea into what is now the Norwegian Sea (compare Figs. 4 and 8).

705 In the Møre and Vøring segments, deep, inherited HVLCBs of Caledonian and/or Precambrian  
706 age controlled rifting (Gernigon et al. 2003, 2004; Abdelmalak et al. 2017; Maystrenko et al.  
707 2017; Zastrozhnov et al. 2018). In the inner Møre margin, basin architecture follows the trends  
708 of late-Caledonian shear zones bordering the margin to the south, specifically the Møre-  
709 Trøndelag Fault Complex (Grunnaleite and Gabrielsen 1995; Hurich 1996; Jongepier et al.  
710 1996; Doré et al. 1997; Nasuti et al. 2011; Theissen-Krah et al. 2017) suggesting a genetic  
711 connection. The dominant NE-SW-trending Caledonian thrust sheets in the Lofoten-Vesterålen  
712 margin interact with the Palaeoproterozoic NW-SE, margin-perpendicular Bothnian-Senja  
713 Fault Complex (Bergh et al. 2007), which appears to run into the younger offshore Senja

714 Fracture Zone, forming the Barents Sea's western transform boundary (Henkel 1991; Doré et  
715 al. 1997).

716 With the exception of the Wandel Sea Basin, the conjugate East Greenland margin is  
717 characterised by approximately N-S trending basins. Extensional faults appear to relate to  
718 Caledonian fabrics (Henriksen 2003) (Figure 9). Late Devonian-Early Carboniferous shear  
719 zones formed during Caledonian collapse (Surlyk 1990; Price et al. 1997; Parsons et al. 2017;  
720 Rotevatn et al. 2018), accompanied and possibly facilitated by major strike-slip deformation  
721 (Dewey and Strachan 2003), which may have reactivated older, pre-Caledonian shear zones  
722 related to the opening of the Iapetus Ocean (Soper and Higgins 1993). Faulting in the Triassic-  
723 Cretaceous East Greenland rift system was episodic, with multiple stages of reactivation  
724 culminating in the final separation of the JMMC (Surlyk 1990; Stemmerik et al. 1991; Hartz  
725 and Andresen 1995; Seidler et al. 2004; Parsons et al. 2017; Rotevatn et al. 2018). The East  
726 Greenland rift system is segmented by right-stepping NW-SE transfer zones (Fossen et al.  
727 2017; Rotevatn et al. 2018). These offsets are thought to be related to reactivation of a NW-SE  
728 Proterozoic fabric (Andresen et al. 1998; White and Hodges 2002; Guarnieri 2015; Rotevatn  
729 et al. 2018).

730 The JMMC is located between the central East Greenland margin and the Møre margin (Gaina  
731 et al. 2009; Gernigon et al. 2015; Blischke et al. 2017, 2019; Polteau et al. 2018; Schiffer et al.  
732 2018). The nature and formation of the JMMC remains enigmatic but its location and  
733 geographic relation to the GIFR and known Caledonian structures suggests inheritance control  
734 (Gernigon et al. this volume; Schiffer et al. 2015b, 2018) (see section 7.3). A lower crustal-  
735 upper mantle fabric, exemplified by a proposed N-S Caledonian (or pre-Caledonian) fossil  
736 suture zone (Schiffer et al. 2015b; Petersen and Schiffer 2016) may also have influenced rifting.  
737 However, direct geological or geophysical evidence for reactivation of older structures remains  
738 sparse.

739 The Wandel Sea Basin formed by transtension or extension during the mid-Cretaceous, and  
740 was modified by Palaeocene-Eocene N-S compression (Svennevig et al. 2016), synchronous  
741 with formation of the West Spitsbergen fold-and-thrust belt. Local structural trends (~NW-SE)  
742 closely mimic the conjugate Bothnia-Senja Fault Complex and Senja Fracture Zone. The  
743 Wandel Sea Basin is thought to have experienced multiple phases of reactivation of earlier rift  
744 structures (Guarnieri 2015).

#### 745 ***Segment 2 – SE Greenland-Rockall-Hatton margins***

746 The NE Atlantic south of the GIFR broke up parallel to Caledonian trends and structures, but  
747 ~500 km west of the Caledonian front through the Laurentian basement of the Rockall-Hatton  
748 margin. The margins in this segment are highly asymmetric. The Hatton margin comprises  
749 thinner and narrower SDRs and HVLCBs compared to SE Greenland (Planke and Alvestad  
750 1999; Hopper et al. 2003). The SE Greenland continental shelf is straight and narrow, whilst  
751 the Rockall-Hatton margin shelf is extremely wide and formed during Jurassic-Cretaceous  
752 lithospheric thinning (Stoker et al. 2017).

753 The Rockall-Hatton margin contains two large failed rift basins (the highly extended, deep  
754 Rockall Basin and the less extended, shallower Hatton Basin) bounded by major marginal highs  
755 (Hatton High, Rockall Bank) (Morewood et al. 2005). The highs are underlain by crustal blocks  
756 up to 30 km thick (Funck et al. 2016a). The Rockall Basin has crustal thicknesses of <10 km  
757 beneath up to 5 km of sediments (Funck et al. 2016a) and is underlain by HVLC or hydrated  
758 mantle peridotite (Roberts 1975; Roberts et al. 1988, 2018; Makris et al. 1991; Shannon et al.  
759 1999; Klingelhöfer et al. 2005; Morewood et al. 2005; Funck et al. 2016a). Reactivation of  
760 NNE-SSW to NE-SW, margin-parallel Caledonian and pre-Caledonian basement lineaments  
761 seems to have led to the initial localisation and segmentation of the Rockall-Hatton shelf.

762 Furthermore, the shelf is transected by NW-trending continental lineaments/transfer zones  
763 (Figure 9) (Rumph et al. 1993; Kimbell et al. 2005a; Stoker et al. 2017). Some of these  
764 lineaments link to faults onshore Ireland (e.g., SHL), others are associated with COB offsets  
765 of the Hatton-Rockall shelf (e.g., SHL, ADL) or are correlated with sedimentary basins (e.g.,  
766 ADL, WTL, JF), and some may have guided magmatic intrusions or be related to oceanic  
767 fractures or accommodation zones in the Iceland Basin (e.g., CL) (Kimbell et al. 2005a; Naylor  
768 and Shannon 2005; Štolfova and Shannon 2009).

769 During Cenozoic compression/transpression, some transfer zones became the loci for inversion  
770 (Doré and Lundin 1996; Doré et al. 1999; Eldholm et al. 2002; Kimbell et al. 2005a; Tuitt et  
771 al. 2010). These are interpreted as rejuvenated Precambrian terrane boundaries or shear zones  
772 that had previously impeded rift propagation (Shannon et al. 1995, 1999; Kimbell et al. 2005a;  
773 Ritchie et al. 2008; Štolfova and Shannon 2009), thereby compartmentalising rift evolution in  
774 the Rockall Basin (Rumph et al. 1993; Kimbell et al. 2005a; Stoker et al. 2017). Such pre-  
775 existing, margin-perpendicular terrane boundaries between different blocks may also explain  
776 why the lithosphere beneath Rockall did not break, while rifting was transferred outboard to a  
777 weaker section (Johnson et al. 2005; Elliott and Parson 2008). At the southern margin of the  
778 Rockall Basin, a probable connection between the Charlie Gibbs Fracture Zone and the Iapetus  
779 Suture, suggests a further reactivation of a pre-existing Caledonian lithospheric feature  
780 (Shannon et al. 1994; Buitter and Torsvik 2014; Ady and Whittaker 2018) (Figure 2).

781 The poorly known, narrow margin in SE Greenland comprises SDRs, HVLC bodies, and  
782 igneous centres and intrusions (Dahl-Jensen et al. 1998; Korenaga et al. 2000; Callot et al.  
783 2001; Klausen and Larsen 2002; Hopper et al. 2003). Palaeoproterozoic discontinuities in SE  
784 Greenland were reactivated as left-lateral shear zones prior to breakup and the margin was  
785 inverted during the Eocene or later (Guarnieri 2015). The highly asymmetric line of Cenozoic  
786 breakup, outboard of the Hatton Basin and close to the SE Greenland coast (e.g. Figs. 4, 8 &  
787 9), is a curious feature that appears to have formed without significant observable initial rifting.  
788 Because data is sparse, it is not possible to make any definite connection with older weaknesses.  
789 Speculatively, both the trend and straightness of this margin segment suggests a connection  
790 with the Late Caledonian shear fabric, as exemplified by faults such as the Møre-Trøndelag  
791 Fault Complex (e.g. Fig. 2). This line forms the shortest path from the Aegir Ridge to the  
792 Labrador Sea, and may have been created or exploited by dextral strike-slip associated with  
793 Labrador Sea opening (Lundin and Doré 2018) or high geopotential energy associated with the  
794 forming ridge triple junction located south of Greenland at that time (Kristoffersen and Talwani  
795 1977; Roest and Srivastava 1989; Guan et al. 2019). An alternative hypothesis is that after  
796 Early Cretaceous rifting, the lithosphere in the Rockall-Hatton shelf re-equilibrated, cooled and  
797 strengthened (Guan et al. 2019), thereby leaving the SE Greenland shelf as the weakest  
798 pathway for breakup due to its thick, warm crust (45-55 km) and weak lithosphere.

### 799 ***Segment 3 – The Greenland-Iceland-Faroe Ridge and adjacent margins***

800 The GIFR forms a WNW-ESE ridge spanning the NE Atlantic from central East Greenland to  
801 the Faroe-Shetland Basin (Foulger et al. 2019). The GIFR has anomalously high topography  
802 with typically 20-30 km thick crust (Foulger et al. 2003; Fedorova et al. 2005; Torsvik et al.  
803 2015; Funck et al. 2016b; Haase et al. 2016), which thickens to 40 km beneath the central  
804 Iceland Plateau (Darbyshire et al. 2000; Du and Foulger 2001; Kaban et al. 2002;  
805 Gudmundsson 2003; Foulger et al. 2003; Fedorova et al. 2005). Thick basaltic lava flows cover  
806 the ridge (Horni et al. 2017; Hjartarson et al. 2017). The origin, structure and composition of  
807 the lithosphere beneath the GIFR remain poorly understood but there is significant evidence  
808 for a component of continental crust (Foulger 2006; Torsvik et al. 2015; Schiffer et al. 2018;  
809 Petersen et al. 2018; Foulger et al. 2019). The role of structural inheritance here is unknown,  
810 but the common location and orientation of the GIFR and the intersection of the North Atlantic

811 rift axis with the Caledonian orogenic front suggest a link (Foulger and Anderson 2005;  
812 Schiffer et al. 2015b, 2018; Foulger et al. 2019). In addition, the recent recognition of Faroe-  
813 Shetland basement terrane immediately north of Scotland and the correlation of its southern  
814 boundary with that of the Rae Craton in Greenland (Holdsworth et al. 2019) mean that the  
815 southern margin of the GIFR follows this ancient terrane boundary.

816 The central East Greenland margin appears to be structurally and magmatically segmented by  
817 margin-perpendicular Precambrian structures that accommodated transform motion and  
818 localised intrusions (Karson and Brooks 1999). This segmentation was controlled by local  
819 magmatic centres, from which magma flow was guided and transfer zones defined (Callot et  
820 al. 2001; Klausen and Larsen 2002; Callot and Geoffroy 2004). Tegner et al. (2008) linked  
821 some of these tectonic lineaments to failed rifts, localised magmatism and breakup between  
822 central East Greenland and the JMMC.

823 The Faroe–Shetland margin consists of basins and highs, formed from the Late Palaeozoic to  
824 early Cenozoic plate breakup, followed by syn- to post-breakup magmatism, compressional  
825 tectonics and differential uplift and subsidence (Doré et al. 1999; Roberts et al. 1999; Johnson  
826 et al. 2005; Ritchie et al. 2008, 2011; Fletcher et al. 2013; Stoker 2016; Stoker et al. 2017,  
827 2018). N–S to NE–SW and ESE–WSW to SE–NW structural trends follow regional fabrics  
828 observed in onshore basement rocks (Doré et al. 1997; Wilson et al. 2010). Many Devonian to  
829 Jurassic rifts exhibit Caledonian structural inheritance with a generally NNE trend such as the  
830 Outer Hebrides/Minch fault zones (Imber et al. 2001) (Fig. 9), faults within the West Orkney  
831 Basin (Bird et al. 2015) and the northeastern Faroe-Shetland Basin (Lamers and Carmichael  
832 1999; Ritchie et al. 2011; Stoker et al. 2017) (Fig. 9).

833 In contrast, some lineaments in the Faroe Shetland Basin, including the southern boundary of  
834 the basin (Judd Fault), have a NW-SE orientation. Similar to the Rockall-Hatton margin, this  
835 structural trend is pre-Caledonian and may have created the transfer zones that  
836 compartmentalised the basin during the Mesozoic and early Palaeogene (Ritchie et al. 2011),  
837 although these features are not ubiquitous (Moy and Imber 2009). In the southern part of the  
838 basin, a W-to-NW trend prevails, including the Wyville-Thomson Lineament (Fig. 9), which  
839 reactivated during the Palaeocene (Kimbell et al. 2005a; Lundin and Doré 2005; Ziska and  
840 Varming 2008). Compressional structures formed in the Late Cretaceous (Booth et al. 1993;  
841 Grant et al. 1999; Stoker 2016) have been attributed to strike-slip tectonics linked to a shear  
842 margin (proto-plate boundary) separating Faroe–Shetland and SE Greenland, which reactivated  
843 old lineaments prior to breakup (Roberts et al. 1999; Guarnieri 2015; Stoker et al. 2018).  
844 Further compressional folding and differential uplift events occurred during the Eocene to early  
845 Neogene (Johnson et al. 2005; Stoker et al. 2005; Ritchie et al. 2008).

#### 846 ***Segment 4 – North Sea & Tornquist Zone***

847 The North Sea formed within basement that had been influenced by the Caledonian orogeny  
848 and Devonian orogenic collapse (Coward 1990; Andersen 1998; McKerrow et al. 2000; Fossen  
849 and Hurich 2005; Fossen 2010), with subsequent generally E-W extension beginning in the  
850 Permian-Triassic (Ziegler 1992; Fossen and Dunlap 1999; Frederiksen et al. 2001; Coward et  
851 al. 2003) and E-W to NW-SE extension in the latest Jurassic to Early Cretaceous (Brun and  
852 Tron 1993; Underhill and Partington 1993; Færseth 1996; Frederiksen et al. 2001; Coward et  
853 al. 2003; Arfai et al. 2014; Bell et al. 2014; Duffy et al. 2015; Deng et al. 2017a). Its  
854 development was also variably influenced by Permo-Carboniferous rifting and magmatism  
855 (Glennie et al. 2003; Heeremans and Faleide 2004; Neumann et al. 2004; Wilson et al. 2004),  
856 and far-field Alpine compression combined with ridge-push and gravitational forces from the  
857 high topography in Norway in the Late Cretaceous and Eocene (Biddle and Rudolph 1988;  
858 Cartwright 1989; Nielsen et al. 2005, 2007; Pascal and Cloetingh 2009; Jackson et al. 2013).

859 The North Sea region exhibits a range of upper mantle fabrics of Precambrian to Devonian age  
860 (Klemperer and Hurich 1990; Blundell et al. 1991; Abramovitz and Thybo 2000; Balling 2000;  
861 Fossen et al. 2014). Large-scale Moho and upper mantle shear zones originating from Devonian  
862 extension are imaged in the Norwegian North Sea (Fossen et al. 2014; Gabrielsen et al. 2015).  
863 HVLCBs in the southwest (Abramovitz and Thybo 2000) and NW (Christiansson et al. 2000)  
864 of the North Sea, and lower crustal fabrics (Klemperer et al. 1990) in the vicinity of the Iapetus  
865 suture offshore NW England are attributed to Caledonian collision and may have exerted  
866 structural control on the development of the rifts. Caledonian or Variscan upper mantle fabric  
867 along the eastern British coastline (Blundell et al. 1991) may also have influenced rifting. Pre-  
868 Caledonian dipping structures in the upper mantle were identified in the Skagerrak Sea between  
869 Norway and Denmark (Lie et al. 1990).

870 Structural inheritance within the North Sea seems to be related to N-S to NE-SW oriented  
871 Caledonian and Devonian lineaments (Bartholomew et al. 1993; Glennie 1998; Fossen 2010),  
872 along with the NW-SE trend of the Tornquist Zone in the south (Pegrum 1984; Bartholomew  
873 et al. 1993; Mogensen 1994). Caledonian nappes and late-Caledonian strike-slip shear zones  
874 in Norway (Andersen and Jamtveit 1990; Fossen 1992; Fossen and Dunlap 1998; Vetti and  
875 Fossen 2012; Fossen et al. 2017) and Scotland (Stewart et al. 1997, 1999) extend offshore  
876 beneath the North Sea rift (Bird et al. 2015; Reeve et al. 2015; Phillips et al. 2016; Fazlikhani  
877 et al. 2017). These were reactivated during later tectonic events (Phillips et al. 2016; Fazlikhani  
878 et al. 2017; Rotevatn et al. 2018) and exerted strong control on the Permo-Triassic structural  
879 development of the North Sea (Færseth et al. 1995; Færseth 1996; Lepercq and Gaulier 1996;  
880 Phillips et al. 2016; Fazlikhani et al. 2017).

881 The lithosphere-scale Tornquist Zone (TZ) spans Central Europe from SE to NW and extends  
882 across the Central North Sea (Figs. 2, 9), marking a major change in lithospheric and crustal  
883 thickness between Baltica to the NE and younger lithosphere to the SW (Berthelsen 1998;  
884 Pharaoh 1999; Cotte and Pedersen 2002; Babuška and Plomerová 2004; Janutyte et al. 2015;  
885 Mazur et al. 2015; Hejrani et al. 2015; Köhler et al. 2015). The TZ is associated with a series  
886 of NW-SE oriented crustal rift systems which have been periodically reactivated (Pegrum  
887 1984; Berthelsen 1998; Mazur et al. 2015; Phillips et al. 2018). The TZ accommodated major  
888 late-Cretaceous compression associated with far-field stresses imposed by the Alpine orogeny  
889 (Berthelsen 1998; Nielsen et al. 2005, 2007; Jackson et al. 2013; Phillips et al. 2018).

890 At the rift scale, lithospheric thinning from Permian-Triassic, Carboniferous-Permian and  
891 Devonian extension, strongly influenced the Late Jurassic-Early Cretaceous rift in the North  
892 Sea (Walsh et al. 2002; Whipp et al. 2014; Duffy et al. 2015; Henstra et al. 2015; Reeve et al.  
893 2015; Childs et al. 2017; Deng et al. 2017a). Thinning localised the thermal perturbation during  
894 later extension, resulting in a narrower and more localised rift focussed in the Viking Graben  
895 (Odinsen et al. 2000; Cowie et al. 2005) which, as indicated earlier, probably represented the  
896 main marine conduit between the Tethyan ocean and the proto-Norwegian Sea.

#### 897 **Segment 5 – Labrador Sea, Baffin Bay & Davis Strait**

898 The Labrador Sea and Baffin Bay form an extinct early Cenozoic spreading system, with the  
899 Ungava Fault Zone running through the Davis Strait separating the two ocean basins (Figure  
900 10). The basins formed by two-phase divergence between Greenland and North America  
901 (Chalmers and Pulvertaft 2001; Hosseinpour et al. 2013). A first phase of NE-SW extension  
902 started in the Early Cretaceous and culminated in Palaeocene continental breakup in the  
903 Labrador Sea (Srivastava and Keen 1995; Chalmers and Laursen 1995; Larsen et al. 2009;  
904 Abdelmalak et al. 2012, 2018; Pinet et al. 2013; Jones et al. 2017). Mesozoic-Early Cenozoic  
905 faulting was controlled by reactivation of pre-existing structures (Peace et al. 2018a, b). A  
906 second phase of NNE-SSW extension caused oblique spreading from the late Palaeocene (C25)

907 to late Eocene (Roest and Srivastava 1989; Abdelmalak et al. 2012), which ceased at about 36  
908 Ma (Roest and Srivastava 1989). The continental Davis Strait underwent sinistral transtension,  
909 but not breakup during the first stage (Wilson et al. 2006; Suckro et al. 2013; Peace et al.  
910 2018b), followed by sinistral transpression during the second stage (Geoffroy et al. 2001;  
911 Suckro et al. 2013).

912 The Labrador Sea and Baffin Bay formed perpendicular to many lithospheric-scale  
913 Precambrian structures and fabrics, perhaps suggesting limited basement inheritance (Figure  
914 2). However, purely based on similar trends of pre-existing structures with the Labrador Sea  
915 and Baffin Bay it is apparent that exceptions may exist. Direct evidence that any of these pre-  
916 existing structures did reactivate and guided the formation of the Labrador Sea and Baffin Bay  
917 is lacking however. For example, the Palaeoproterozoic Rinkian Orogen along the West  
918 Greenland margin of Baffin Bay (Grocott and McCaffrey 2017) and Precambrian normal faults  
919 (McWhae 1981) and strike-slip faults (van Gool et al. 2002; St-Onge et al. 2009) are sub-  
920 parallel to the Labrador Sea margin (Fig. 2). Early Cretaceous sinistral transform motion  
921 (Lundin and Doré 2018) and/or Jurassic mafic dyke swarms (Watt 1969; Larsen et al. 2009;  
922 Peace et al. 2016) could also have played a role in strain localisation in the Labrador Sea.  
923 Additionally, Neoproterozoic and Palaeoproterozoic dyke swarms in West Greenland and  
924 Baffin Island are parallel to sub-parallel to coastlines and continental margins of Baffin Bay  
925 and the Labrador Sea. In particular the Late Palaeoproterozoic-Early Mesoproterozoic Melville  
926 Bugt dyke swarm is strikingly parallel to the Baffin Bay continental margins (Buchan and Ernst  
927 2006b). Klausen and Nilsson (2018) proposed a continuation of this dyke swarm through  
928 southern Greenland. Similarly, the Palaeoproterozoic BN-1 dyke swarm in SW Greenland is  
929 parallel to Labrador Sea breakup (Ernst and Buchan 2004). The Neoproterozoic Franklin-Thule  
930 dyke swarm is sub-parallel to the Baffin Bay continental margins on the Greenland side, but  
931 largely parallel to breakup on Baffin Island (Buchan and Ernst 2006a). Direct reactivation of  
932 these dykes or lithospheric rheological anisotropies reworked during dyke emplacement may  
933 have facilitated or guided rifting and breakup in Baffin Bay and Labrador Sea.

934 The Ungava Fault Zone in the Davis Strait is a major structural discontinuity (Geoffroy et al.  
935 2001; Peace et al. 2017, 2018b; Abdelmalak et al. 2018) that may be related to Proterozoic  
936 basement structures and mantle scars (Geoffroy et al. 2001; Peace et al. 2018b; Heron et al.  
937 2019). For example, the Palaeoproterozoic Torngat-Nagssugtoquidian orogenic belt (van Gool  
938 et al. 2002; Grocott and McCaffrey 2017) could have formed a rheological barrier, preserving  
939 thicker, continental-affinity crust and lithosphere in the Davis Strait (Heron et al. 2019). The  
940 HVLC underlying Davis Strait (Funck et al. 2007, 2012) could represent remnants of pre-  
941 existing metamorphosed or metasomatised crust or mantle (Petersen and Schiffer 2016; Peace  
942 et al. 2017).

943 The Labrador Sea and Baffin Bay margins are subdivided into magma-rich and magma-poor  
944 segments by major lithospheric structures, such as the Upernavik Escarpment in Baffin Bay  
945 (Chauvet et al., 2019) and the Grenville Front or the Ketillidian Mobile Belt in the Labrador  
946 Sea (Keen et al. 2018; Gouiza and Paton 2019). The poorly defined onshore continuation of  
947 the Upernavik Escarpment trends parallel to the Precambrian crustal fabric. A potential  
948 interplay between lithospheric inheritance and magmatism in the NW Atlantic has been  
949 proposed (Foley 1989; Larsen et al. 1992; Tappe et al. 2007; Peace et al. 2017). Excessive  
950 melting along the Davis Strait may also be related to older lithospheric structures (Larsen et al.  
951 1992; Koopmann et al. 2014; Peace et al. 2017). Clarke and Beutel (this volume) link the Davis  
952 Strait Palaeogene picrites to sudden rupture of the thick Nagssugtoquidian lithosphere during  
953 breakup.

954 The conjugate margins of the Labrador Sea and Baffin Bay display significant structural and  
955 magmatic asymmetry (Chalmers and Pulvertaft 2001; Funck et al. 2012; Suckro et al. 2012;  
956 Welford and Hall 2013; Peace et al. 2016; Keen et al. 2017; Welford et al. 2018; Chauvet et al.  
957 2019). This asymmetry could indicate that the Greenland lithosphere was weaker prior to  
958 rifting compared to the conjugate Labrador margin (Welford and Hall 2013). It could also be  
959 the consequence of strain migration associated with hyperextension (Brune et al. 2014) and, in  
960 the southern Baffin Bay, to the usual development of VPMs away from previous amagmatic  
961 rift systems due to strain hardening (Guan et al. 2019). Major shear zones, faults and basement  
962 structures onshore (Figure 10) may have controlled the fracture zones, structural divisions and  
963 basin architecture offshore (Welford and Hall 2013; Jauer et al. 2014; Peace et al. 2018b).

964 Moho topography seen in northern Baffin Bay may result from reactivation of large-scale pre-  
965 existing structures (Jackson and Reid 1994). Approximately N-S faults produced during  
966 Cretaceous rifting were reactivated during the Palaeogene deformation phase, when Greenland  
967 moved north relative to North America (Gregersen et al. 2016), causing the Eureka Orogeny  
968 (Oakey and Chalmers 2012) during which Palaeozoic and Proterozoic structures were  
969 reactivated (Piepjohn et al. 2016; Schiffer and Stephenson 2017; Stephenson et al. 2017).

## 970 7 Discussion

### 971 7.1 Rifting, segmentation and breakup in the CNAR

972 Our review suggests that in the NE Atlantic (*segments 1-4*), many of the late Palaeozoic to  
973 Cretaceous rift systems follow the trend of Caledonian structures, particularly the NE-SW-  
974 oriented sub-vertical, orogen-parallel sinistral strike-slip faults formed during the Silurian-  
975 Devonian (e.g. GGF-WBF, HBF, SUF, MTFC; Figures 3,9). There are, however, some  
976 exceptions such as the noted obliquity of the N-S Triassic-Jurassic rift trend expressed in (for  
977 example) the Viking Graben and Halten Terrace. This may have reactivated duplex structures  
978 formed during the late Caledonian (Doré et al., 1997) but could simply represent a newly  
979 created trend resulting from northwards Tethyan propagation (Figs. 4 & 8). In many cases NW-  
980 SE to WNW-ESE lineaments and transfer zones (Figure 9) further partitioned the structure and  
981 evolution of the NE Atlantic margins (Doré et al. 1997, 1999; Kimbell et al. 2005b). Some of  
982 these lineaments had pre-Caledonian history while others formed during the development of  
983 post-Caledonian basins. Of significance is the relation between continental transfer zones and  
984 oceanic fracture zones. In some cases, continental lineaments pass laterally into oceanic  
985 transfer faults (Figure 9). Many other margin-perpendicular lineaments are expressed by offsets  
986 in sedimentary basin architecture, but direct evidence of strike-slip motion is often lacking. A  
987 connection between continental transfer faults and oceanic fracture zones in the Vøring margin  
988 (Tsikalas et al. 2002; Mjelde et al. 2005) is questioned in more recent studies of modern  
989 magnetic data (Olesen et al. 2007).

990 A key observation in the northernmost NE Atlantic (essentially the Vøring margin) is the  
991 obliquity of its breakup axis with earlier rift basins and the Caledonian (surface) trend in the  
992 northern part (*segment 1*), compared to other areas where Caledonian structures appear to be  
993 more parallel to breakup. The late-Caledonian shear zones are strikingly parallel to the line of  
994 breakup (Figure 4 & 8) suggesting a causal link. As we explain below, a primary reason for  
995 this obliquity may lie in the existence of lithospheric layers in which differently oriented pre-  
996 existing fabrics rejuvenate at different times in response to changes in the regional stress field.  
997 This may be additionally linked to the magmatic development, as the extent of the Cenozoic  
998 pre- and syn-rift magmatism of the NAIP is also generally parallel to the final line of breakup,  
999 which may have been “perforated” by magmatic intrusions (Gernigon et al., this volume),  
1000 and/or strike-slip deformation (Lundin & Doré, 2018).

1001 Numerical modelling suggests that the dominating weaknesses may lie within the mantle  
1002 lithosphere, rather than the crust (e.g. Heron et al. 2016) (see also section 2.2). We hypothesise  
1003 that at the onset of rifting, the crustal and mantle lithospheric fabrics were oblique to one  
1004 another. There existed an older, orogen-parallel, brittle crustal fabric and an oblique, younger,  
1005 upper mantle shear fabric. Rifting in the North Atlantic experienced phases of varying stress  
1006 orientations that rejuvenated either the less dominant, shallow crustal fabric or the dominant  
1007 mantle fabric.

1008 We propose a scenario for the NE Atlantic rifting and breakup as follows:

- 1009 • The Caledonides formed as a notably linear orogen in the NE Atlantic resulting in a  
1010 predominantly orogen-parallel fabric of crustal blocks, terranes, nappes and thrust  
1011 faults (Figure 4, 8). At this time, lithospheric mantle fabric was parallel to the brittle  
1012 crustal features. During late Caledonian sinistral transpression (Soper et al. 1992) the  
1013 pre-existing discrete, brittle crustal fabric was reactivated as strike-slip faults,  
1014 preserving their original orogen-parallel orientation. In contrast, the pervasive ductile  
1015 lower crustal-upper mantle fabric was reworked and reoriented to ENE-WSW (rotated  
1016 20-30° clockwise about the orogenic axis).
- 1017 • Devonian orogenic collapse was driven by body forces created by the high Caledonian  
1018 topography mainly perpendicular to the axis of the mountain range (England and  
1019 Houseman 1986; Molnar et al. 1993; Schiffer and Nielsen 2016), however, with local  
1020 structural and kinematic complexities (Seranne 1992; Braathen et al. 2000; Osmundsen  
1021 et al. 2003). The Devonian collapse was partly driven by major strike-slip shearing  
1022 along reactivating Caledonian fault and shear zones (MTFC, HFZ, GGF, WBF, HBF)  
1023 (Osmundsen and Andersen 1994; Dewey and Strachan 2003; Fossen 2010), during  
1024 which the Devonian basins of southern Norway, East Greenland and Britain were  
1025 formed (Seranne and Seguret 1987; Seguret et al. 1989; Fossen 1992) and lower crustal  
1026 and high pressure metamorphic rocks were exhumed, as prominently displayed in the  
1027 Western Gneiss Region in southern Norway (Andersen et al. 1991; Brueckner and van  
1028 Roermund 2004; Hacker et al. 2010) and East Greenland (Hartz et al. 2001; Gilotti et  
1029 al. 2014).
- 1030 • In late Palaeozoic to Triassic(?) times, rifting still essentially reflected orogenic  
1031 collapse, and NE-SW-oriented shallow, brittle crustal structures were reactivated that  
1032 were favourably aligned with the dominant stress field.
- 1033 • Beginning in the Triassic and particularly during the Jurassic, complex fragmentation  
1034 of Pangea took place, with rifting including the dominant N-S trend of the Viking  
1035 Graben and Halten Terrace. This extensional trend probably represents a linkage  
1036 between Tethys and proto-Norwegian Sea. This period represents a long time interval  
1037 (circa 100 million years) during which the dominant E-W stress field was highly  
1038 oblique to the lithospheric-scale Caledonian orogenic structures, preventing full  
1039 lithospheric rupture and breakup. This was probably a significant contributing factor in  
1040 the anomalously long period between initial rifting and breakup in the North Atlantic  
1041 (c. 350 million years).
- 1042 • A major change in extension vector from E-W to NW-SE in the Early Cretaceous (Doré  
1043 et al. 1999) resulted in favourable alignment with the pervasive mantle-lithospheric  
1044 fabric and late-Caledonian shear zones. Major basins such as the Rockall, Faroe-  
1045 Shetland, Møre, Vøring and Thetis basins, oblique to the earlier Jurassic N-S trend, had  
1046 their principal expression at this time. These crust beneath the basins was  
1047 hyperextended (Lundin and Doré 2011) but never achieved full oceanic status.

- 1048 • Apparent cessation of extensional stress in the mid-Cretaceous (although with minor  
1049 extension in some sub-basins) resulted in a significant time gap (60-70 million years)  
1050 before final early Cenozoic breakup. This hiatus further contributed to the anomalously  
1051 long time between initial rifting and breakup.
- 1052 • Rupturing to form the North Atlantic was highly asymmetric in the south (*segment 2*)  
1053 and oblique to the preceding basin trend in the north (*segment 1*) (Fig. 8). We suggest  
1054 that the late Caledonian shear trend, deeply ingrained in the mantle, was now  
1055 reactivated, but did not follow the axes of the previously formed basins that followed  
1056 the shallower crustal trends and where cooling and strengthening may have occurred  
1057 (e.g. Naliboff and Buitter 2015). The obliquity in *segment 1*, where the Thetis and  
1058 Vøring basins may represent a single basin that has been diagonally bisected by breakup  
1059 (Fig. 8), is an interesting issue; it is difficult to see why basin-parallel breakup akin to  
1060 that of the Møre Basin did not occur. Cut-across of the basin by pre-breakup strike-slip,  
1061 either newly formed or reactivating elements of the late Caledonian shear fabric, is one  
1062 potential explanation for this geometry (Lundin & Doré, 2018; see also Section 7.2).  
1063 Additionally, the oblique geometry of this segment may have been also controlled by  
1064 pre-breakup magmatic intrusions.

1065 One model for rift relocation suggests strengthening of the lithosphere by cooling after  
1066 cessation of initial rifting (Van Wijk and Cloetingh 2002; Naliboff and Buitter 2015). This  
1067 model might apply to the abandonment of the Møre and Rockall-Hatton shelves (Gernigon et  
1068 al. this volume; Kimbell et al. 2017; Guan et al. 2019). However, this would not explain why  
1069 the initial rifting stopped in the first place. Another mechanism is strain hardening in the  
1070 vicinity of rift basins that may lead to development of a new rift offset from the early one  
1071 (Kusznir and Park 1987; Sonder and England 1989; Newman and White 1997; Yamasaki and  
1072 Stephenson 2009).

## 1073 **7.2 Magmatism, rifting and breakup**

1074 In the North Atlantic, variations in the magmatic budget during the onset of breakup were often  
1075 controlled by complex interactions between the pre-existing lithosphere state (including  
1076 discrete pre-existing structures, lithospheric thickness variations, thermal state and  
1077 composition) and the timing and degree of decompression melting (Gernigon et al. this volume;  
1078 Gouiza and Paton 2019).

1079 As discussed earlier, the amount of pre- and syn-breakup decompression melting beneath  
1080 continental margins is dependent on extension rate and pre-existing lithospheric rheology and  
1081 composition (Buck 1991; Armitage et al. 2010; Huisman and Beaumont 2011; Petersen and  
1082 Schiffer 2016), as well as on the geotherm (White and McKenzie 1989; Hill 1991). Petersen &  
1083 Schiffer, (2016) suggest that a hot, weak crust over a relatively strong lithospheric mantle can  
1084 produce wide, asymmetric, magma-rich margins. In contrast, a cold, strong crustal layer above  
1085 a weaker mantle lithosphere may facilitate, magma-poor margins with abrupt necking zones  
1086 (Petersen & Schiffer, 2016). As indicated in section 7.3, the abrupt margins observed in the NE  
1087 Atlantic between Greenland and Norway may also related to exploitation of deep-seated and  
1088 lithospheric-scale shear faults (Lundin & Doré, 2018).

1089 Literature on the origin of magma-rich margins in the North Atlantic is dominated by the plume  
1090 concept; in this hypothesis, the impingement of the Icelandic plume on the base of the  
1091 lithosphere has variously been implicated in raised mantle temperatures, elevated margins,  
1092 voluminous magmatism and break-up itself. A full description of this model is beyond the  
1093 scope of this paper; it has been well-described in (for example) (White and McKenzie 1989;  
1094 White 1992; Skogseid et al. 1992, 2000) while problems with the hypothesis have been  
1095 highlighted by (for example) (Foulger 2002, 2010; Lundin and Doré 2005). Other ideas exist

1096 to explain the anomalous magmatism. These include a relationship to extension rate during  
1097 breakup (Lundin et al. 2014) and the generation of small-scale edge-driven convection at abrupt  
1098 steps in the lithosphere (Mutter et al. 1988; van Wijk et al. 2001).

1099 Independent of the origin of anomalous magmatism in the North Atlantic, magmatic processes  
1100 guided by pre-existing faults and shear zones may have influenced and governed final plate  
1101 separation. Lithosphere softening associated with melts and lithospheric hardening associated  
1102 with emplaced and cooled mafic rocks can occur at different depths and can accommodate and  
1103 localise strain. Magma-supported lithospheric breakup may occur at far lower differential stress  
1104 levels than those needed for lithosphere breakup via brittle faulting (Buck and Karner 2004).

1105 Most of the magmas feeding plateau basalts and SDRs in the North Atlantic are associated with  
1106 large Palaeocene to Eocene igneous centres (Callot et al. 2001; Callot and Geoffroy 2004;  
1107 Geoffroy et al. 2007). These may have been related to small-scale convection cells that initiated  
1108 at the base of the lithosphere and grew upward by thermal erosion, feeding these localised  
1109 igneous centres and creating “soft spots” in the lithosphere (Geoffroy et al. 2007; Gac and  
1110 Geoffroy 2009). These small-scale convection cells appear to correlate with areas of high  
1111 mantle heat flow suggesting a relationship with lithospheric thickness variations (Geoffroy et  
1112 al., 2007). The pattern and development of such instabilities, marking the potential locus of the  
1113 future breakup axis, could thus reflect the pre-existing thermal, compositional and structural  
1114 configuration of the lithosphere.

1115 Cenozoic breakup of the NE-Atlantic did not occur within previously (Late Jurassic-Early  
1116 Cretaceous) tectonically thinned lithosphere, such as the Hatton-Rockall shelf. These areas  
1117 thermally re-equilibrated and strengthened after early rifting events (Guan et al., 2019;  
1118 Gernigon et al., 2019). On the Hatton-Rockall shelf, the distance between the Palaeogene  
1119 igneous centres is approximately 100 km – about twice as large as along the continental  
1120 margins of East Greenland and Hatton-Rockall (Geoffroy et al. 2007; Horni et al. 2017).

1121 In the British Tertiary Igneous Province an abnormally dense spacing of igneous centres is  
1122 observed (Dobre and Geoffroy 2003). This dense pattern may indicate that the pattern of  
1123 Palaeogene small-scale convection or loci of mantle diapirism interacted with  
1124 compartmentalised lithospheric blocks and terranes originating with Caledonian and post-  
1125 Caledonian shear motions. The developing igneous centres then exploited lithospheric  
1126 structural and compositional heterogeneities.

1127 Edge convection along the eastern border of the Greenland craton (King and Anderson 1998)  
1128 may have increased magmatic production rates and reduced the spacing between small-scale  
1129 convection cells, forming igneous centres and weakening and thinning the lithosphere. This  
1130 model could be one explanation for the development of the breakup axis oblique to most failed  
1131 rift systems in the NE Atlantic (Gernigon et al., 2019), along with an oblique inherited  
1132 lithospheric mantle fabric and lithospheric perforation by pre-syn-breakup strike-slip motion  
1133 (see next section), or a combination of these end-member mechanisms (Fig. 12).

### 1134 **7.3 Role of strike-slip faults**

1135 Lundin & Doré (2018) recently proposed that the instigation of oceanic spreading in the North  
1136 Atlantic-Arctic region was facilitated by the development of transform faults. Such faults are  
1137 strike-slip faults that segment plates or form plate boundaries, juxtaposing oceanic and  
1138 continental crust. According to Lundin and Doré (2018), some of these faults were inherited  
1139 structures while others formed first during the breakup process. The basis of this model is that  
1140 a) pre-existing lines of lithospheric-scale strike-slip faults are zones of weakness, which can be  
1141 separated by orthogonal forces without initial stretching, and b), that oblique slip more easily  
1142 facilitates breakup (Brune et al. 2012a). Thus, such zones should fail first (Brune et al. 2018).

1143 A clear example of a margin influenced by transform faulting is found on the SW Barents Sea  
1144 margin, which opened along the De Geer transform fault. This fault was probably instigated  
1145 during late-stage sinistral movements along the Caledonian Orogen in the Late Devonian  
1146 (Harland 1969), but its role in oceanic development did not start until the Eocene opening of  
1147 the NE Atlantic, when it enabled Greenland to be translated dextrally past Eurasia. In the  
1148 earliest Oligocene, the De Geer transform fault opened obliquely as a zone of deformation that  
1149 developed into an oblique transform margin, along which the Knipovich Ridge ultimately  
1150 formed between Eurasia and Greenland (Faleide et al. 2008). The De Geer transform fault and  
1151 rigid crustal/lithospheric blocks in the SW Barents Sea may have acted as a barrier to the  
1152 straight propagation of the North Atlantic. A further example is found in the southernmost  
1153 CNAR, where the Aptian opening of the Bay of Biscay utilised the North Pyrenean Fault, an  
1154 established Variscan transform fault (Vissers et al. 2016).

1155 Margins influenced by strike-slip faulting may be characterised by the reduced role of  
1156 extension prior to breakup as well as the potential for the breakup axis to be oblique to earlier  
1157 rifting. The NE Atlantic, as shown earlier, is an example where older (Mesozoic) rift systems  
1158 are cut obliquely by the axis of Early Eocene breakup, resulting in highly asymmetric conjugate  
1159 margins (Lundin et al. 2013).

1160 Based on these observations, Lundin & Doré (2018) suggested that the old rift systems were  
1161 bisected by transform faulting, which facilitated orthogonal opening in the Early Eocene.  
1162 Kinematic evidence along the line of breakup provides some support for this hypothesis.  
1163 Indications of dextral motion are provided by the Hel Graben in the northern Vøring Basin.  
1164 The Hel Graben would be located at a right-stepping releasing bend in the proposed pre-NE  
1165 Atlantic shear, offset by the Surt Lineament (Blystad 1995; Brekke 2000). Within the graben  
1166 are a series of E-W trending normal faults (Ren et al. 2003), consistent with cross-basin fault  
1167 systems in a dextral pull-apart basin (Dooley and McClay 1997).

1168 The strike slip deformation and associated breakup may have acted rapidly (on geological  
1169 scale) along long segments of the North Atlantic rift. Such a model is consistent with the rapid  
1170 lithospheric relaxation observed in the shift of depocentres in the Danish Basin (Nielsen et al.  
1171 2007). Other authors prefer a rift propagation model characterised by highly diachronous and  
1172 fragmented breakup (Gernigon et al. this volume). In such a model, the North Atlantic rift  
1173 would have propagated along the weakest path for the background stresses and this may have  
1174 been governed by basement inheritance or pre-syn-rift magmatism that has perforated the  
1175 lithosphere. These two models may not necessarily be incompatible: A rift propagation model  
1176 could have had a strong component of strike-slip deformation, or strike-slip may have acted  
1177 only on certain segments rather than the whole length of the NE Atlantic margins.

1178 Whether or not one accepts the evidence for strike-slip motion immediately preceding breakup  
1179 in the NE Atlantic, a further key observation is that of the close correlation of the breakup axis  
1180 and NE-SW-trending late Caledonian shears, such as the MTFC and GGF. This suggests that  
1181 a more ancient and deep-seated strike-slip trend was implicated in the eventual line of opening.

1182 Both, the Labrador Sea and Baffin Bay appear to cut through cratonic elements and across  
1183 Proterozoic orogenic belts (Section 1.3) (St-Onge et al. 2009). As it is unusual that such  
1184 features would form in a mid-cratonic setting, the possibility exists that they were facilitated  
1185 by transform faults. Indirect support for such a fault in the proto-Labrador Sea is provided from  
1186 the c. 1000 km long fault system in Hudson Strait and Foxe Channel, the projected continuation  
1187 of the Canadian Labrador Sea margin. The fault system has been interpreted as an abandoned  
1188 rift tip to the Labrador Sea rift (Pinet et al. 2013), but vertical offsets are small compared with  
1189 the length of the fault system, and terminate northwards in a horse-tail geometry.

1190 The fault system is marked by shallow rhomboid basins, suggesting sinistral movement. It may,  
1191 therefore, have originated as a sinistral transform that experienced minor extensional overprint  
1192 during early opening of the Labrador Sea. When the Ungava Transform linked the Labrador  
1193 Sea and Baffin Bay in the Palaeogene (Funck et al. 2012), the Hudson Strait-Foxe Basin fault  
1194 system was abandoned. However, the Labrador Sea transform fault might have had a much  
1195 older origin. Whereas there is no evidence of a suture beneath the Labrador Sea, there is  
1196 abundant evidence on the Labrador margin of sinistral shear sub-parallel to the ocean, which  
1197 van Gool et al. (2002) and St-Onge et al. (2009) relate to the Palaeoproterozoic (c. 1.8 Ga)  
1198 indentation of the North Atlantic Craton into northern Greenland. Thus, it is possible that these  
1199 older shears were exploited during development of the Labrador Sea in a similar way as  
1200 suggested for the NE Atlantic.

#### 1201 **7.4 Microcontinent formation**

1202 A complication in North Atlantic breakup was formation of the JMMC (Gaina et al. 2009;  
1203 Blischke et al. 2011, 2017; Schiffer et al. 2015b, 2018) and other smaller continental fragments  
1204 (Døssing et al. 2008; Péron-Pinvidic and Manatschal 2010; Nemčok et al. 2016). The central  
1205 segment of the NE Atlantic, between the GIFR and the Jan Mayen Fracture zone (Figure 1,2),  
1206 underwent breakup and initially fast spreading along the Aegir Ridge in the early Eocene (~55  
1207 Ma) that then slowed down in the mid-Eocene (~47 Ma) (Gernigon et al. this volume, 2015).  
1208 In the mid-Cenozoic, the JMMC began to separate from East Greenland's Liverpool Land  
1209 margin along the new Kolbeinsey Ridge, and the Aegir Ridge became extinct, between ~28  
1210 Ma and ~21 Ma (Nemčok et al. 2016; Lundin and Doré 2018), when the JMMC separated from  
1211 the East Greenland margin. The two mid-oceanic ridges were, therefore, simultaneously active  
1212 for possibly up to 10 Ma, but probably longer (Doré et al. 2008; Gernigon et al. 2012, 2015;  
1213 Peron-Pinvidic et al. 2012; Ellis and Stoker 2014).

1214 The JMMC consists of Cenozoic igneous rocks and older thinned and intruded continental crust  
1215 (Kuvaas and Kodaira 1997; Breivik et al. 2012; Blischke et al. 2017). Breakup on the eastern  
1216 side of the JMMC was magmatic, forming subaerial seaward-dipping reflectors (SDRs)  
1217 (Planke and Alvestad 1999) underlain by HVLCBs (Breivik et al. 2012). SDRs are not  
1218 observed along the western margin of the JMMC (Kodaira et al. 1998), nor are they reported  
1219 from the conjugate Liverpool Land margin (Horni et al. 2017). Wide-angle seismic data suggest  
1220 that the northern part of the JMMC is underlain by "Icelandic-type" crust (Kandilarov et al.  
1221 2015). The central Jan Mayen Ridge comprises ~15 km thick continental crust (Kodaira et al.  
1222 1998; Breivik et al. 2012) with no evidence of HVLC (Kodaira et al. 1998; Mjelde et al. 2007a),  
1223 but HVLC is observed in the transition zone to the Iceland plateau (Gernigon et al. this volume;  
1224 Brandsdóttir et al. 2015).

1225 The mechanisms responsible for breakoff of the JMMC are poorly understood. Plume impact  
1226 has been suggested (Müller et al. 2001; Mittelstaedt et al. 2008; Howell et al. 2014). In such a  
1227 scenario a plume heats and weakens the lithosphere to cause renewed continental breakup and  
1228 a ridge jump. However, breakup-related volcanism, such as SDRs, are absent between  
1229 Greenland and the JMMC (Kodaira et al. 1998; Horni et al. 2017), at odds with expectations  
1230 of this model.

1231 Also mechanical explanations for the formation of microcontinents and rifted continental  
1232 blocks via detachment along pre-existing lithospheric weaknesses have been suggested  
1233 (Nemčok et al. 2016; Molnar et al. 2018; Schiffer et al. 2018). Recent analogue modelling  
1234 illustrates how microplates may be formed by propagating rifts that form new oceans.  
1235 Microcontinents may separate from the continental margin with rotational motion during the  
1236 latest breakup stages, such that location and shape of fragmentation is controlled by  
1237 lithospheric weaknesses (Molnar et al. 2018). Analogue modelling produces rotating

1238 microplates “trapped” between overlapping spreading centres (Katz et al. 2005). Geoffroy et  
1239 al. (2015) suggested microcontinent formation through large-scale, symmetric and continental-  
1240 vergent detachment faulting – the so-called “C-Block”. Other models involve the separation of  
1241 continental lithosphere along overlapping spreading centres (Auzende et al. 1980; Ellis and  
1242 Stoker 2014). Foulger et al. (this volume) suggest that extension in the southern JMMC was  
1243 initially diffuse, and westward migration of the axes of extension on the GIFR induced  
1244 extension in the JMMC, focusing on its most westerly axis to form the proto-Kolbeinsey Ridge.  
1245 This resulted in breakoff of the JMMC from Greenland.

1246 Several authors have linked separation of the JMMC to mid-Eocene plate-kinematic  
1247 reorganisations in the North Atlantic (Gaina et al. 2009). For instance, Schiffer et al. (2018)  
1248 proposed a model linking the formation of the JMMC to global plate tectonic reconfigurations  
1249 to rejuvenation of old and pre-existing lower-crustal/upper mantle orogenic fabric (Schiffer et  
1250 al. 2015b; Petersen and Schiffer 2016). In this model, the apparent rotation of North Atlantic  
1251 spreading from NW-SE to W-E put the NW-SE oriented accommodation zone between the  
1252 Aegir and Reykjanes Ridges – the proto-GIFR – under transpression. This “locked” the right-  
1253 lateral deformation along the proto-GIFR and forced extension to divert to a more favourable  
1254 position/path – possibly pre-existing Caledonian weak zones along the East Greenland margin.

1255

## 1256 **7.5 The Wilson Cycle revisited**

1257 The breakup of Pangaea to form the NE Atlantic was a protracted and piecemeal process with  
1258 many local complexities (Gernigon et al. this volume; Peace et al. this volume; Roberts et al.  
1259 1999; Ady and Whittaker 2018). The original Wilson cycle theory does not conclusively  
1260 explain how and why the opening of the North Atlantic occurred and why its manifestation  
1261 varies across the CNAR. During the past 50 years, more data have been acquired, and new  
1262 theories proposed, but the mechanisms driving the Wilson Cycle are still a matter of debate.  
1263 The simplest explanation for breakup along former orogens is that mountain ranges are usually  
1264 the weakest zones in supercontinents and hence regions where deformation is expected to  
1265 concentrate.

1266 We show that most rifts are associated with former collision zones, implying that structural  
1267 inhomogeneity may be preserved long term. However, the North Atlantic did not necessarily  
1268 focus exactly along suture zones, but in some places broke through regions of apparently  
1269 previously undisturbed cratonic lithosphere such as SE Greenland (Buitter and Torsvik 2014).  
1270 The Labrador Sea and Baffin Bay broke through pre-existing cratons (the Archean North  
1271 Atlantic and Rae cratons) and almost orthogonally across Precambrian orogenic belts (the  
1272 Meosoproterozoic Grenville and Makkovik-Ketilidian orogens, and the Paleoproterozoic  
1273 Nagssugtoqidian orogen) (Buchan et al. 2000; St-Onge et al. 2009; Peace et al. 2017).

1274 These events may have been enabled by the development of transform faults that can also  
1275 nucleate at a distance from old suture zones (Lundin & Doré, 2018), or by the regional rift,  
1276 magmatic and thermal history that modified lithospheric strength distribution and guided  
1277 lithospheric breakup away from suture zones – for example, the pronounced N-S rift fabric that  
1278 developed in the Jurassic, oblique to the main Caledonian trend. Alternatively, they may have  
1279 occurred simply for kinematic compatibility reasons, for example if the pathway through a  
1280 craton was the shortest.

1281 The Wilson Cycle is one of the most crucial and basic concepts regarding inheritance in a plate  
1282 tectonic framework. However, the Wilson Cycle concept only addresses large-scale, first-order  
1283 events and is insufficient to explain all the complexities of developing oceans and continental  
1284 margins. (Super)continents do not simply re-open along the surface traces of suture zones.

1285 Structures and fabric are 3D entities and dominant weaknesses are not at the surface.  
1286 Inheritance at all scales is important in explaining rejuvenation at regional and global scales.  
1287 Structures can be preserved over billions of years and may still impose an inheritance control.  
1288 Intraplate deformation and “non-rigid” plates and magmatism must also be incorporated in  
1289 inheritance models and plate tectonic theory.

1290

## 1291 **8 Conclusions**

1292

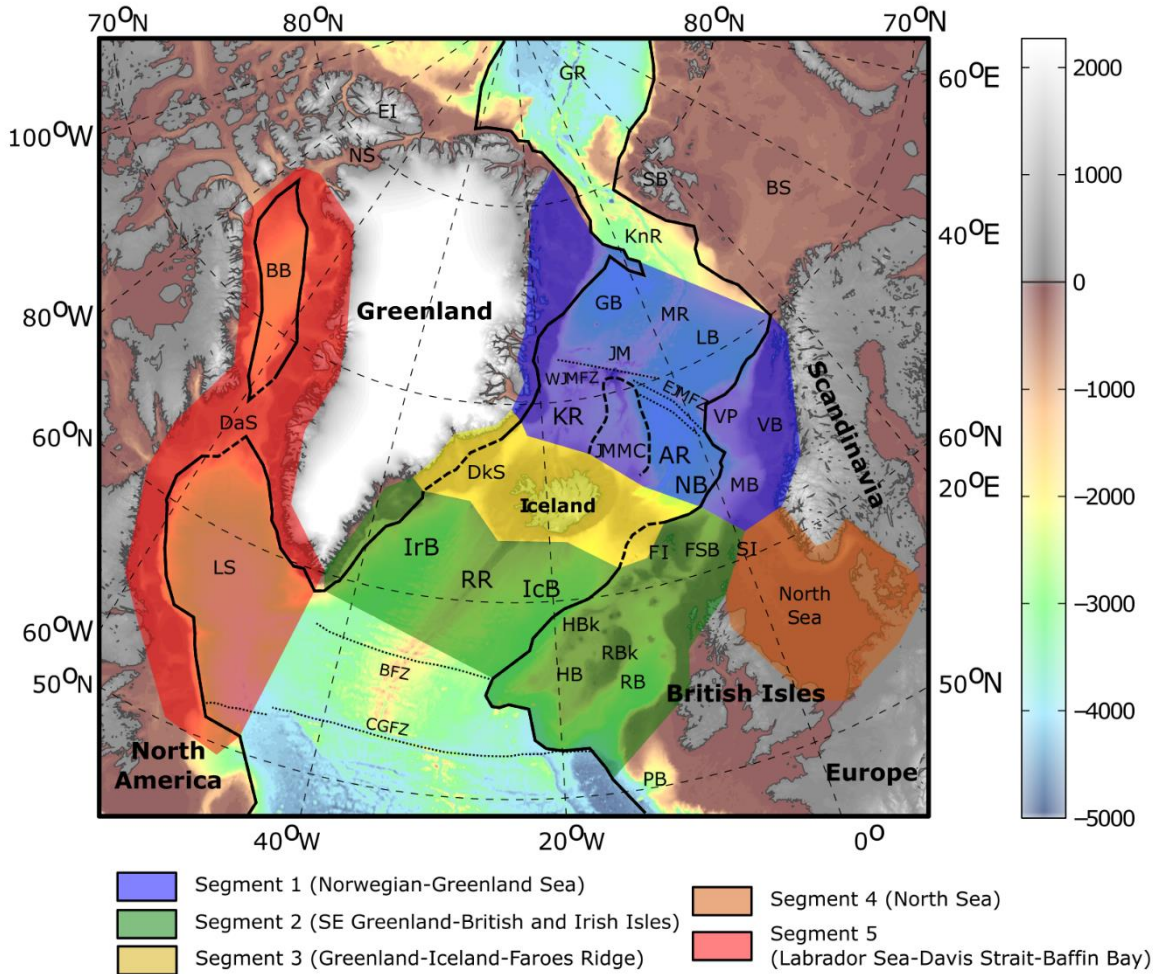
- 1293 1. The CNAR is the type example of the Wilson Cycle concept and, in general, reopened  
1294 elements of the Caledonian fold belt. However, evidence from the CNAR and  
1295 elsewhere clearly demonstrates that the Wilson Cycle only partially accounts for the  
1296 observations. Where breakup does occur along an older orogenic belt, it does not simply  
1297 re-open the older suture, and intact cratons may fragment.
- 1298 2. Rift evolution and opening of the CNAR is to varying degrees linked to structural  
1299 inheritance at lithospheric, continental, basin, fault and micro-scales. However, other  
1300 factors were influential, such as changing stress directions imposed by plate boundary  
1301 effects and supercontinent (Pangaea) breakup and magmatism.
- 1302 3. Caledonian rejuvenation of anisotropies imparted at different depths (crust vs. mantle)  
1303 and different stages of the orogenic evolution (collision vs. late Caledonian  
1304 transpression-transtension) played the major role in regional rift evolution and breakup  
1305 of the NE Atlantic. Precambrian structures (e.g., the Nagssugtoquidian suture, Bothnia-  
1306 Senja Fault Zone) may have also controlled the margin segmentation of the NE Atlantic  
1307 on the largest scale.
- 1308 4. Many, but not all, of the rift systems that preceded the CNAR followed major orogenic  
1309 trends expressed at the surface. However, final breakup seems to have followed the late  
1310 Caledonian strike-slip shear fabric exemplified by the MTFC. In the NE Atlantic  
1311 (*Segment 1*), breakup cut obliquely across the preceding rifts. We suggest that breakup  
1312 occurred when stress directions became favourable to exploit a deeper and more  
1313 pervasive mantle fabric, probably related to lithospheric-scale shear zones that  
1314 developed in the late Caledonian. The radical cut-across of a Cretaceous basin by the  
1315 breakup line in Segment 1, defining the Thetis and Vøring margins, may represent  
1316 reactivation of this trend by pre-breakup strike-slip and/or was guided by pre-breakup  
1317 magmatic intrusions weakening the crust.
- 1318 5. Breakup between SE Greenland and the Rockall-Hatton margin does not appear to fit  
1319 the classic Wilson-Cycle model. This may have been related to the pre-breakup rift  
1320 history of the Hatton-Rockall shelf which thinned crust but created an overall stronger  
1321 lithospheric column. Breakup occurred where the crust was thicker above weaker  
1322 lithosphere, and may have been assisted by strike-slip/transform motion. This region  
1323 then formed the southern CNAR link, which was offset from the Northern CNAR  
1324 breakup axis between the Central Atlantic and the Aegir Ridge
- 1325 6. The extremely long interval between initial post-orogenic rifting and final plate  
1326 separation – some 350 million years – is highly anomalous and an order of magnitude  
1327 greater than that of most other oceans – for example the Central and South Atlantic. It  
1328 was probably a result of radical changes in the regional stress field – for example in the  
1329 Triassic-Jurassic interval, and significant hiatuses in extension (for example in the mid-  
1330 Late Cretaceous), which allowed the pre-existing rifts to cool and strengthen.

- 1331 7. The “magma-poor” nature of the western margin of the JMMC and adjacent ocean  
1332 favours mechanical models for microcontinent formation, rather than weakening by a  
1333 thermal anomaly.
- 1334 8. High velocity lower crustal bodies beneath the basins flanking the North Atlantic have  
1335 been variously attributed to syn-rift serpentinitised mantle, syn-rift mafic and ultramafic  
1336 rocks and pre-existing metamorphic and metasomatised rocks such as granulites and  
1337 eclogites. Some of these interpretations and the question of whether these HVLCBs  
1338 have a pre-or syn-rift origin remain controversial. Some HVLCBs formed before the  
1339 onset of rifting and breakup, forming rheological inhomogeneities in the lithosphere  
1340 that can control the location, deformation and type of breakup and continental margins.
- 1341 9. The temperature- and composition-dependent strength profile of a lithospheric column,  
1342 which controls crust vs. mantle thinning (among other properties), but also the  
1343 extension rate, structural and rift obliquity determine whether a wide, asymmetric,  
1344 diffuse rift zone develops or whether sharply localised rifts with narrow necking zones  
1345 develop.
- 1346 10. The GIFR may contain a significant component of continental lithosphere. It may owe  
1347 its existence to diffuse extension of a zone of Precambrian terranes and Caledonian  
1348 fossil structures running parallel to the direction of extension between central East  
1349 Greenland and northern Scotland.
- 1350 11. At the basin-scale, the CNAR displays a wide variety of structural inheritance effects  
1351 including brittle reactivation of basement faults and fabrics creating syn-rift faults that  
1352 are complex in terms of kinematics or growth history. Oblique extension on pre-existing  
1353 orogenic, post-orogenic or early rift structures may partition deformation into strike-  
1354 slip and dip-slip components at different scales. Complex fault displacement patterns  
1355 are produced by multiphase rifting where later extension collinear with, or rotated  
1356 relative, to earlier phases by local stresses. Basin inversion structures by definition are  
1357 inherited features where intense localisation of contractional deformation is guided by  
1358 pre-existing extensional features. Igneous activity and other mobilised materials such  
1359 as salt interact with local stress fields to partition deformation within basins both  
1360 spatially and temporally.

1361  
1362

### 1363 **Acknowledgements**

1364 Christian Schiffer’s Carlsberg Foundation postdoctoral fellowship was held at Durham  
1365 University, where the series of North Atlantic workshops that led to this special issue were  
1366 planned and held. Thomas Phillip’s postdoctoral fellowship at Durham University is funded by  
1367 the Leverhulme Foundation. M. Stoker gratefully acknowledges the award of Visiting Research  
1368 Fellow at the Australian School of Petroleum. The authors thank all participants of the North  
1369 Atlantic workshop series. Four anonymous reviewers and the handling editor are thanked for  
1370 constructive and useful comments, and John Kipps (Equinor) for help with some of the figures.

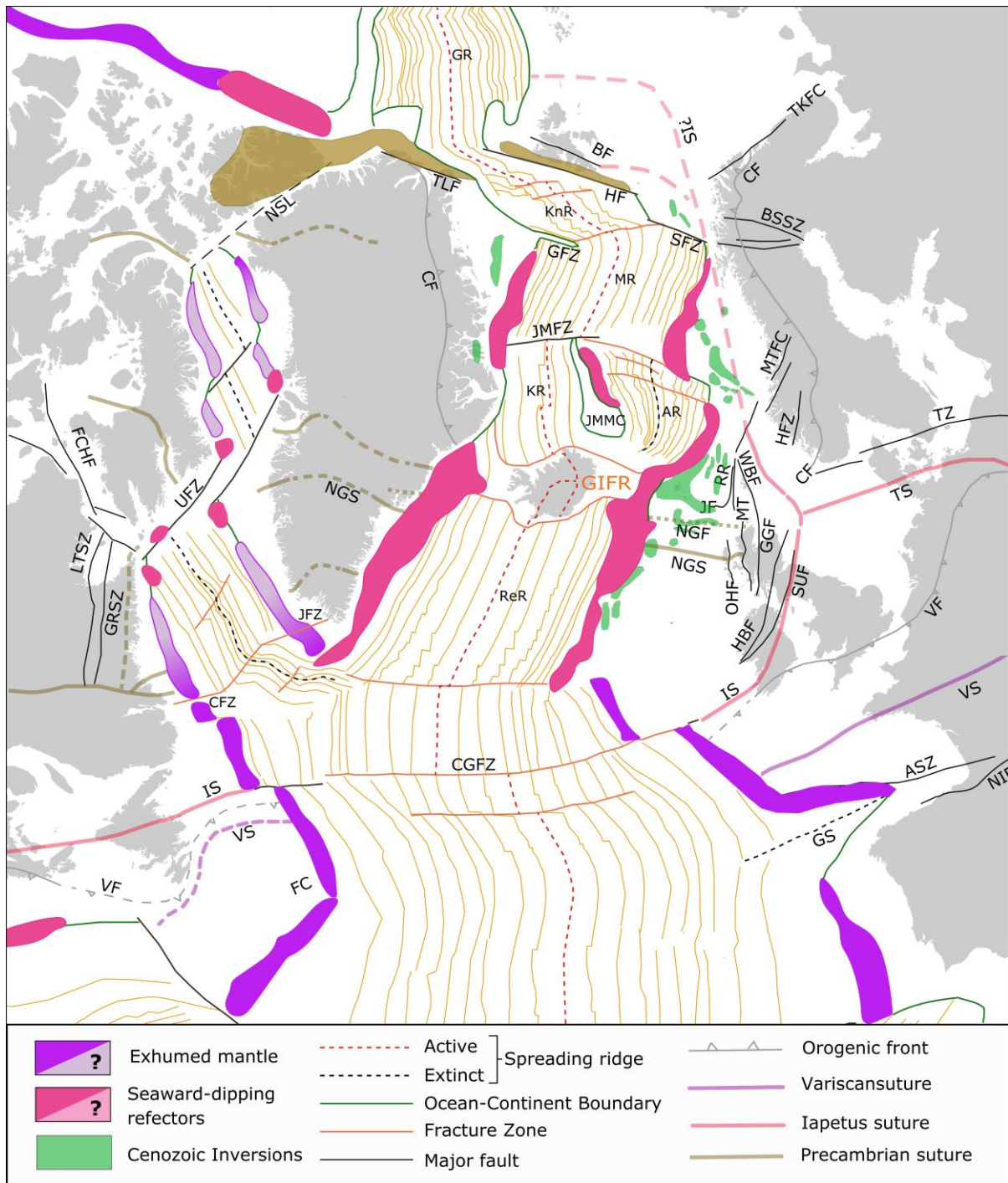


1372

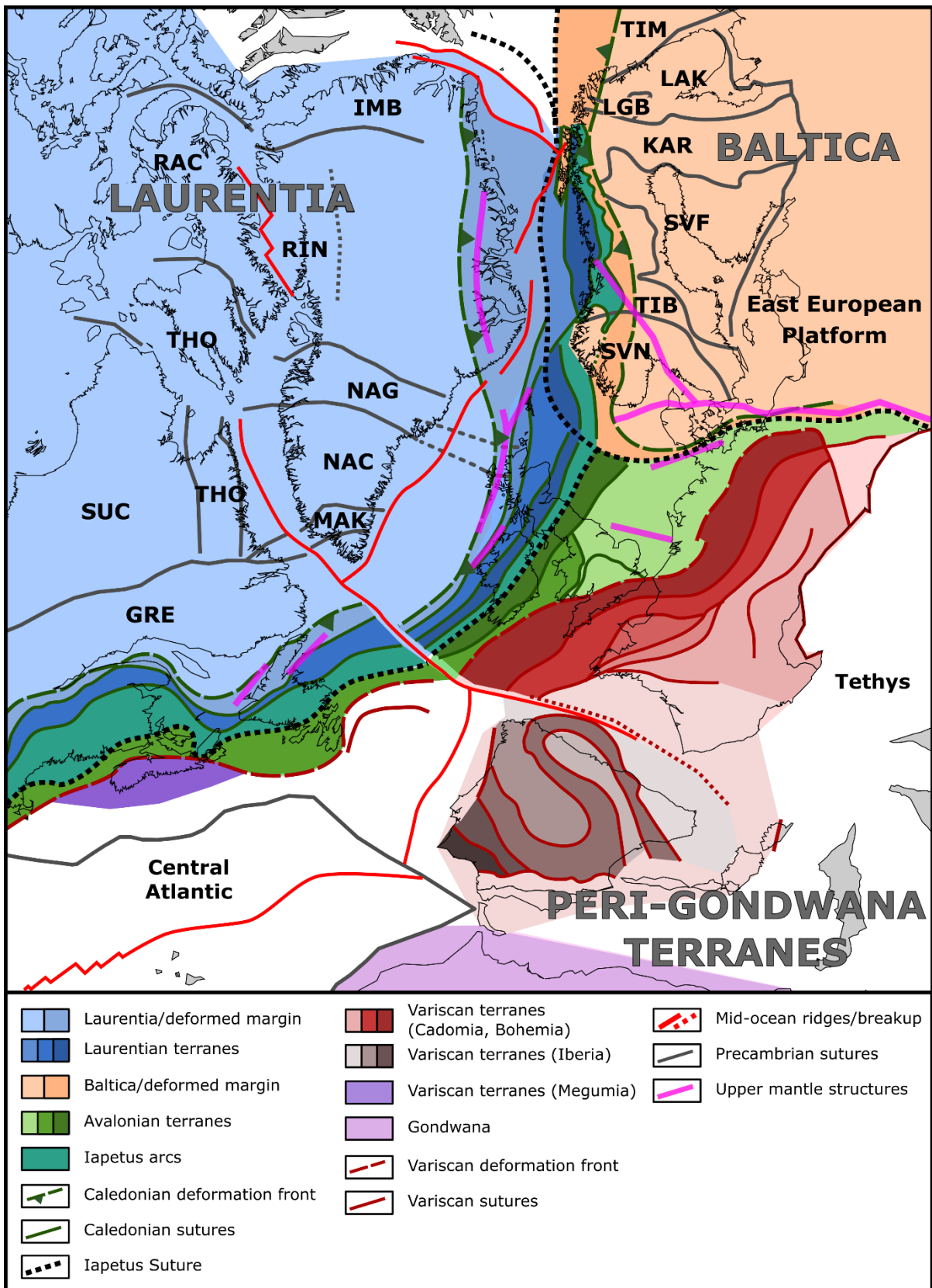
1373 **Figure 1: Physiographic map of the present-day Circum-North Atlantic region showing**  
 1374 **geographic names and places, as well as the five segments discussed in the paper.**  
 1375 **Abbreviations: AR = Aegir Ridge, BB = Baffin Bay, BFZ = Night Fracture Zone, BS =**  
 1376 **Barents Sea, CGFZ = Charlie Gibbs Fracture Zone, DaS = Davis Strait, DkS = Denmark**  
 1377 **Strait, EI = Ellesmere Island, EJMfZ = East Jan Mayen Fracture Zone, FI = Faroe Islands,**  
 1378 **FSB = Faroe-Shetland Basin, GB = Greenland Basin, GR = Gakkel Ridge, HB = Hatton**  
 1379 **Basin, HBk = Hatton Bank, IcB = Iceland Basin, IrB = Irminger Basin, JM = Jan Mayen**  
 1380 **Island, JMfZ = Jan Mayen Microplate Complex, KnR = Knipovich Ridge, KR = Kolbeinsey**  
 1381 **Ridge, LB = Lofoten Basin, LS = Labrador Sea, MB = Møre Basin, MR = Mohn's Ridge,**  
 1382 **NB = Norway Basin, NS = Nares Strait, PB = Porcupine Basin, RB = Rockall Basin, RBk =**  
 1383 **Rockall Bank, RR = Reykjanes Ridge, SB = Svalbard, SI = Shetland Islands, VB = Vøring**  
 1384 **Basin, WJMfZ = West Jan Mayen Fracture Zone. Solid black lines are an interpretation of**  
 1385 **the continent-ocean transition. Stippled black lines indicate uncertain locations of the**  
 1386 **continent-ocean transition.**

1387

1388



1401 *MTFC = Møre-Trøndelag Fault Complex, NGF = Nagssugtoquidian Front; NGS =*  
1402 *Nagssugtoquidian Suture, NIF = North Iberian Fault, NSL = Nares Strait lineament, OHF*  
1403 *= Outer Hebrides Fault, ReR= Reykjanes Ridge, RR = Rona Ridge, SFZ = Senja Fracture*  
1404 *Zone, SUF = Southern Uplands Fault, TKFC = Trollfjord-Komagelv Fault Complex, TLF*  
1405 *= Trolle Land Fault, TZ = Tornquist Zone, TS = Thor Suture, UFZ = Ungava Fault Zone,*  
1406 *VF = Variscan Front, VS = Variscan Suture, WBF = Walls Boundary Fault.*

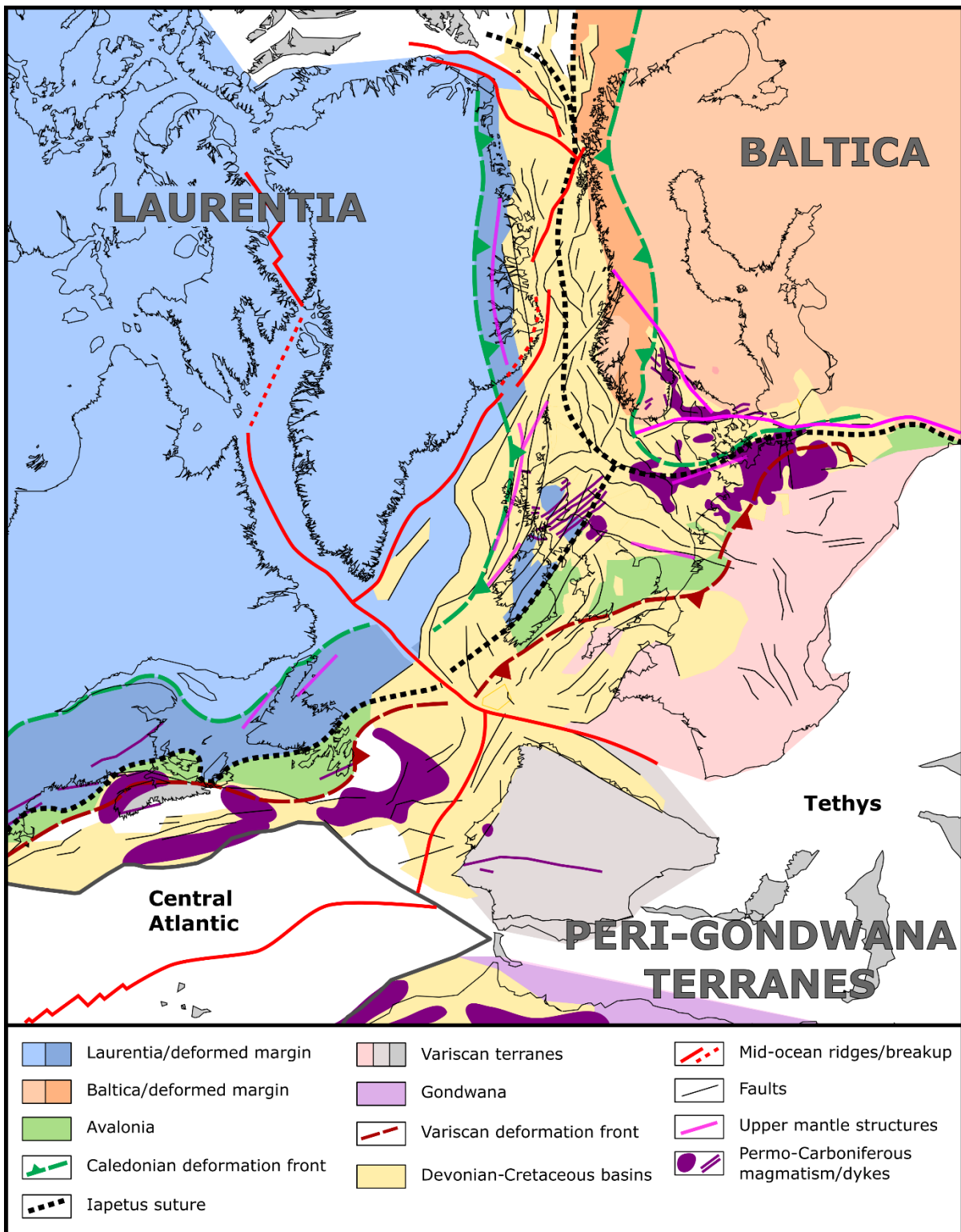


1407  
 1408 *Figure 3: Terrane and structure map of the Circum-North Atlantic region at 145 Ma*  
 1409 *showing continents, terranes, suture zones and upper mantle structures. Caledonian and*  
 1410 *Variscan terranes and structures are generally closely aligned with the breakup axes In the*  
 1411 *NE Atlantic, breakup occurred west of the Iapetus Suture; In contrast, breakup occurred to*  
 1412 *the east of the Iapetus Suture in the northern Central Atlantic. Precambrian terranes are*

1413 *generally perpendicularly aligned, but have therefore probably affected margin*  
1414 *segmentation and the formation of transform zones and faults during rifting. The NW*  
1415 *Atlantic is a region where an ocean opened (Labrador Sea and Baffin Bay) not following*  
1416 *any known Phanerozoic structures or terranes and cross-cutting Precambrian lineaments.*  
1417 *However, the Rinkian Orogen may have played a role during the formation of Baffin Bay.*  
1418 *GRE – Grenvillian Orogen, IMB – Inglefield Mobile Belt, KAR – Karelian, LGB – Lapland*  
1419 *Granulite Belt, MAK – Makkovik-Ketilidian Orogen, NAC – North Atlantic Craton, NAG –*  
1420 *Nagssugtoqidian Orogen, RAC – Rae Craton, RIN – Rinkian Orogen, SUC – Superior*  
1421 *Craton, SVF – Svecofennian, SVN – Sveconorwegian Orogen, THO – Trans-Hudson*  
1422 *Orogen, TIB – Transscandinavian Igenous Belt, TIM – Timanian Orogen*

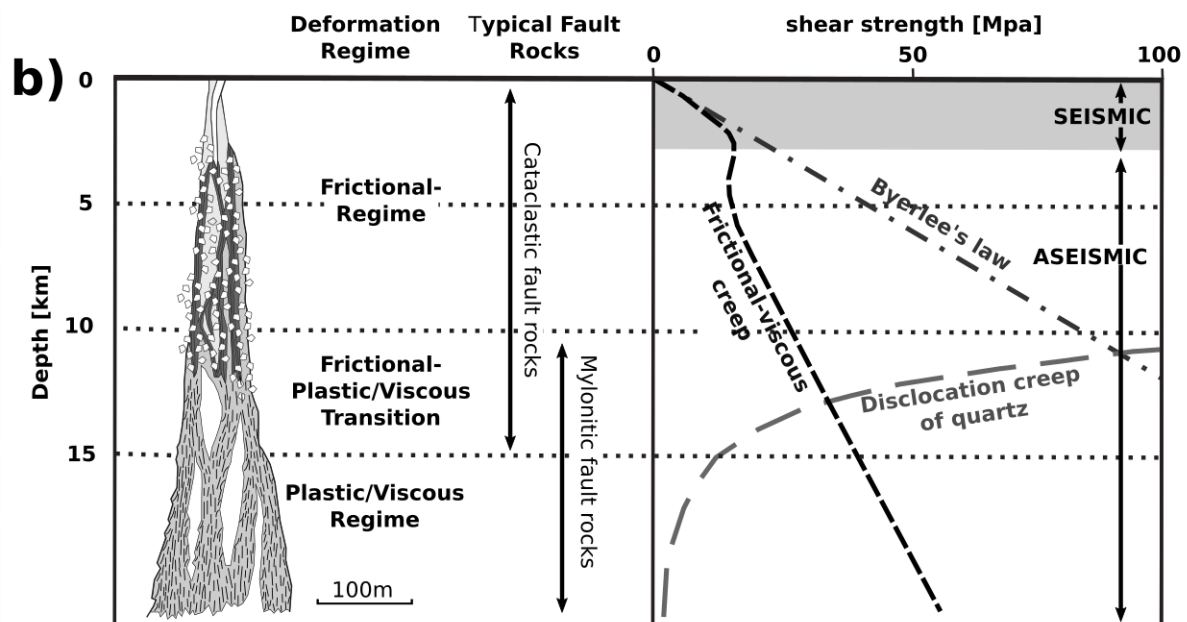
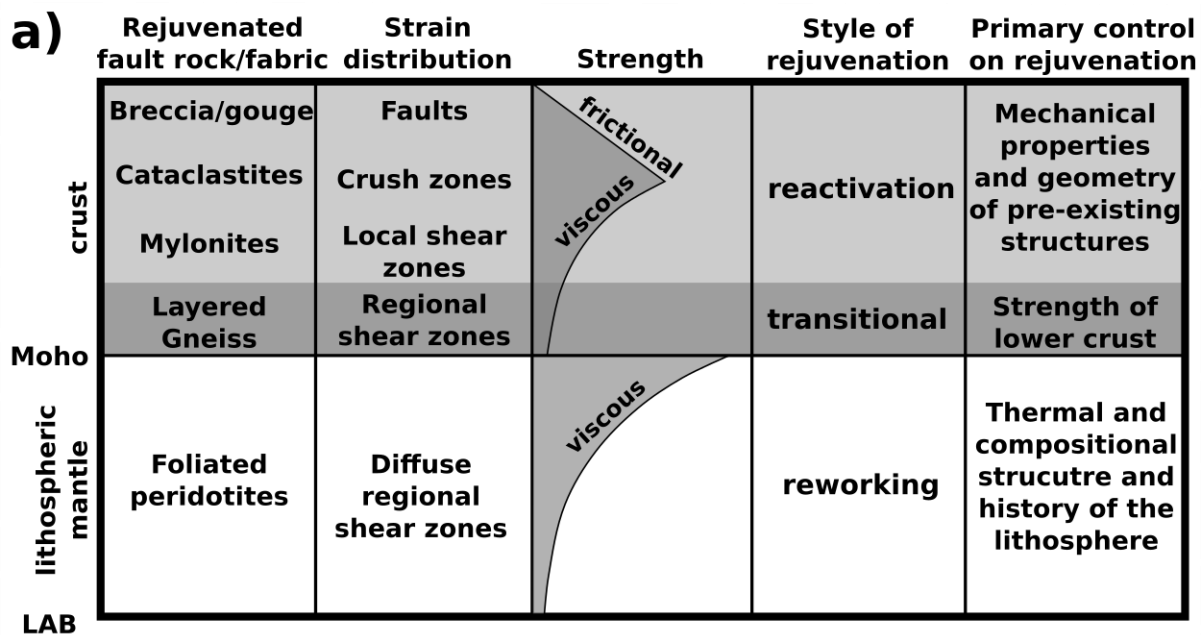
1423

1424



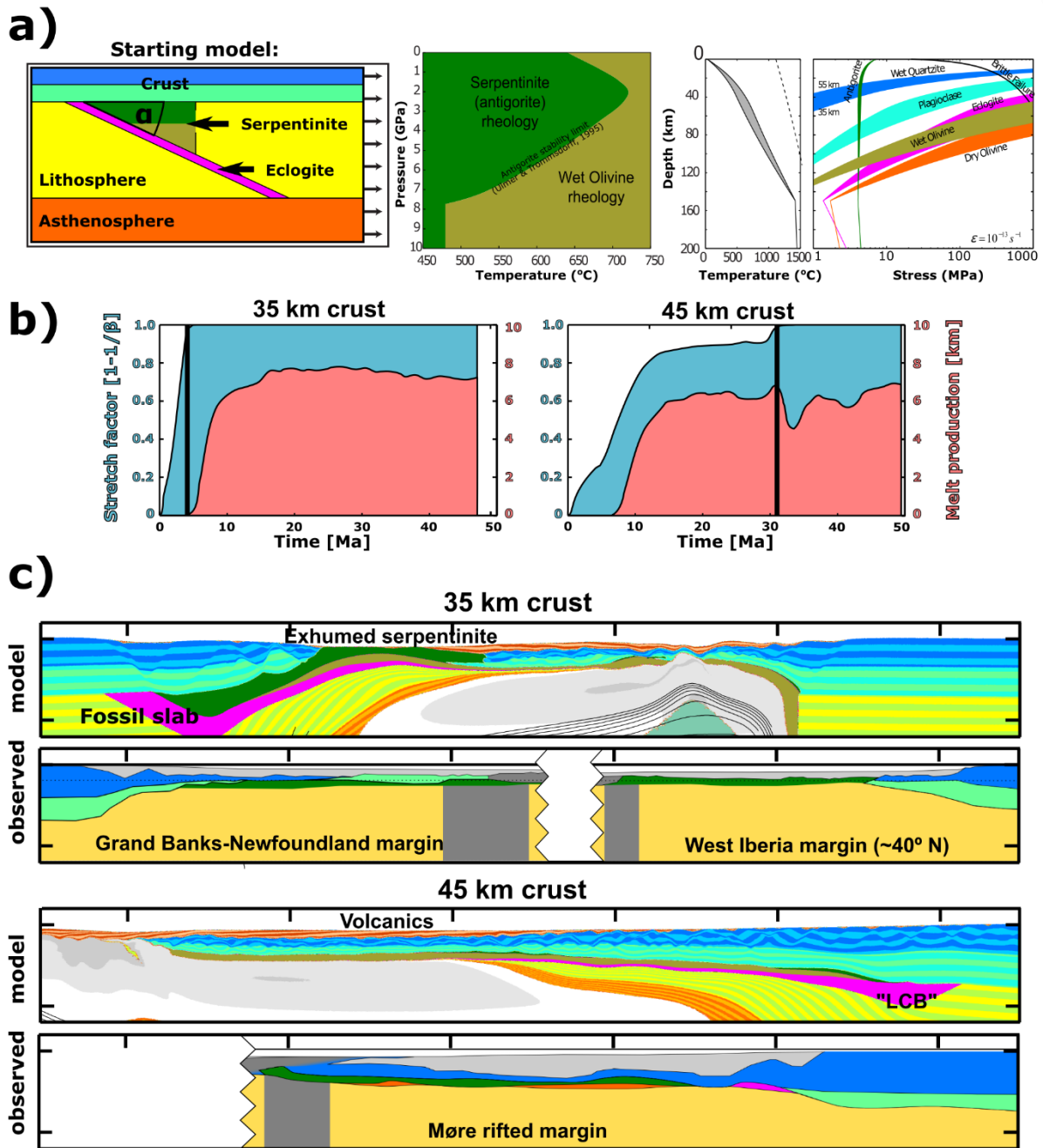
1425

1426 *Figure 4: Basin and structure map of the Circum-North Atlantic region at 145 Ma showing*  
 1427 *continents, basins, faults, upper mantle structures and Permo-Carboniferous magmatism.*  
 1428 *Almost all of the early, Devonian-Jurassic basins illustrated in this figure have formed*  
 1429 *within the Caledonian or Variscan orogens (within their deformation fronts) and oblique to*  
 1430 *the axis of breakup.*



1431

1432 *Figure 5: (a) Schematic diagram showing typical fault rocks/fabrics, the strain distribution,*  
 1433 *strength, tectonic style and primary rheological controls during rejuvenation at different*  
 1434 *depth through the lithosphere (Holdsworth et al. 2001; Jefferies et al. 2006). The regimes of*  
 1435 *reactivation and reworking are separated by a gradual transition somewhere in the lower*  
 1436 *crust. Note that the strength profile is for a simplified and averaged continental lithosphere.*  
 1437 *Any tectonic processes (orogenesis, delamination, rifting) and compositional heterogeneity*  
 1438 *will perturb the strength profile of the lithosphere. (b) Schematic diagrams illustrating*  
 1439 *variations in shear deformation, deformation regime and typical fault rocks with depth in a*  
 1440 *crustal profile, (left) and a crustal strength profile with different representative rheologies*  
 1441 *(right) (Holdsworth et al. 2001; Alsop and Holdsworth 2004; Jefferies et al. 2006; Imber et al.*  
 1442 *2008).*



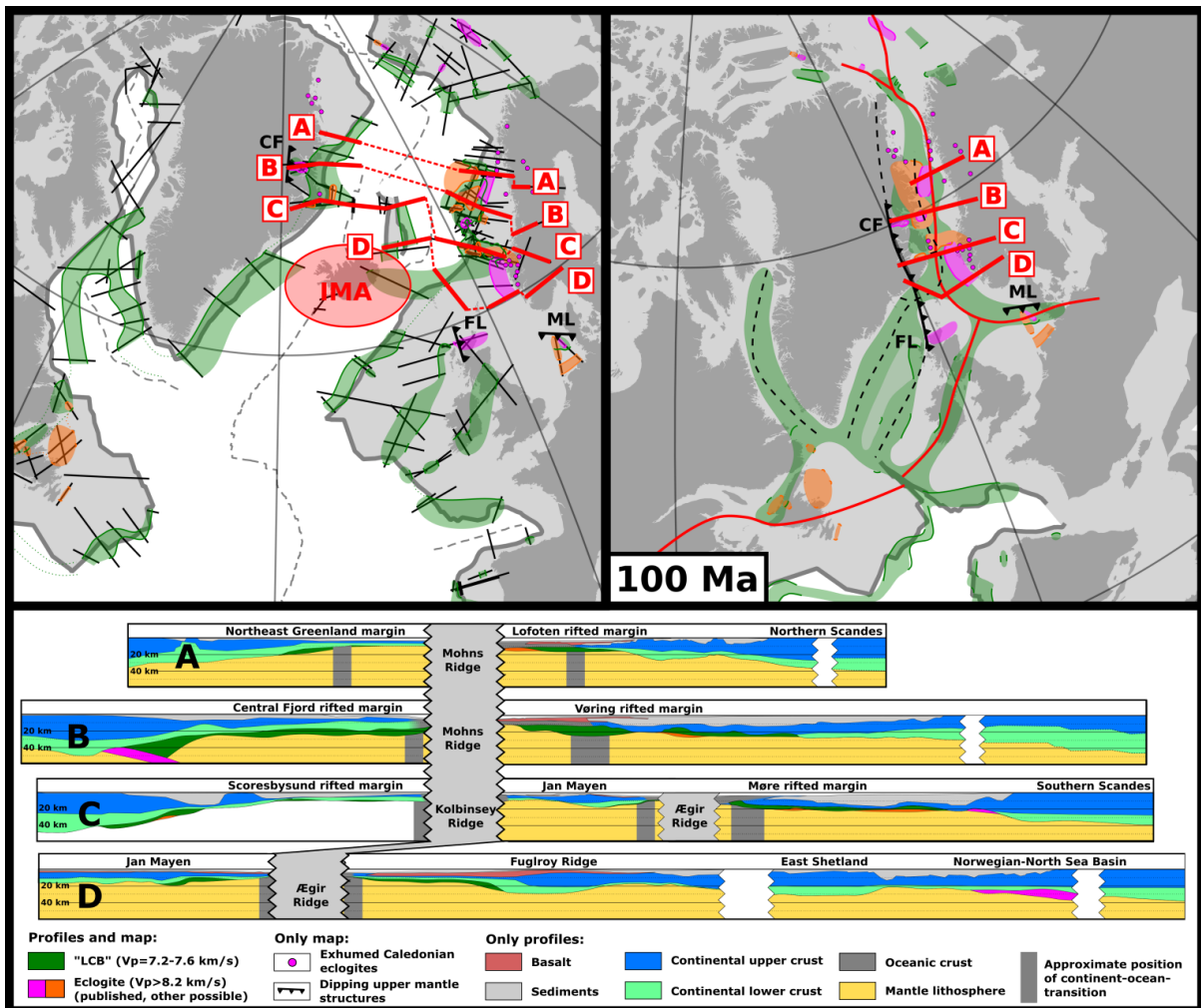
1443

1444 *Figure 6: 2D numerical modelling setup and results modified from Petersen & Schiffer*  
 1445 *(2016) illustrating the effect of crustal thickness and a preserved subduction zone complex*  
 1446 *on rifting and passive margin formation. The crust vs. mantle (depth-dependent) thinning is*  
 1447 *in agreement with many other studies (e.g. Buck, 1991; Huismans and Beaumont, 2011) (a)*  
 1448 *Starting model setup with crust (upper and lower), lithospheric mantle with discrete*  
 1449 *heterogeneities (eclogite, serpentinite and hydrated peridotite) on top of the asthenospheric*  
 1450 *mantle (upper panel). The binary phase diagram for antigorite/serpentinite stability is shown*  
 1451 *(lower left panel), the different tested initial geotherms for a range of crustal thicknesses*  
 1452 *(35-55 km) (lower middle panel) as well as the resulting strength profiles for the involved*  
 1453 *lithologies (wet quartz, plagioclase, dry and wet olivine, and antigorite/serpentinite) (lower*  
 1454 *right panel). (b) Modelling evolution in terms of relative crustal thinning (blue, stretch factor*  
 1455 *=  $1-1/\beta$ ; 0 is no thinning, 1 represent separation of the continental crust – marked by the*  
 1456 *vertical black line) and melt production (red, in terms of equivalent thickness of flood*

1457 *basalts). It can be noticed that melt production first starts with separation (breakup) of the*  
 1458 *continental crust, therefore, no flood basalts cover the continental crust. For a thick crust*  
 1459 *(45 km) it can be observed that melt production starts several tens of Ma before crustal*  
 1460 *separation (breakup), therefore intruding and extruding magmatic products into and on top*  
 1461 *of continental crust. (c) Models and possible analogues in the North Atlantic passive*  
 1462 *margins. The thin crust template is able to explain many first-order observations in magma-*  
 1463 *poor margins, such as the Iberia-Newfoundland conjugate passive margins. Here, the*  
 1464 *surrounding continents have thinner crust (~35 km). The margins have sharp, abrupt*  
 1465 *necking zones, thin continental slivers, separated from the margin lie within exhumed and*  
 1466 *hydrated mantle lithosphere covering the ocean floor and few (pre-breakup) magmatic*  
 1467 *products are observed on the continental margin. Volcanic products cover hundreds of km*  
 1468 *of the preserved hyperextended continental crust. The conjugate (not shown here) would be*  
 1469 *– in contrast – very narrow forming a highly asymmetric conjugate margin pair. This*  
 1470 *“magma-rich” margin shows evidence of high velocity lower crust that – in this case – is*  
 1471 *derived from the deformed and re-replaced lithospheric heterogeneities. This template*  
 1472 *shows many similar first order features with many observed magma-rich margins, for*  
 1473 *example the Møre margin.*

1474

1475



1476

1477

1478

*Figure 7: Top left: Map of the high-velocity lower crustal bodies in the Circum-North Atlantic region. Green colours illustrate HVLCBs in the P-wave velocity range 7.2-7.6 km/s*

1479 *and magenta shows occurrences of ultra-HVLCBs with P-wave velocity larger than 8.2 km/s*  
1480 *that is indicative of eclogite. Thick black lines show dipping upper mantle structures and*  
1481 *triangles the dip direction: CF, Central Fjord structure; FL, Flannan structure; ML, Mona*  
1482 *Lisa Caledonian suture. Orange indicates other possible occurrences of the  $V_p > 8.2$  km/s*  
1483 *ultra-HVLCBs. Four transects are defined through the NE Atlantic based on seismic lines*  
1484 *(thin black lines) illustrates the position of the transects (red) and wide-angle seismic lines*  
1485 *(black lines) in the North Atlantic. Top right: Same map in a 100 Ma pre-breakup*  
1486 *reconstruction showing how well the interpreted eclogite bodies coincide with the location*  
1487 *of the Iapetus Suture (thin red line). Lower panel shows the four transects (A-D) at present*  
1488 *day from wide-angle seismic lines* (Theilen and Meissner 1979; Goldschmidt-Rokita et al.  
1489 1994; Weigel et al. 1995; Mandler and Jokat 1998; Christiansson et al. 2000; Tsikalas et al.  
1490 2005; Mjelde et al. 2009, 2013; Roberts et al. 2009; Voss et al. 2009; Breivik et al. 2012;  
1491 Maupin et al. 2013; Schiffer et al. 2015a).

1492

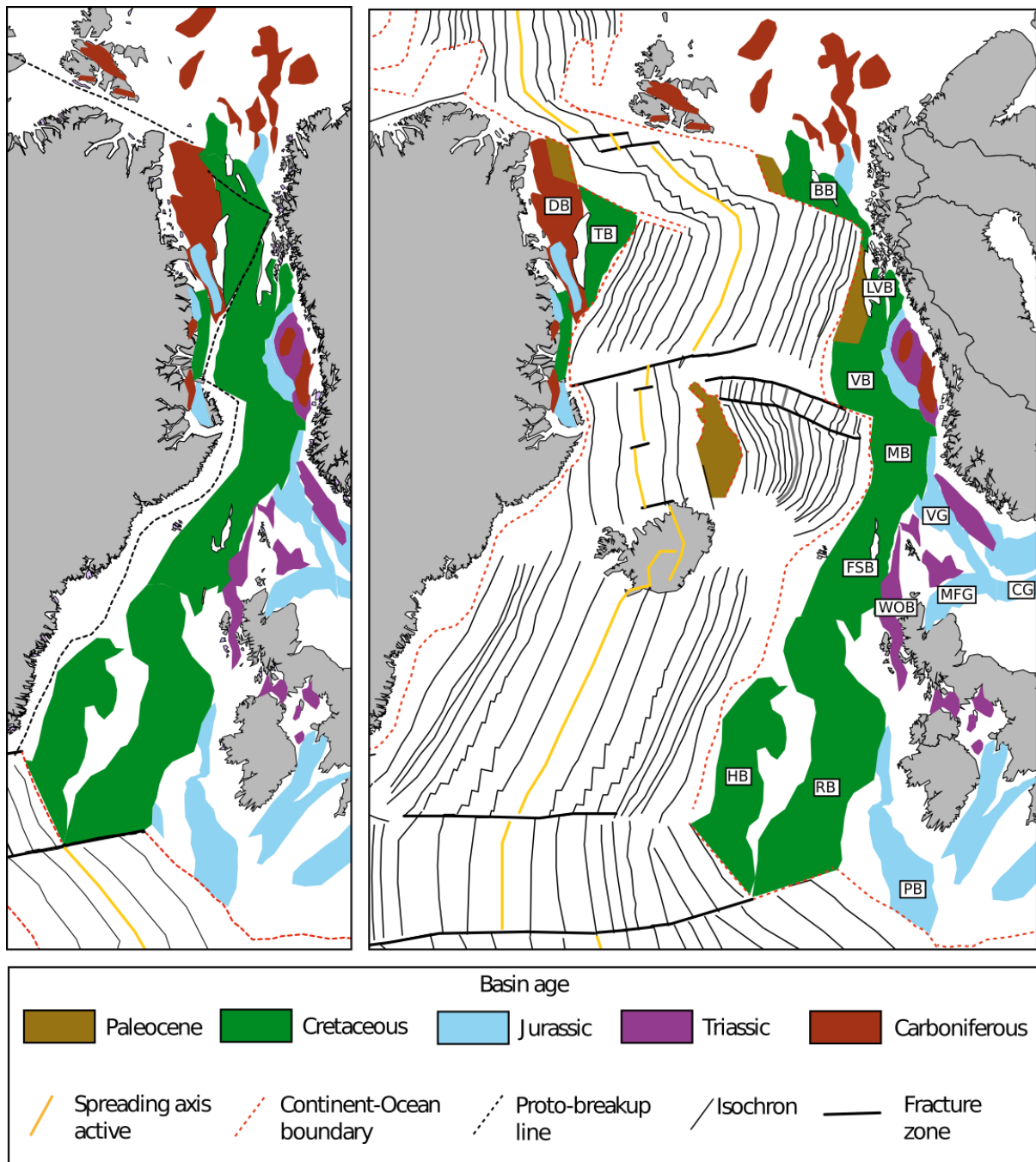
1493

1494

1495

1496

1497

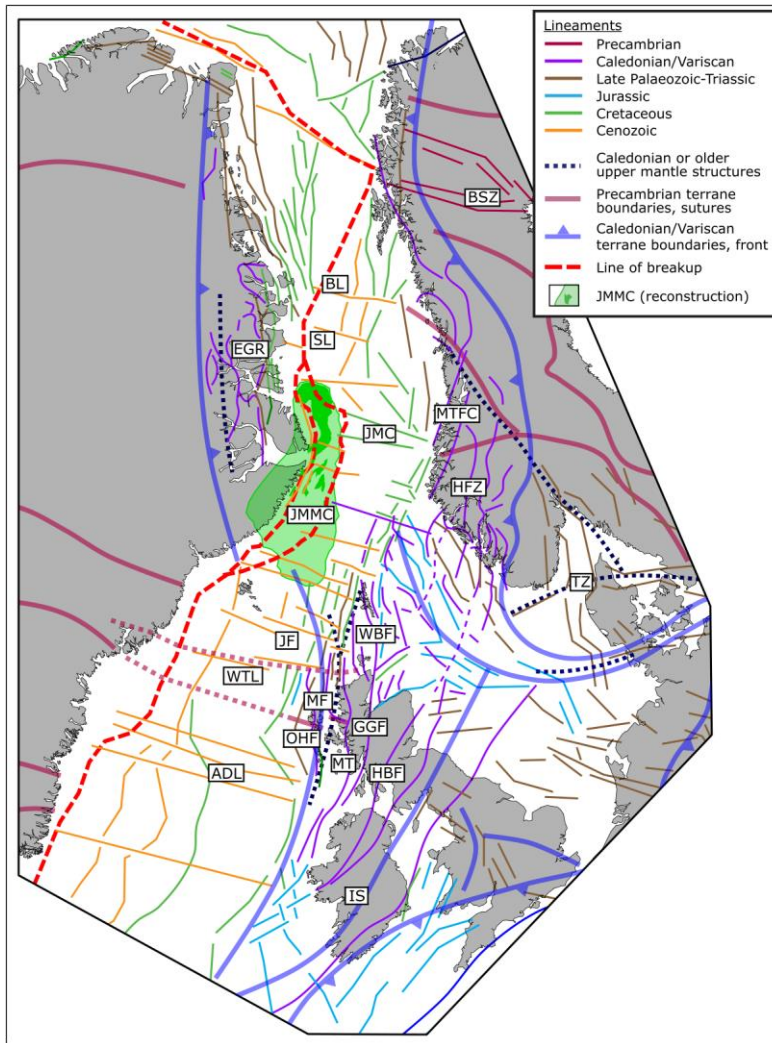


1498

1499 **Figure 8: Basin age map of the North Atlantic, shown before breakup at 53 Ma (left), and**  
 1500 **present day (right). Basins are coloured according to the age of the crustal extension that**  
 1501 **mainly created the basin. The general asymmetry of the breakup (much of pre-existing basin**  
 1502 **system left on the European margin) and the obliquity of the breakup in the NE are clearly**  
 1503 **shown. Abbreviations: BB, Bjørnøya Basin; CG, Central Graben; DB, Danmarkshavn**  
 1504 **Basin; FSB, Faroe-Shetland Basin; HB, Hatton Basin; LVB, Lofoten-Vestrålen Basin; MB,**  
 1505 **Møre Basin; MFG, Moray Firth Graben; PB, Porcupine Basin; RB, Rockall Basin; TB,**  
 1506 **Thetis Basin; VB, Vøring Basin; VG, Viking Graben; WB=Wandel Sea Basin, WOB, West**  
 1507 **Orkney Basin.**

1508

1509



1510

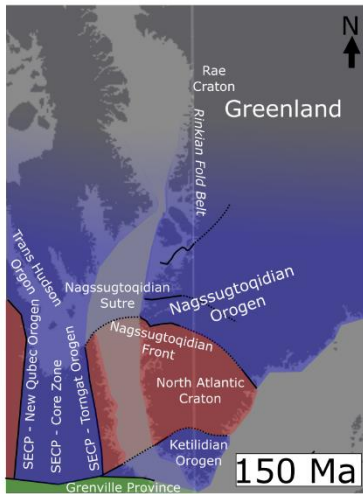
1511 **Figure 9: Basement terranes and lineaments of the NE Atlantic margins in a plate**  
 1512 **reconstruction at 60 Ma. Lineaments are coloured according to their main observed age of**  
 1513 **expression** (Gernigon et al. this volume; Karson and Brooks 1999; Doré et al. 1999; Heeremans  
 1514 and Faleide 2004; Kimbell et al. 2005a; Guarnieri 2015; Fossen et al. 2017; Rotevatn et al.  
 1515 2018; Holdsworth et al. 2019). **Abbreviations: ADL, Anton Dohrn Lineament; BL, Bivrost**  
 1516 **Lineament; BSZ, Bothnian-Senja Shear Zone; EGR, East Greenland Rift System; GGF,**  
 1517 **Great Glen Fault; HBF, Highland Boundary Fault; HFZ, Hardangerfjord Fault Zone; IS,**  
 1518 **Iapetus Suture; JF, Judd Fault; JMMC, Jan Mayen Microplate Complex; JMC, Jan Mayen**  
 1519 **Corridor; MF, Mich Fault Zone; MTFZ, Møre-Trøndelag Fault Zone; MT, Moine Thrust;**  
 1520 **OHF, Outer Hebrides Fault Zone; SL, Surt Lineament; TZ, Tornquist Zone; WTL, Wyville-**  
 1521 **Thomson Lineament.**

1522

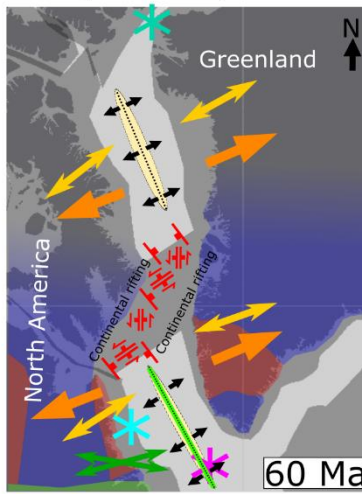
1523

1524

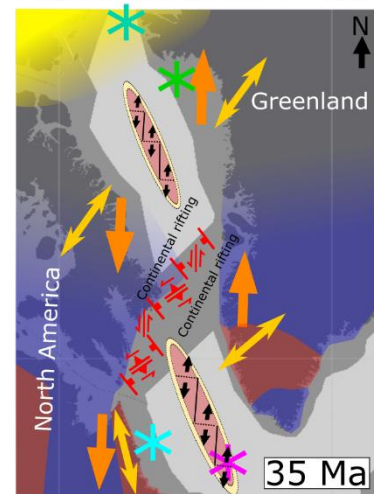
A) Pre-rift stage and onshore structures



B) Stage 1: Rifting  
Ch27(or earlier) - Ch24



C) Stage 2:  
Rift/transform Ch24 - Ch13



Age of pre-rift crust (St-Onge et al., 2009)

1.5 - 1.0 Ga    2.3 - 1.7 Ga    >2.5 Ga

Reactivated fault kinematics (Peace et al., 2017b)

Normal    Oblique normal  
Oblique reverse    Strike slip

Oceanic crust (schematic)

Regional Extension directions (Abdelmalak et al., 2012)

Regional extension from geopotential stress field modelling (Peace et al., 2018a)

Regional compression (Eurekan orogeny; reactivation)

Breakup following pre-existing normal faults (McWhae, 1981)

Fracture zones related to Grenville front (Welford and Hall, 2013)

Reactivated faults offsetting Moho (Jackson and Reid, 1994)

Reactivated faults (Jauer et al., 2014)

Reactivated faults (Gregersen et al., 2016)

Stress inversion results (Peace et al., 2018a)

1525

1526

1527

1528

1529

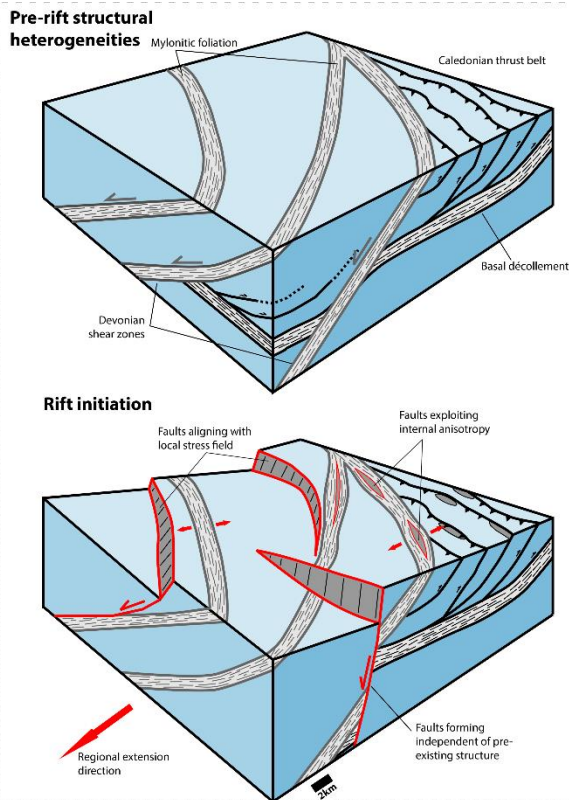
1530

1531

1532

1533

**Figure 10: Schematic diagram summarising the kinematic and structural development, as well as seismic, mapping and modelling results of the Labrador Sea and Baffin Bay spreading system after (Peace et al. 2018b). A) Pre-rift configuration of North America and Greenland with graphical representations of the onshore structure and basement terrains of West Greenland (e.g. Wilson et al., 2006). B) Kinematic model for the first rift phase. C) Kinematic model for the second rift phase, after a change of stress field from ~SE-NW to N-S, at which the Ungava Transform Fault system develops as a result of the lateral offset between the Baffin Bay and Labrador Sea spreading centres.**

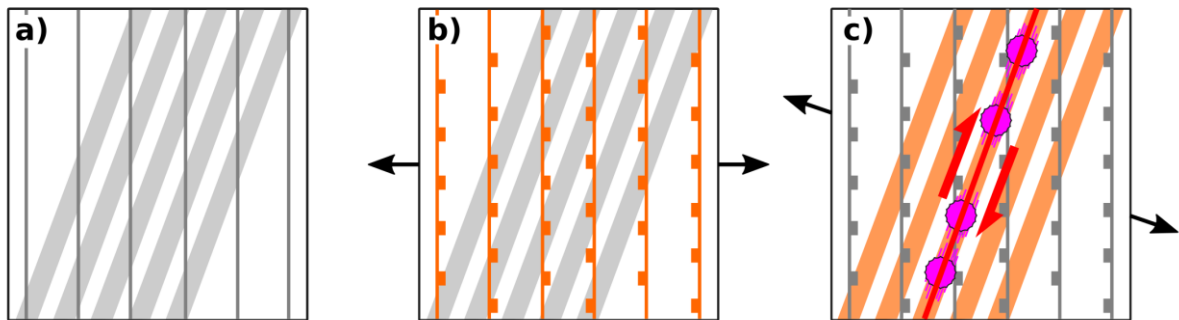


1534

1535 **Figure 11: Schematic block diagram showing the Caledonian thrust belt and Devonian**  
 1536 **shear zones present within the lithosphere (above) and the various interactions with rift-**  
 1537 **related faults (below). After Phillips et al. (2016).**

1538

1539



1540

1541 **Figure 12: Simplified schematic diagram illustrating large-scale inheritance and**  
 1542 **reactivation in the NE Atlantic. The diagram is not to scale and is conceptual (i.e. does not**  
 1543 **show specific structures) (a) The initial shallow (crustal) Caledonian thrust fault systems**  
 1544 **(thin, dark grey lines) were oblique to the late Caledonian mantle shear fabric (light grey**  
 1545 **bands). (b) During early basin formation, the shallow Caledonian thrust faults were**  
 1546 **reactivated as normal faults (orange). Breakup, however, was not accommodated as the**  
 1547 **stress field was oblique to the stronger mantle shear fabric (light grey). (c) First later, after**  
 1548 **rotation of the stress field, the mantle shear fabric (orange) was favourably aligned**  
 1549 **allowing lithospheric breakup (red line). This may have been assisted by the formation of**  
 1550 **magmatic centres (magenta circles) and dykes exploiting lithospheric weaknesses**

1551 (Gernigon et al. this volume; Geoffroy et al. 2007) and/or strike slip motion, perforating  
1552 the lithosphere prior to breakup (Lundin and Doré 2018).

1553

1554

1555

## 1556 **10 References**

1557

1558 Aarseth I, Mjelde R, Breivik AJ, et al (2017) Crustal structure and evolution of the Arctic Caledonides:  
1559 results from controlled-source seismology. *Tectonophysics* 718:9–24

1560 Abdelmalak MM, Faleide JJ, Planke S, et al (2017) The T-Reflection and the Deep Crustal Structure of  
1561 the Vøring Margin, Offshore mid-Norway. *Tectonics* 36:2497–2523

1562 Abdelmalak MM, Geoffroy L, Angelier J, et al (2012) Stress fields acting during lithosphere breakup  
1563 above a melting mantle: A case example in West Greenland. *Tectonophysics* 581:132–143.  
1564 <https://doi.org/10.1016/j.tecto.2011.11.020>

1565 Abdelmalak MM, Planke S, Polteau S, et al (2018) Breakup volcanism and plate tectonics in the NW  
1566 Atlantic. *Tectonophysics*. <https://doi.org/10.1016/j.tecto.2018.08.002>

1567 Abramovitz T, Thybo H (2000) Seismic images of Caledonian, lithosphere-scale collision structures in  
1568 the southeastern North Sea along Mona Lisa Profile 2. *Tectonophysics* 317:27–54.  
1569 [https://doi.org/10.1016/S0040-1951\(99\)00266-8](https://doi.org/10.1016/S0040-1951(99)00266-8)

1570 Ady BE, Whittaker RC (2018) Examining the influence of tectonic inheritance on the evolution of the  
1571 North Atlantic using a palinspastic deformable plate reconstruction. *Geol Soc Lond Spec Publ*  
1572 470:SP470–9

1573 Alsop GI, Holdsworth RE (2004) Shear zones—an introduction and overview. *Geol Soc Lond Spec*  
1574 *Publ* 224:1–9

1575 Andersen TB (1998) Extensional tectonics in the Caledonides of southern Norway, an overview.  
1576 *Tectonophysics* 285:333–351

1577 Andersen TB, Jamtveit B (1990) Uplift of deep crust during orogenic extensional collapse: A model  
1578 based on field studies in the Sogn-Sunnfjord Region of western Norway. *Tectonics* 9:1097–  
1579 1111

1580 Andersen TB, Jamtveit B, Dewey J, Swensson E (1991) Subduction and exhumation of continental crust:  
1581 major mechanisms during continent-continent collision and orogenic extensional collapse, a  
1582 model based on the south Norwegian Caledonides. *Terra Nova* 3:303–310.  
1583 <https://doi.org/10.1111/j.1365-3121.1991.tb00148.x>

1584 Andréasson PG, Gee DG, Whitehouse MJ, Schöberg H (2003) Subduction-flip during Iapetus Ocean  
1585 closure and Baltica–Laurentia collision, Scandinavian Caledonides. *Terra Nova* 15:362–369.  
1586 <https://doi.org/10.1046/j.1365-3121.2003.00486.x>

1587 Andresen A, Hartz EH, Vold J (1998) A late orogenic extensional origin for the infracrustal gneiss  
1588 domes of the East Greenland Caledonides (72–74 N). *Tectonophysics* 285:353–369

- 1589 Arfai J, Jähne F, Lutz R, et al (2014) Late Palaeozoic to Early Cenozoic geological evolution of the  
1590 northwestern German North Sea (Entenschnabel): new results and insights. *Neth J Geosci*  
1591 93:147–174
- 1592 Armitage JJ, Collier JS, Minshull TA (2010) The importance of rift history for volcanic margin  
1593 formation. *Nature* 465:913
- 1594 Asimow PD, Langmuir CH (2003) The importance of water to oceanic mantle melting regimes. *Nature*  
1595 421:815–820. <https://doi.org/10.1038/nature01429>
- 1596 Audet P, Sole C, Schaeffer AJ (2016) Control of lithospheric inheritance on neotectonic activity in  
1597 northwestern Canada? *Geology* 44:807–810
- 1598 Auzende JM, Beuzart P, Bonnin J, et al (1980) Mode de dislocation des continents lors des stades  
1599 initiaux d'ouverture. 8<sup>ème</sup> La Réunion Sci Terre Société Géologique Fr
- 1600 Babuška V, Plomerová J (2004) The Sorgenfrei–Tornquist Zone as the mantle edge of Baltica  
1601 lithosphere: new evidence from three-dimensional seismic anisotropy. *Terra Nova* 16:243–  
1602 249
- 1603 Balling N (2000) Deep seismic reflection evidence for ancient subduction and collision zones within  
1604 the continental lithosphere of northwestern Europe. *Tectonophysics* 329:269–300.  
1605 [https://doi.org/10.1016/S0040-1951\(00\)00199-2](https://doi.org/10.1016/S0040-1951(00)00199-2)
- 1606 Barruol G, Bonnin M, Pedersen H, et al (2011) Belt-parallel mantle flow beneath a halted continental  
1607 collision: The Western Alps. *Earth Planet Sci Lett* 302:429–438
- 1608 Barruol G, Helffrich G, Vauchez A (1997) Shear wave splitting around the northern Atlantic: frozen  
1609 Pangaeian lithospheric anisotropy? *Tectonophysics* 279:135–148
- 1610 Bartholomew ID, Peters JM, Powell CM (1993) Regional structural evolution of the North Sea:  
1611 oblique slip and the reactivation of basement lineaments. In: Geological Society, London,  
1612 Petroleum Geology Conference series. Geological Society of London, pp 1109–1122
- 1613 Baudon C, Cartwright J (2008) The kinematics of reactivation of normal faults using high resolution  
1614 throw mapping. *J Struct Geol* 30:1072–1084
- 1615 Bell RE, Jackson CA-L, Whipp PS, Clements B (2014) Strain migration during multiphase extension:  
1616 Observations from the northern North Sea. *Tectonics* 33:1936–1963
- 1617 Bellahsen N, Fournier M, d'Acremont E, et al (2006) Fault reactivation and rift localization:  
1618 Northeastern Gulf of Aden margin. *Tectonics* 25:
- 1619 Beniest A, Willingshofer E, Sokoutis D, Sassi W (2018) Extending continental lithosphere with lateral  
1620 strength variations: effects on deformation localization and margin geometries. *Front Earth*  
1621 *Sci* 6:148
- 1622 Bergh SG, Eig K, Kløvjan OS, et al (2007) The Lofoten-Vesterålen continental margin: a multiphase  
1623 Mesozoic-Palaeogene rifted shelf as shown by offshore-onshore brittle fault-fracture  
1624 analysis. *Nor J Geol Geol Foren* 87:
- 1625 Berthelsen A (1998) The Tornquist Zone northwest of the Carpathians: An intraplate pseudosuture.  
1626 *GFF* 120:223–230. <https://doi.org/10.1080/11035899801202223>

- 1627 Biddle KT, Rudolph KW (1988) Early tertiary structural inversion in the Stord basin, Norwegian north  
1628 sea. *J Geol Soc* 145:603–611
- 1629 Bingen B, Andersson J, Söderlund U, Möller C (2008a) The Mesoproterozoic in the Nordic countries.  
1630 In: *Episodes*. Episodes, pp 29–34
- 1631 Bingen B, Nordgulen O, Viola G (2008b) A four-phase model for the Sveconorwegian orogeny, SW  
1632 Scandinavia. *Nor Geol Tidsskr* 88:43
- 1633 Bird P (1979) Continental delamination and the Colorado Plateau. *J Geophys Res Solid Earth*  
1634 84:7561–7571
- 1635 Bird PC, Cartwright JA, Davies TL (2015) Basement reactivation in the development of rift basins: an  
1636 example of reactivated Caledonide structures in the West Orkney Basin. *J Geol Soc* 172:77–  
1637 85
- 1638 Bladon AJ, Burley SD, Clarke SM, Beaumont H (2015) Geology and regional significance of the Sarnoo  
1639 Hills, eastern rift margin of the Barmer Basin, NW India. *Basin Res* 27:636–655
- 1640 Blakey RC (2008) Gondwana paleogeography from assembly to breakup—A 500 my odyssey. *Geol*  
1641 *Soc Am Spec Pap* 441:1–28
- 1642 Blischke A, Arnarson TS, Gunnarsson K (2011) The Structural History of the Jan Mayen Micro-  
1643 Continent (JMMC) and Its Role During the Rift “Jump” Between the Aegir to the Kolbeinsey  
1644 Ridge. In: AAPG, 3P Arctic-The Polar Petroleum Potential Conference & Exhibition, extended  
1645 Abstract, Halifax, Nova Scotia, Canada
- 1646 Blischke A, Gaina C, Hopper JR, et al (2017) The Jan Mayen microcontinent: an update of its  
1647 architecture, structural development and role during the transition from the Ægir Ridge to  
1648 the mid-oceanic Kolbeinsey Ridge. *Geol Soc Lond Spec Publ* 447:299–337
- 1649 Blischke A, Stoker MS, Brandsdóttir B, et al (2019) The Jan Mayen microcontinent’s Cenozoic  
1650 stratigraphic succession and structural evolution within the NE-Atlantic. *Mar Pet Geol*  
1651 103:702–737. <https://doi.org/10.1016/j.marpetgeo.2019.02.008>
- 1652 Blundell DJ, Hobbs RW, Klemperer SL, et al (1991) Crustal structure of the central and southern  
1653 North Sea from BIRPS deep seismic reflection profiling. *J Geol Soc* 148:445–457.  
1654 <https://doi.org/10.1144/gsjgs.148.3.0445>
- 1655 Blystad P (1995) Structural elements of the Norwegian continental shelf. Part 2: The Norwegian Sea  
1656 region. *NPD Bull* 8:
- 1657 Booth J, Swiecicki T, Wilcockson P (1993) The tectono-stratigraphy of the Solan Basin, west of  
1658 Shetland. In: Geological Society, London, Petroleum Geology Conference series. Geological  
1659 Society of London, pp 987–998
- 1660 Bott MHP, Tuson J (1973) Deep structure beneath the Tertiary volcanic regions of Skye, Mull and  
1661 Ardnamurchan, north-west Scotland. *Nat Phys Sci* 242:114–116
- 1662 Bowling JC, Harry DL (2001) Geodynamic models of continental extension and the formation of non-  
1663 volcanic rifted continental margins. *Geol Soc Lond Spec Publ* 187:511–536.  
1664 <https://doi.org/10.1144/GSL.SP.2001.187.01.25>

1665 Braathen A, Nordgulen Ø, Osmundsen P-T, et al (2000) Devonian, orogen-parallel, opposed  
1666 extension in the Central Norwegian Caledonides. *Geology* 28:615–618.  
1667 [https://doi.org/10.1130/0091-7613\(2000\)28<615:DOOEIT>2.0.CO;2](https://doi.org/10.1130/0091-7613(2000)28<615:DOOEIT>2.0.CO;2)

1668 Brandsdóttir B, Hooft EEE, Mjelde R, Murai Y (2015) Origin and evolution of the Kolbeinsey Ridge and  
1669 Iceland Plateau, N-Atlantic. *Geochem Geophys Geosystems* 16:612–634.  
1670 <https://doi.org/10.1002/2014GC005540>

1671 Braun J, Chéry J, Poliakov A, et al (1999) A simple parameterization of strain localization in the  
1672 ductile regime due to grain size reduction: A case study for olivine. *J Geophys Res Solid Earth*  
1673 104:25167–25181

1674 Breivik AJ, Mjelde R, Faleide JJ, Murai Y (2012) The eastern Jan Mayen microcontinent volcanic  
1675 margin. *Geophys J Int* 188:798–818. <https://doi.org/10.1111/j.1365-246X.2011.05307.x>

1676 Breivik AJ, Mjelde R, Grogan P, et al (2005) Caledonide development offshore-onshore Svalbard  
1677 based on ocean bottom seismometer, conventional seismic, and potential field data.  
1678 *Tectonophysics* 401:79–117. <https://doi.org/10.1016/j.tecto.2005.03.009>

1679 Breivik AJ, Mjelde R, Grogan P, et al (2002) A possible Caledonide arm through the Barents Sea  
1680 imaged by OBS data. *Tectonophysics* 355:67–97. [https://doi.org/10.1016/S0040-1951\(02\)00135-X](https://doi.org/10.1016/S0040-1951(02)00135-X)

1682 Brekke H (2000) The tectonic evolution of the Norwegian Sea continental margin, with emphasis on  
1683 the Voring and More basins. *Spec Publ-Geol Soc Lond* 167:327–378

1684 Brueckner HK (2006) Dunk, dunkless and re-dunk tectonics: A model for metamorphism, lack of  
1685 metamorphism, and repeated metamorphism of HP/UHP terranes. *Int Geol Rev* 48:978–995.  
1686 <https://doi.org/10.2747/0020-6814.48.11.978>

1687 Brueckner HK, Van Roermund HL (2007) Concurrent HP metamorphism on both margins of Iapetus:  
1688 Ordovician ages for eclogites and garnet pyroxenites from the Seve Nappe Complex, Swedish  
1689 Caledonides. *J Geol Soc* 164:117–128

1690 Brueckner HK, van Roermund HLM (2004) Dunk tectonics: A multiple subduction/eduction model for  
1691 the evolution of the Scandinavian Caledonides. *Tectonics* 23:TC2004.  
1692 <https://doi.org/10.1029/2003TC001502>

1693 Brun J-P, Tron V (1993) Development of the North Viking Graben: inferences from laboratory  
1694 modelling. *Sediment Geol* 86:31–51

1695 Brune S, Corti G, Ranalli G (2017) Controls of inherited lithospheric heterogeneity on rift linkage:  
1696 Numerical and analog models of interaction between the Kenyan and Ethiopian rifts across  
1697 the Turkana depression. *Tectonics* 36:1767–1786

1698 Brune S, Heine C, Pérez-Gussinyé M, Sobolev SV (2014) Rift migration explains continental margin  
1699 asymmetry and crustal hyper-extension. *Nat Commun* 5:  
1700 <https://doi.org/10.1038/ncomms5014>

1701 Brune S, Popov AA, Sobolev SV (2012a) Modeling suggests that oblique extension facilitates rifting  
1702 and continental break-up. *J Geophys Res Solid Earth* 117:

- 1703 Brune S, Popov AA, Sobolev SV (2012b) Modeling suggests that oblique extension facilitates rifting  
1704 and continental break-up. *J Geophys Res Solid Earth* 117:
- 1705 Brune S, Williams SE, Müller RD (2018) Oblique rifting: the rule, not the exception. *Solid Earth*  
1706 9:1187–1206
- 1707 Buchan KL, Ernst R (2006a) Giant dyke swarms and the reconstruction of the Canadian Arctic islands,  
1708 Greenland, Svalbard and Franz Josef Land. In: *Dyke Swarms - Time Markers of Crustal*  
1709 *Evolution*. Taylor & Francis, pp 27–48
- 1710 Buchan KL, Ernst RE (2006b) The High Arctic Large Igneous Province (HALIP): Evidence for an  
1711 Associated Giant Radiating Dyke Swarm. In: *High Arct. Large Igneous Prov. HALIP Evid. Assoc.*  
1712 *Giant Radiat. Dyke Swarm*. <http://www.largeigneousprovinces.org/06apr>
- 1713 Buchan KL, Mertanen S, Park RG, et al (2000) Comparing the drift of Laurentia and Baltica in the  
1714 Proterozoic: the importance of key palaeomagnetic poles. *Tectonophysics* 319:167–198.  
1715 [https://doi.org/10.1016/S0040-1951\(00\)00032-9](https://doi.org/10.1016/S0040-1951(00)00032-9)
- 1716 Buchanan JG, Buchanan PG (1995) Introduction. *Geol Soc Lond Spec Publ* 88:vii–ix.  
1717 <https://doi.org/10.1144/GSL.SP.1995.088.01.01>
- 1718 Buck WR (1991) Modes of continental lithospheric extension. *J Geophys Res Solid Earth* 96:20161–  
1719 20178. <https://doi.org/10.1029/91JB01485>
- 1720 Buck WR (2006) The role of magma in the development of the Afro-Arabian Rift System. *Geol Soc*  
1721 *Lond Spec Publ* 259:43–54
- 1722 Buck WR, Karner GD (2004) Consequences of asthenospheric variability on continental rifting. *Rheol*  
1723 *Deform Lithosphere Cont Margins* 62:1–30
- 1724 Buitter SJH, Torsvik TH (2014) A review of Wilson Cycle plate margins: A role for mantle plumes in  
1725 continental break-up along sutures? *Gondwana Res* 26:627–653.  
1726 <https://doi.org/10.1016/j.gr.2014.02.007>
- 1727 Burg JP, Iglesias M, Laurent Ph, et al (1981) Variscan intracontinental deformation: The Coimbra—  
1728 Cordoba shear zone (SW Iberian Peninsula). *Tectonophysics* 78:161–177.  
1729 [https://doi.org/10.1016/0040-1951\(81\)90012-3](https://doi.org/10.1016/0040-1951(81)90012-3)
- 1730 Burov EB (2011) Rheology and strength of the lithosphere. *Mar Pet Geol* 28:1402–1443.  
1731 <https://doi.org/10.1016/j.marpetgeo.2011.05.008>
- 1732 Callot J-P, Geoffroy L (2004) Magma flow in the East Greenland dyke swarm inferred from study of  
1733 anisotropy of magnetic susceptibility: magmatic growth of a volcanic margin. *Geophys J Int*  
1734 159:816–830
- 1735 Callot J-P, Geoffroy L, Aubourg C, et al (2001) Magma flow directions of shallow dykes from the East  
1736 Greenland volcanic margin inferred from magnetic fabric studies. *Tectonophysics* 335:313–  
1737 329. [https://doi.org/10.1016/S0040-1951\(01\)00060-9](https://doi.org/10.1016/S0040-1951(01)00060-9)
- 1738 Cartwright JA (1989) The kinematics of inversion in the Danish Central Graben. *Geol Soc Lond Spec*  
1739 *Publ* 44:153–175

- 1740 Cawood PA, Nemchin AA, Strachan R, et al (2007) Sedimentary basin and detrital zircon record along  
1741 East Laurentia and Baltica during assembly and breakup of Rodinia. *J Geol Soc* 164:257–275
- 1742 Cawood PA, Pisarevsky SA (2017) Laurentia-Baltica-Amazonia relations during Rodinia assembly.  
1743 *Precambrian Res* 292:386–397. <https://doi.org/10.1016/j.precamres.2017.01.031>
- 1744 Cawood PA, Strachan R, Cutts K, et al (2010) Neoproterozoic orogeny along the margin of Rodinia:  
1745 Valhalla orogen, North Atlantic. *Geology* 38:99–102. <https://doi.org/10.1130/G30450.1>
- 1746 Chalmers JA, Laursen KH (1995) Labrador Sea: the extent of continental and oceanic crust and the  
1747 timing of the onset of seafloor spreading. *Mar Pet Geol* 12:205–217.  
1748 [https://doi.org/10.1016/0264-8172\(95\)92840-5](https://doi.org/10.1016/0264-8172(95)92840-5)
- 1749 Chalmers JA, Pulvertaft TCR (2001) Development of the continental margins of the Labrador Sea: a  
1750 review. *Geol Soc Lond Spec Publ* 187:77–105.  
1751 <https://doi.org/10.1144/GSL.SP.2001.187.01.05>
- 1752 Chauvet F, Geoffroy L, Guillou H, et al (2019) Eocene continental breakup in Baffin Bay.  
1753 *Tectonophysics* 757:170–186
- 1754 Chenin P, Manatschal G, Lavier LL, Erratt D (2015) Assessing the impact of orogenic inheritance on  
1755 the architecture, timing and magmatic budget of the North Atlantic rift system: a mapping  
1756 approach. *J Geol Soc* 172:711–720. <https://doi.org/10.1144/jgs2014-139>
- 1757 Chenin P, Picazo S, Jammes S, et al (2018) Potential role of lithospheric mantle composition in the  
1758 Wilson cycle: a North Atlantic perspective. *Geol Soc Lond Spec Publ* 470:SP470–10
- 1759 Childs C, Holdsworth RE, Jackson CA-L, et al (2017) Introduction to the geometry and growth of  
1760 normal faults. *Geol Soc Lond Spec Publ* 439:SP439–23
- 1761 Christiansson P, Faleide JJ, Berge AM (2000) Crustal structure in the northern North Sea: an  
1762 integrated geophysical study. *Geol Soc Lond Spec Publ* 167:15–40.  
1763 <https://doi.org/10.1144/GSL.SP.2000.167.01.02>
- 1764 Claringbould JS, Bell RE, Jackson CA-L, et al (2017) Pre-existing normal faults have limited control on  
1765 the rift geometry of the northern North Sea. *Earth Planet Sci Lett* 475:190–206
- 1766 Clarke DB, Beutel EK (this volume) Davis Strait paleocene picrites: Products of a plume or plates?  
1767 *Earth-Sci Rev*
- 1768 Clerc C, Jolivet L, Ringenbach JC (2015) Ductile extensional shear zones in the lower crust of a passive  
1769 margin. *Earth Planet Sci Lett* 431:1–7
- 1770 Clerc C, Ringenbach J-C, Jolivet L, Ballard J-F (2018) Rifted margins: Ductile deformation, boudinage,  
1771 continentward-dipping normal faults and the role of the weak lower crust. *Gondwana Res*  
1772 53:20–40. <https://doi.org/10.1016/j.gr.2017.04.030>
- 1773 Cloetingh S, Van Wees JD, Van der Beek PA, Spadini G (1995) Role of pre-rift rheology in kinematics  
1774 of extensional basin formation: constraints from thermomechanical models of  
1775 Mediterranean and intracratonic basins. *Mar Pet Geol* 12:793–807

- 1776 Cocks LRM, Torsvik TH (2006) European geography in a global context from the Vendian to the end  
1777 of the Palaeozoic. *Geol Soc Lond Mem* 32:83–95.  
1778 <https://doi.org/10.1144/GSL.MEM.2006.032.01.05>
- 1779 Cocks LRM, Torsvik TH (2011) The Palaeozoic geography of Laurentia and western Laurussia: A stable  
1780 craton with mobile margins. *Earth-Sci Rev* 106:1–51.  
1781 <https://doi.org/10.1016/j.earscirev.2011.01.007>
- 1782 Collanega L, Massironi M, Breda A, Kjølhamar BE (2017) Onset of N-Atlantic rifting in the Hoop Fault  
1783 Complex (SW Barents Sea): An orthorhombic dominated faulting? *Tectonophysics* 706:59–70
- 1784 Corfu F, Gasser D, Chew DM (2014) New Perspectives on the Caledonides of Scandinavia and Related  
1785 Areas. Geological Society, London
- 1786 Corti G, van Wijk J, Cloetingh S, Morley CK (2007) Tectonic inheritance and continental rift  
1787 architecture: Numerical and analogue models of the East African Rift system. *Tectonics*  
1788 26:TC6006. <https://doi.org/10.1029/2006TC002086>
- 1789 Cotte N, Pedersen HA (2002) Sharp contrast in lithospheric structure across the Sorgenfrei–Tornquist  
1790 Zone as inferred by Rayleigh wave analysis of TOR1 project data. *Tectonophysics* 360:75–88.  
1791 [https://doi.org/10.1016/S0040-1951\(02\)00348-7](https://doi.org/10.1016/S0040-1951(02)00348-7)
- 1792 Coward MP (1990) The Precambrian, Caledonian and Variscan framework to NW Europe. *Geol Soc  
1793 Lond Spec Publ* 55:1–34
- 1794 Coward MP, Dewey J, Hempton M, Holroyd J (2003) Tectonic evolution. *Millenn Atlas Pet Geol Cent  
1795 North North Sea Geol Soc Lond* 17:33
- 1796 Cowie PA, Underhill JR, Behn MD, et al (2005) Spatio-temporal evolution of strain accumulation  
1797 derived from multi-scale observations of Late Jurassic rifting in the northern North Sea: A  
1798 critical test of models for lithospheric extension. *Earth Planet Sci Lett* 234:401–419
- 1799 Dahl-Jensen T, Thybo H, Hopper J, Rosing M (1998) Crustal structure at the SE Greenland margin  
1800 from wide-angle and normal incidence seismic data. *Tectonophysics* 288:191–198
- 1801 Daly MC, Chorowicz J, Fairhead JD (1989) Rift basin evolution in Africa: the influence of reactivated  
1802 steep basement shear zones. *Geol Soc Lond Spec Publ* 44:309–334
- 1803 Dalziel IWD, Dewey JF (2018) The classic Wilson cycle revisited. *Geol Soc Lond Spec Publ*  
1804 470:SP470.1. <https://doi.org/10.1144/SP470.1>
- 1805 Darbyshire FA, Bastow ID, Forte AM, et al (2015) Variability and origin of seismic anisotropy across  
1806 eastern Canada: Evidence from shear wave splitting measurements. *J Geophys Res Solid  
1807 Earth* 120:8404–8421
- 1808 Darbyshire FA, White RS, Priestley KF (2000) Structure of the crust and uppermost mantle of Iceland  
1809 from a combined seismic and gravity study. *Earth Planet Sci Lett* 181:409–428.  
1810 [https://doi.org/10.1016/S0012-821X\(00\)00206-5](https://doi.org/10.1016/S0012-821X(00)00206-5)
- 1811 De Paola N, Mirabella F, Barchi MR, Burchielli F (2006) Early orogenic normal faults and their  
1812 reactivation during thrust belt evolution: the Gubbio Fault case study, Umbria-Marche  
1813 Apennines (Italy). *J Struct Geol* 28:1948–1957

- 1814 Deng C, Fossen H, Gawthorpe RL, et al (2017a) Influence of fault reactivation during multiphase  
1815 rifting: the Oseberg area, Northern North Sea rift. *Mar Pet Geol* 86:1252–1272
- 1816 Deng C, Gawthorpe RL, Finch E, Fossen H (2017b) Influence of a pre-existing basement weakness on  
1817 normal fault growth during oblique extension: Insights from discrete element modeling. *J*  
1818 *Struct Geol* 105:44–61
- 1819 Deng C, Gawthorpe RL, Fossen H, Finch E (2018) How does the orientation of a pre-existing  
1820 basement weakness influence fault development during renewed rifting? Insights from  
1821 three-dimensional discrete element modeling. *Tectonics*
- 1822 Dewey J, Spall H (1975) Pre-Mesozoic plate tectonics: How far back in Earth history can the Wilson  
1823 Cycle be extended? *Geology* 3:422–424. [https://doi.org/10.1130/0091-  
1824 7613\(1975\)3<422:PPTHFB>2.0.CO;2](https://doi.org/10.1130/0091-7613(1975)3<422:PPTHFB>2.0.CO;2)
- 1825 Dewey JF (2005) Orogeny can be very short. *Proc Natl Acad Sci* 102:15286–15293.  
1826 <https://doi.org/10.1073/pnas.0505516102>
- 1827 Dewey JF, Ryan PD, Andersen TB (1993) Orogenic uplift and collapse, crustal thickness, fabrics and  
1828 metamorphic phase changes: the role of eclogites. *Geol Soc Lond Spec Publ* 76:325–343.  
1829 <https://doi.org/10.1144/GSL.SP.1993.076.01.16>
- 1830 Dewey JF, Strachan RA (2003) Changing Silurian–Devonian relative plate motion in the Caledonides:  
1831 sinistral transpression to sinistral transtension. *J Geol Soc* 160:219–229.  
1832 <https://doi.org/10.1144/0016-764902-085>
- 1833 Dineva S, Eaton D, Ma S, Mereu R (2007) The October 2005 Georgian Bay, Canada, earthquake  
1834 sequence: Mafic Dykes and their role in the mechanical heterogeneity of Precambrian crust.  
1835 *Bull Seismol Soc Am* 97:457–473
- 1836 Dobrzhinetskaya LF, Eide EA, Larsen RB, et al (1995) Microdiamond in high-grade metamorphic rocks  
1837 of the Western Gneiss region, Norway. *Geology* 23:597–600. [https://doi.org/10.1130/0091-  
1838 7613\(1995\)023<0597:MIHGMR>2.3.CO;2](https://doi.org/10.1130/0091-7613(1995)023<0597:MIHGMR>2.3.CO;2)
- 1839 Dooley T, McClay K (1997) Analog modeling of pull-apart basins. *AAPG Bull* 81:1804–1826
- 1840 Doré AG (1991) The structural foundation and evolution of Mesozoic seaways between Europe and  
1841 the Arctic. *Palaeogeogr Palaeoclimatol Palaeoecol* 87:441–492
- 1842 Doré AG, Lundin ER (1996) Cenozoic compressional structures on the NE Atlantic margin; nature,  
1843 origin and potential significance for hydrocarbon exploration. *Pet Geosci* 2:299–311.  
1844 <https://doi.org/10.1144/petgeo.2.4.299>
- 1845 Doré AG, Lundin ER, Fichler C, Olesen O (1997) Patterns of basement structure and reactivation  
1846 along the NE Atlantic margin. *J Geol Soc* 154:85–92.  
1847 <https://doi.org/10.1144/gsjgs.154.1.0085>
- 1848 Doré AG, Lundin ER, Gibbons A, et al (2015) Transform margins of the Arctic: a synthesis and re-  
1849 evaluation. *Geol Soc Lond Spec Publ* 431:SP431.8. <https://doi.org/10.1144/SP431.8>
- 1850 Doré AG, Lundin ER, Jensen LN, et al (1999) Principal tectonic events in the evolution of the  
1851 northwest European Atlantic margin. *Geol Soc Lond Pet Geol Conf Ser* 5:41–61.  
1852 <https://doi.org/10.1144/0050041>

- 1853 Doré AG, Lundin ER, Kuszniir NJ, Pascal C (2008) Potential mechanisms for the genesis of Cenozoic  
1854 domal structures on the NE Atlantic margin: pros, cons and some new ideas. *Geol Soc Lond*  
1855 *Spec Publ* 306:1–26. <https://doi.org/10.1144/SP306.1>
- 1856 Døssing A, Dahl-Jensen T, Thybo H, et al (2008) East Greenland Ridge in the North Atlantic Ocean: an  
1857 integrated geophysical study of a continental sliver in a boundary transform fault setting. *J*  
1858 *Geophys Res Solid Earth* 113:
- 1859 Doubre C, Geoffroy L (2003) Rift-zone development around a plume-related magma centre on the  
1860 Isle of Skye (Scotland): a model for stress inversions. *Terra Nova* 15:230–237
- 1861 Dovzhikova E, Pease V, Remizov D (2004) Neoproterozoic island arc magmatism beneath the  
1862 Pechora Basin, NW Russia. *Gff* 126:353–362
- 1863 Du Z, Foulger GR (2001) Variation in the crustal structure across central Iceland. *Geophys J Int*  
1864 145:246–264. <https://doi.org/10.1111/j.1365-246X.2001.00377.x>
- 1865 Duffy OB, Bell RE, Jackson CA-L, et al (2015) Fault growth and interactions in a multiphase rift fault  
1866 network: Horda Platform, Norwegian North Sea. *J Struct Geol* 80:99–119
- 1867 Duffy OB, Nixon CW, Bell RE, et al (2017) The topology of evolving rift fault networks: Single-phase vs  
1868 multi-phase rifts. *J Struct Geol* 96:192–202
- 1869 Dunbar JA, Sawyer DS (1989a) Patterns of continental extension along the conjugate margins of the  
1870 central and North Atlantic Oceans and Labrador Sea. *Tectonics* 8:1059–1077
- 1871 Dunbar JA, Sawyer DS (1989b) How preexisting weaknesses control the style of continental breakup.  
1872 *J Geophys Res Solid Earth* 94:7278–7292. <https://doi.org/10.1029/JB094iB06p07278>
- 1873 Duret T, Petri B, Mohn G, et al (2016) The importance of structural softening for the evolution and  
1874 architecture of passive margins. *Sci Rep* 6:38704. <https://doi.org/10.1038/srep38704>
- 1875 Eagles G, Pérez-Díaz L, Scarselli N (2015) Getting over continent ocean boundaries. *Earth-Sci Rev*  
1876 151:244–265. <https://doi.org/10.1016/j.earscirev.2015.10.009>
- 1877 Ebbing J, Lundin E, Olesen O, Hansen EK (2006) The mid-Norwegian margin: a discussion of crustal  
1878 lineaments, mafic intrusions, and remnants of the Caledonian root by 3D density modelling  
1879 and structural interpretation. *J Geol Soc* 163:47–59. <https://doi.org/10.1144/0016-764905-029>  
1880
- 1881 Ebinger CJ, Casey M (2001) Continental breakup in magmatic provinces: An Ethiopian example.  
1882 *Geology* 29:527–530
- 1883 Ebinger CJ, van Wijk J, Keir D (2013) The time scales of continental rifting: Implications for global  
1884 processes. *Geol Soc Am Spec Pap* 500:371–396
- 1885 Eldholm O, Grue K (1994) North Atlantic volcanic margins: Dimensions and production rates. *J*  
1886 *Geophys Res Solid Earth* 99:2955–2968. <https://doi.org/10.1029/93JB02879>
- 1887 Eldholm O, Tsikalas F, Faleide JJ (2002) Continental margin off Norway 62–75 N: Palaeogene tectono-  
1888 magmatic segmentation and sedimentation. *Geol Soc Lond Spec Publ* 197:39–68

- 1889 Elkins-Tanton LT (2005) Continental magmatism caused by lithospheric delamination. In: Special  
1890 Paper 388: Plates, plumes and paradigms. Geological Society of America, pp 449–461
- 1891 Elliott GM, Parson LM (2008) Influence of margin segmentation upon the break-up of the Hatton  
1892 Bank rifted margin, NE Atlantic. *Tectonophysics* 457:161–176
- 1893 Ellis D, Stoker MS (2014) The Faroe–Shetland Basin: a regional perspective from the Paleocene to the  
1894 present day and its relationship to the opening of the North Atlantic Ocean. *Geol Soc Lond*  
1895 *Spec Publ* 397:SP397.1. <https://doi.org/10.1144/SP397.1>
- 1896 England P, Houseman G (1986) Finite strain calculations of continental deformation: 2. Comparison  
1897 with the India-Asia Collision Zone. *J Geophys Res Solid Earth* 91:3664–3676.  
1898 <https://doi.org/10.1029/JB091iB03p03664>
- 1899 Ernst RE, Buchan KL (2004) Igneous rock associations in Canada 3. Large Igneous Provinces (LIPs) in  
1900 Canada and adjacent regions: 3 Ga to present. *Geosci Can* 31:
- 1901 Escartín J, Mével C, MacLeod CJ, McCaig AM (2003) Constraints on deformation conditions and the  
1902 origin of oceanic detachments: The Mid-Atlantic Ridge core complex at 15 45' N. *Geochem*  
1903 *Geophys Geosystems* 4:
- 1904 Færseth RB (1996) Interaction of Permo-Triassic and Jurassic extensional fault-blocks during the  
1905 development of the northern North Sea. *J Geol Soc* 153:931–944
- 1906 Færseth RB, Gabrielsen RH, Hurich CA (1995) Influence of basement in structuring of the North Sea  
1907 basin, offshore southwest Norway. *Nor Geol Tidsskr* 75:105–119
- 1908 Faleide JJ, Tsikalas F, Breivik AJ, et al (2008) Structure and evolution of the continental margin off  
1909 Norway and the Barents Sea. *Episodes* 31:82–91
- 1910 Fazlikhani H, Fossen H, Gawthorpe RL, et al (2017) Basement structure and its influence on the  
1911 structural configuration of the northern North Sea rift. *Tectonics* 36:1151–1177
- 1912 Fedorova T, Jacoby WR, Wallner H (2005) Crust–mantle transition and Moho model for Iceland and  
1913 surroundings from seismic, topography, and gravity data. *Tectonophysics* 396:119–140.  
1914 <https://doi.org/10.1016/j.tecto.2004.11.004>
- 1915 Fichler C, Odinsen T, Rueslåtten H, et al (2011) Crustal inhomogeneities in the Northern North Sea  
1916 from potential field modeling: Inherited structure and serpentinites? *Tectonophysics*  
1917 510:172–185. <https://doi.org/10.1016/j.tecto.2011.06.026>
- 1918 Fletcher R, Kuszniir N, Roberts A, Hunsdale R (2013) The formation of a failed continental breakup  
1919 basin: The Cenozoic development of the Faroe-Shetland Basin. *Basin Res* 25:532–553.  
1920 <https://doi.org/10.1111/bre.12015>
- 1921 Foley SF (1989) Emplacement features of lamprophyre and carbonatitic lamprophyre dykes at Aillik  
1922 Bay, Labrador. *Geol Mag* 126:29–42. <https://doi.org/10.1017/S0016756800006129>
- 1923 Fossen H (2010) Extensional tectonics in the North Atlantic Caledonides: a regional view. *Geol Soc*  
1924 *Lond Spec Publ* 335:767–793. <https://doi.org/10.1144/SP335.31>
- 1925 Fossen H (1992) The role of extensional tectonics in the Caledonides of south Norway. *J Struct Geol*  
1926 14:1033–1046. [https://doi.org/10.1016/0191-8141\(92\)90034-T](https://doi.org/10.1016/0191-8141(92)90034-T)

- 1927 Fossen H, Cavalcante GC, Almeida RP de (2017) Hot Versus Cold Orogenic Behavior: Comparing the  
 1928 Araçuaí-West Congo and the Caledonian Orogens. *Tectonics* 36:2159–2178.  
 1929 <https://doi.org/10.1002/2017TC004743>
- 1930 Fossen H, Dunlap WJ (1998) Timing and kinematics of Caledonian thrusting and extensional collapse,  
 1931 southern Norway: evidence from <sup>40</sup>Ar/<sup>39</sup>Ar thermochronology. *J Struct Geol* 20:765–781.  
 1932 [https://doi.org/10.1016/S0191-8141\(98\)00007-8](https://doi.org/10.1016/S0191-8141(98)00007-8)
- 1933 Fossen H, Dunlap WJ (1999) On the age and tectonic significance of Permo-Triassic dikes in the  
 1934 Bergen-Sunnhordland region, southwestern Norway. *Nor Geol Tidsskr* 79:169–178
- 1935 Fossen H, Gabrielsen RH, Faleide JJ, Hurich CA (2014) Crustal stretching in the Scandinavian  
 1936 Caledonides as revealed by deep seismic data. *Geology* 42:791–794
- 1937 Fossen H, Hurich CA (2005) The Hardangerfjord Shear Zone in SW Norway and the North Sea: a  
 1938 large-scale low-angle shear zone in the Caledonian crust. *J Geol Soc* 162:675–687
- 1939 Fossen H, Pedersen RB, Bergh S, Andresen A (2008) Creation of a mountain chain. *Mak Land - Geol*  
 1940 *Nor*
- 1941 Foulger GR (2006) Older crust underlies Iceland. *Geophys J Int* 165:672–676.  
 1942 <https://doi.org/10.1111/j.1365-246X.2006.02941.x>
- 1943 Foulger GR (2002) Plumes, or plate tectonic processes? *Astron Geophys* 43:6–19
- 1944 Foulger GR (2010) *Plates vs Plumes: A Geological Controversy*, 1 edition. Wiley-Blackwell, Hoboken,  
 1945 N.J
- 1946 Foulger GR, Anderson DL (2005) A cool model for the Iceland hotspot. *J Volcanol Geotherm Res*  
 1947 141:1–22. <https://doi.org/10.1016/j.jvolgeores.2004.10.007>
- 1948 Foulger GR, Doré T, Emeleus CH, et al (2019) A continental Greenland-Iceland-Faroe Ridge. *Earth-Sci*  
 1949 *Rev* 102926. <https://doi.org/10.1016/j.earscirev.2019.102926>
- 1950 Foulger GR, Du Z, Julian BR (2003) Icelandic-type crust. *Geophys J Int* 155:567–590.  
 1951 <https://doi.org/10.1046/j.1365-246X.2003.02056.x>
- 1952 Foulger GR, Natland JH, Anderson DL (2005) Genesis of the Iceland melt anomaly by plate tectonic  
 1953 processes. *Geol Soc Am Spec Pap* 388:595–625. <https://doi.org/10.1130/0-8137-2388-4.595>
- 1954 Franke D (2013) Rifting, lithosphere breakup and volcanism: Comparison of magma-poor and  
 1955 volcanic rifted margins. *Mar Pet Geol* 43:63–87.  
 1956 <https://doi.org/10.1016/j.marpetgeo.2012.11.003>
- 1957 Franke W (2006) The Variscan orogen in Central Europe: construction and collapse. *Geol Soc Lond*  
 1958 *Mem* 32:333–343
- 1959 Frederiksen S, Nielsen SB, Balling N (2001) Post-Permian evolution of the Central North Sea: a  
 1960 numerical model. *Tectonophysics* 343:185–203
- 1961 Funck T, Erlendsson Ö, Geissler WH, et al (2016a) A review of the NE Atlantic conjugate margins  
 1962 based on seismic refraction data. *Geol Soc Lond Spec Publ* 447:SP447.9.  
 1963 <https://doi.org/10.1144/SP447.9>

- 1964 Funck T, Geissler WH, Kimbell GS, et al (2016b) Moho and basement depth in the NE Atlantic Ocean  
 1965 based on seismic refraction data and receiver functions. *Geol Soc Lond Spec Publ*  
 1966 447:SP447.1. <https://doi.org/10.1144/SP447.1>
- 1967 Funck T, Gohl K, Damm V, Heyde I (2012) Tectonic evolution of southern Baffin Bay and Davis Strait:  
 1968 Results from a seismic refraction transect between Canada and Greenland. *J Geophys Res*  
 1969 *Solid Earth* 117:. <https://doi.org/10.1029/2011JB009110>
- 1970 Funck T, Jackson HR, Loudon KE, Klingelhöfer F (2007) Seismic study of the transform-rifted margin in  
 1971 Davis Strait between Baffin Island (Canada) and Greenland: What happens when a plume  
 1972 meets a transform. *J Geophys Res Solid Earth* 112:B04402.  
 1973 <https://doi.org/10.1029/2006JB004308>
- 1974 Gabrielsen RH, Fossen H, Faleide JJ, Hurich CA (2015) Mega-scale Moho relief and the structure of  
 1975 the lithosphere on the eastern flank of the Viking Graben, offshore southwestern Norway.  
 1976 *Tectonics* 34:803–819
- 1977 Gabrielsen RH, Nystuen JP, Olesen O (2018) Fault distribution in the Precambrian basement of South  
 1978 Norway. *J Struct Geol* 108:269–289
- 1979 Gac S, Geoffroy L (2009) 3D Thermo-mechanical modelling of a stretched continental lithosphere  
 1980 containing localized low-viscosity anomalies (the soft-point theory of plate break-up).  
 1981 *Tectonophysics* 468:158–168
- 1982 Gaina C, Gernigon L, Ball P (2009) Palaeocene–Recent plate boundaries in the NE Atlantic and the  
 1983 formation of the Jan Mayen microcontinent. *J Geol Soc* 166:601–616.  
 1984 <https://doi.org/10.1144/0016-76492008-112>
- 1985 Gaina C, Nasuti A, Kimbell GS, Blischke A (2017) Break-up and seafloor spreading domains in the NE  
 1986 Atlantic. *Geol Soc Lond Spec Publ* 447:SP447–12
- 1987 Gasser D (2013) The Caledonides of Greenland, Svalbard and other Arctic areas: status of research  
 1988 and open questions. *Geol Soc Lond Spec Publ* 390:93–129.  
 1989 <https://doi.org/10.1144/SP390.17>
- 1990 Gee DG (2015) Caledonides of Scandinavia, Greenland, and Svalbard. In: *Reference Module in Earth*  
 1991 *Systems and Environmental Sciences*. Elsevier
- 1992 Gee DG, Bogolepova OK, Lorenz H (2006) The Timanide, Caledonide and Uralide orogens in the  
 1993 Eurasian high Arctic, and relationships to the palaeo-continent Laurentia, Baltica and  
 1994 Siberia. *Geol Soc Lond Mem* 32:507–520. <https://doi.org/10.1144/GSL.MEM.2006.032.01.31>
- 1995 Gee DG, Fossen H, Henriksen N, Higgins AK (2008) From the early Paleozoic platforms of Baltica and  
 1996 Laurentia to the Caledonide orogen of Scandinavia and Greenland. In: *Episodes*. Episodes
- 1997 Gee DG, Pease V (2004) The Neoproterozoic Timanide Orogen of eastern Baltica: introduction. *Geol*  
 1998 *Soc Lond Mem* 30:1–3. <https://doi.org/10.1144/GSL.MEM.2004.030.01.01>
- 1999 Geoffroy L (2005) Volcanic passive margins. *Comptes Rendus Geosci* 337:1395–1408.  
 2000 <https://doi.org/10.1016/j.crte.2005.10.006>
- 2001 Geoffroy L (1998) Diapirism and intraplate extension: cause or consequence? *Comptes Rendus Acad*  
 2002 *Sci Ser IIA Earth Planet Sci* 4:267–273

- 2003 Geoffroy L, Aubourg C, Callot J-P, Barrat J-A (2007) Mechanisms of crustal growth in large igneous  
2004 provinces: The north Atlantic province as a case study. *Geol Soc Am Spec Pap* 430:747–774.  
2005 [https://doi.org/10.1130/2007.2430\(34\)](https://doi.org/10.1130/2007.2430(34))
- 2006 Geoffroy L, Burov EB, Werner P (2015) Volcanic passive margins: another way to break up  
2007 continents. *Sci Rep* 5:. <https://doi.org/10.1038/srep14828>
- 2008 Geoffroy L, Callot J-P, Scaillet S, et al (2001) Southeast Baffin volcanic margin and the North  
2009 American-Greenland plate separation. *Tectonics* 20:566–584
- 2010 Geoffroy L, Huchon P, Khanbari K (1998) Did Yemeni Tertiary granites intrude neck zones of a  
2011 stretched continental upper crust? *Terra Nova* 10:196–200
- 2012 Gernigon L, Blischke A, Nasuti A, Sand M (2015) Conjugate volcanic rifted margins, sea-floor  
2013 spreading and microcontinent: Insights from new high-resolution aeromagnetic surveys in  
2014 the Norway Basin. *Tectonics* 2014TC003717. <https://doi.org/10.1002/2014TC003717>
- 2015 Gernigon L, Brönnner M (2012) Late Palaeozoic architecture and evolution of the southwestern  
2016 Barents Sea: insights from a new generation of aeromagnetic data. *J Geol Soc* 169:449–459
- 2017 Gernigon L, Brönnner M, Dumais M-A, et al (2018) Basement inheritance and salt structures in the SE  
2018 Barents Sea: Insights from new potential field data. *J Geodyn* 119:82–106.  
2019 <https://doi.org/10.1016/j.jog.2018.03.008>
- 2020 Gernigon L, Brönnner M, Roberts D, et al (2014) Crustal and basin evolution of the southwestern  
2021 Barents Sea: From Caledonian orogeny to continental breakup. *Tectonics* 33:2013TC003439.  
2022 <https://doi.org/10.1002/2013TC003439>
- 2023 Gernigon L, Franke D, Geoffroy L, et al (this volume) Crustal fragmentation, magmatism, and the  
2024 diachronous opening of the Norwegian-Greenland Sea. *Earth-Sci Rev.*  
2025 <https://doi.org/10.1016/j.earscirev.2019.04.011>
- 2026 Gernigon L, Gaina C, Olesen O, et al (2012) The Norway Basin revisited: From continental breakup to  
2027 spreading ridge extinction. *Mar Pet Geol* 35:1–19.  
2028 <https://doi.org/10.1016/j.marpetgeo.2012.02.015>
- 2029 Gernigon L, Lucazeau F, Brigaud F, et al (2006) A moderate melting model for the Vøring margin  
2030 (Norway) based on structural observations and a thermo-kinematical modelling: Implication  
2031 for the meaning of the lower crustal bodies. *Tectonophysics* 412:255–278.  
2032 <https://doi.org/10.1016/j.tecto.2005.10.038>
- 2033 Gernigon L, Ringenbach JC, Planke S, et al (2003) Extension, crustal structure and magmatism at the  
2034 outer Vøring Basin, Norwegian margin. *J Geol Soc* 160:197–208
- 2035 Gernigon L, Ringenbach J-C, Planke S, Le Gall B (2004) Deep structures and breakup along volcanic  
2036 rifted margins: insights from integrated studies along the outer Vøring Basin (Norway). *Mar*  
2037 *Pet Geol* 21:363–372. <https://doi.org/10.1016/j.marpetgeo.2004.01.005>
- 2038 Gerya T (2012) Origin and models of oceanic transform faults. *Tectonophysics* 522–523:34–54.  
2039 <https://doi.org/10.1016/j.tecto.2011.07.006>
- 2040 Gilotti JA, McClelland WC (2011) Geochemical and geochronological evidence that the North-East  
2041 Greenland ultrahigh-pressure terrane is Laurentian crust. *J Geol* 119:439–456

- 2042 Gilotti JA, McClelland WC, Wooden JL (2014) Zircon captures exhumation of an ultrahigh-pressure  
2043 terrane, North-East Greenland Caledonides. *Gondwana Res* 25:235–256.  
2044 <https://doi.org/10.1016/j.gr.2013.03.018>
- 2045 Glennie KW (1998) *Petroleum Geology of the North Sea 4e: Basic Concepts and Recent Advances*, 4  
2046 edition. John Wiley & Sons, Oxford ; Malden, MA
- 2047 Glennie KW, Higham J, Stemmerik L (2003) The Permian of the Northern North Sea. In: *Millennium*  
2048 *Atlas: Petroleum Geology of the Central and Northern North Sea*. Geological Society of  
2049 London, pp 91–103
- 2050 Goldschmidt-Rokita A, Hansch KJF, Hirschleber HB, et al (1994) The ocean/continent transition along  
2051 a profile through the Lofoten basin, Northern Norway. *Mar Geophys Res* 16:201–224.  
2052 <https://doi.org/10.1007/BF01237514>
- 2053 Gorbatshev R, Bogdanova S (1993) Frontiers in the Baltic Shield. *Precambrian Res* 64:3–21.  
2054 [https://doi.org/10.1016/0301-9268\(93\)90066-B](https://doi.org/10.1016/0301-9268(93)90066-B)
- 2055 Gorczyk W, Vogt K (2015) Tectonics and melting in intra-continental settings. *Gondwana Res* 27:196–  
2056 208. <https://doi.org/10.1016/j.gr.2013.09.021>
- 2057 Gordon RG (1998) The plate tectonic approximation: Plate nonrigidity, diffuse plate boundaries, and  
2058 global plate reconstructions. *Annu Rev Earth Planet Sci* 26:615–642
- 2059 Gouiza M, Paton DA (2019) The role of inherited lithospheric heterogeneities in defining the crustal  
2060 architecture of rifted margins and the magmatic budget during continental breakup.  
2061 *Geochem Geophys Geosystems*
- 2062 Grant N, Bouma A, McIntyre A (1999) The Turonian play in the Faeroe–Shetland Basin. In: *Geological*  
2063 *Society, London, Petroleum Geology Conference series*. Geological Society of London, pp  
2064 661–673
- 2065 Gregersen U, Knutz PC, Hopper JR (2016) New geophysical and geological mapping of the eastern  
2066 Baffin Bay region, offshore West Greenland. *Geol Surv Den Greenl Bull* 83–86
- 2067 Grocott J, McCaffrey KJW (2017) Basin evolution and destruction in an Early Proterozoic continental  
2068 margin: the Rinkian fold–thrust belt of central West Greenland. *J Geol Soc* 174:453–467.  
2069 <https://doi.org/10.1144/jgs2016-109>
- 2070 Grunnaleite I, Gabrielsen RH (1995) Structure of the Møre Basin, mid-Norway continental margin.  
2071 *Tectonophysics* 252:221–251
- 2072 Guan H, Geoffroy L, Gernigon L, et al (2019) Magmatic ocean-continent transitions. *Mar Pet Geol*  
2073 104:438–450
- 2074 Guarnieri P (2015) Pre-break-up palaeostress state along the East Greenland margin. *J Geol Soc*  
2075 172:727–739
- 2076 Gudlaugsson ST, Faleide JJ, Johansen SE, Breivik AJ (1998) Late Palaeozoic structural development of  
2077 the South-western Barents Sea. *Mar Pet Geol* 15:73–102. [https://doi.org/10.1016/S0264-](https://doi.org/10.1016/S0264-8172(97)00048-2)  
2078 [8172\(97\)00048-2](https://doi.org/10.1016/S0264-8172(97)00048-2)

- 2079 Gudmundsson Ó (2003) The dense root of the Iceland crust. *Earth Planet Sci Lett* 206:427–440.  
2080 [https://doi.org/10.1016/S0012-821X\(02\)01110-X](https://doi.org/10.1016/S0012-821X(02)01110-X)
- 2081 Gueydan F, Précigout J, Montési LGJ (2014) Strain weakening enables continental plate tectonics.  
2082 *Tectonophysics* 631:189–196. <https://doi.org/10.1016/j.tecto.2014.02.005>
- 2083 Haase C, Ebbing J, Funck T (2016) A 3D regional crustal model of the NE Atlantic based on seismic  
2084 and gravity data. *Geol Soc Lond Spec Publ* SP447.8. <https://doi.org/10.1144/SP447.8>
- 2085 Hacker BR, Andersen TB, Johnston S, et al (2010) High-temperature deformation during continental-  
2086 margin subduction & exhumation: The ultrahigh-pressure Western Gneiss Region of Norway.  
2087 *Tectonophysics* 480:149–171. <https://doi.org/10.1016/j.tecto.2009.08.012>
- 2088 Hansen J, Jerram DA, McCaffrey K, Passey SR (2009) The onset of the North Atlantic Igneous  
2089 Province in a rifting perspective. *Geol Mag* 146:309–325.  
2090 <https://doi.org/10.1017/S0016756809006347>
- 2091 Harland WB (1971) Tectonic transpression in Caledonian Spitsbergen. *Geol Mag* 108:27–41.  
2092 <https://doi.org/10.1017/S0016756800050937>
- 2093 Harland WB (1969) Contribution of Spitsbergen to Understanding of Tectonic Evolution of North  
2094 Atlantic Region: Chapter 58: Arctic Regions
- 2095 Harry DL, Bowling JC (1999) Inhibiting magmatism on nonvolcanic rifted margins. *Geology* 27:895–  
2096 898
- 2097 Hartz E, Andresen A (1995) Caledonian sole thrust of central East Greenland: A crustal-scale  
2098 Devonian extensional detachment? *Geology* 23:637–640. [https://doi.org/10.1130/0091-7613\(1995\)023<0637:CSTOCE>2.3.CO;2](https://doi.org/10.1130/0091-7613(1995)023<0637:CSTOCE>2.3.CO;2)
- 2100 Hartz EH, Andresen A, Hodges KV, Martin MW (2001) Syncontractional extension and exhumation of  
2101 deep crustal rocks in the East Greenland Caledonides. *Tectonics* 20:58–77
- 2102 Hatcher RD (2002) Alleghanian (Appalachian) orogeny, a product of zipper tectonics: Rotational  
2103 transpressive continent-continent collision and closing of ancient oceans along irregular  
2104 margins. *Spec Pap-Geol Soc Am* 199–208
- 2105 Hatcher RD, Tollo RP, Bartholomew MJ, et al (2010) The Appalachian orogen: A brief summary.  
2106 *Rodinia Pangea Lithotectonic Rec Appalach Reg Geol Soc Am Mem* 206:1–19
- 2107 Healy D, Blenkinsop TG, Timms NE, et al (2015) Polymodal faulting: time for a new angle on shear  
2108 failure. *J Struct Geol* 80:57–71
- 2109 Heeremans M, Faleide JJ (2004) Late Carboniferous-Permian tectonics and magmatic activity in the  
2110 Skagerrak, Kattegat and the North Sea. *Geol Soc Lond Spec Publ* 223:157–176
- 2111 Hejrani B, Balling N, Jacobsen BH, Tilmann F (2015) Upper-mantle P- and S-wave velocities across the  
2112 Northern Tornquist Zone from travelttime tomography. *Geophys J Int* 203:437–458.  
2113 <https://doi.org/10.1093/gji/ggv291>
- 2114 Helffrich G (1995) Lithospheric deformation inferred from teleseismic shear wave splitting  
2115 observations in the United Kingdom. *J Geophys Res Solid Earth* 100:18195–18204

- 2116 Henkel H (1991) Magnetic crustal structures in northern Fennoscandia. *Tectonophysics* 192:57–79
- 2117 Henriksen N (2003) Caledonian Orogen, East Greenland 70–82 N. *Geological Map* 1: 1 000 000. GEUS  
2118 Den
- 2119 Henstra GA, Gawthorpe RL, Helland-Hansen W, et al (2017) Depositional systems in multiphase rifts:  
2120 seismic case study from the Lofoten margin, Norway. *Basin Res* 29:447–469
- 2121 Henstra GA, Rotevatn A, Gawthorpe RL, Ravnås R (2015) Evolution of a major segmented normal  
2122 fault during multiphase rifting: The origin of plan-view zigzag geometry. *J Struct Geol* 74:45–  
2123 63
- 2124 Henza AA, Withjack MO, Schlische RW (2010) Normal-fault development during two phases of non-  
2125 coaxial extension: An experimental study. *J Struct Geol* 32:1656–1667.  
2126 <https://doi.org/10.1016/j.jsg.2009.07.007>
- 2127 Henza AA, Withjack MO, Schlische RW (2011) How do the properties of a pre-existing normal-fault  
2128 population influence fault development during a subsequent phase of extension? *J Struct*  
2129 *Geol* 33:1312–1324
- 2130 Heron P, Peace A, McCaffrey K, et al (2019) Segmentation of rifts through structural inheritance:  
2131 Creation of the Davis Strait
- 2132 Heron PJ (2018) Mantle plumes and mantle dynamics in the Wilson cycle. *Geol Soc Lond Spec Publ*  
2133 470:SP470.18. <https://doi.org/10.1144/SP470.18>
- 2134 Heron PJ, Pysklywec RN, Stephenson R (2016) Lasting mantle scars lead to perennial plate tectonics.  
2135 *Nat Commun* 7:11834. <https://doi.org/10.1038/ncomms11834>
- 2136 Hibbard JP, van Staal CR, Rankin DW (2010) Comparative analysis of the geological evolution of the  
2137 northern and southern Appalachian orogen: Late Ordovician-Permian. In: *Geological Society*  
2138 *of America Memoirs*. Geological Society of America, pp 51–69
- 2139 Hill RI (1991) Starting plumes and continental break-up. *Earth Planet Sci Lett* 104:398–416.  
2140 [https://doi.org/10.1016/0012-821X\(91\)90218-7](https://doi.org/10.1016/0012-821X(91)90218-7)
- 2141 Hjartarson Á, Erlendsson Ö, Blischke A (2017) The Greenland–Iceland–Faroe Ridge Complex. *Geol*  
2142 *Soc Lond Spec Publ* 447:SP447.14. <https://doi.org/10.1144/SP447.14>
- 2143 Holdsworth RE (2004) Weak faults–rotten cores. *Science* 303:181–182
- 2144 Holdsworth RE, Butler CA, Roberts AM (1997) The recognition of reactivation during continental  
2145 deformation. *J Geol Soc* 154:73–78. <https://doi.org/10.1144/gsjgs.154.1.0073>
- 2146 Holdsworth RE, Morton A, Frei D, et al (2019) The nature and significance of the Faroe-Shetland  
2147 Terrane: Linking Archaean basement blocks across the North Atlantic. *Precambrian Res*  
2148 321:154–171
- 2149 Holdsworth RE, Stewart M, Imber J, Strachan RA (2001) The structure and rheological evolution of  
2150 reactivated continental fault zones: a review and case study. *Geol Soc Lond Spec Publ*  
2151 184:115–137

- 2152 Hole MJ, Millett JM (2016) Controls of Mantle Potential Temperature and Lithospheric Thickness on  
 2153 Magmatism in the North Atlantic Igneous Province. *J Petrol* 57:417–436.  
 2154 <https://doi.org/10.1093/petrology/egw014>
- 2155 Hole MJ, Natland JH (2019) Magmatism in the North Atlantic Igneous Province; mantle  
 2156 temperatures, rifting and geodynamics. *Earth-Sci Rev.*  
 2157 <https://doi.org/10.1016/j.earscirev.2019.02.011>
- 2158 Hopper JR, Dahl-Jesnen T, Holbrook WS, et al (2003) Structure of the SE Greenland margin from  
 2159 seismic reflection and refraction data: Implications for nascent spreading center subsidence  
 2160 and asymmetric crustal accretion during North Atlantic opening. *J Geophys Res B Solid Earth*  
 2161 108:EPM 13-1-13-22
- 2162 Horni JÁ, Hopper JR, Blischke A, et al (2017) Regional distribution of volcanism within the North  
 2163 Atlantic Igneous Province. *Geol Soc Lond Spec Publ* 447:105–125.  
 2164 <https://doi.org/10.1144/SP447.18>
- 2165 Hosseinpour M, Müller RD, Williams SE, Whittaker JM (2013) Full-fit reconstruction of the Labrador  
 2166 Sea and Baffin Bay. *Solid Earth* 4:461–479. <https://doi.org/10.5194/se-4-461-2013>
- 2167 Howell SM, Ito G, Breivik AJ, et al (2014) The origin of the asymmetry in the Iceland hotspot along  
 2168 the Mid-Atlantic Ridge from continental breakup to present-day. *Earth Planet Sci Lett*  
 2169 392:143–153
- 2170 Huang B-S, Huang W-G, Liang W-T, et al (2006) Anisotropy beneath an active collision orogen of  
 2171 Taiwan: Results from across islands array observations. *Geophys Res Lett* 33:L24302.  
 2172 <https://doi.org/10.1029/2006GL027844>
- 2173 Huismans R, Beaumont C (2011) Depth-dependent extension, two-stage breakup and cratonic  
 2174 underplating at rifted margins. *Nature* 473:74–78. <https://doi.org/10.1038/nature09988>
- 2175 Hurich CA (1996) Kinematic evolution of the lower plate during intracontinental subduction: An  
 2176 example from the Scandinavian Caledonides. *Tectonics* 15:1248–1263
- 2177 Hynes A, Rivers T (2010) Protracted continental collision—Evidence from the Grenville orogen. *Can J*  
 2178 *Earth Sci* 47:591–620
- 2179 Imber J, Holdsworth RE, Butler CA, Strachan RA (2001) A reappraisal of the Sibson-Scholz fault zone  
 2180 model: The nature of the frictional to viscous (“brittle-ductile”) transition along a long-lived,  
 2181 crustal-scale fault, Outer Hebrides, Scotland. *Tectonics* 20:601–624
- 2182 Imber J, Holdsworth RE, Smith S a. F, et al (2008) Frictional-viscous flow, seismicity and the geology  
 2183 of weak faults: a review and future directions. *Geol Soc Lond Spec Publ* 299:151–173.  
 2184 <https://doi.org/10.1144/SP299.10>
- 2185 Jackson C-L, Chua S-T, Bell RE, Magee C (2013) Structural style and early stage growth of inversion  
 2186 structures: 3D seismic insights from the Egersund Basin, offshore Norway. *J Struct Geol*  
 2187 46:167–185
- 2188 Jackson HR, Reid I (1994) Crustal thickness variations between the Greenland and Ellesmere Island  
 2189 margins determined from seismic refraction. *Can J Earth Sci* 31:1407–1418.  
 2190 <https://doi.org/10.1139/e94-124>

- 2191 Jammes S, Lavier LL (2016) The effect of bimineralic composition on extensional processes at  
2192 lithospheric scale. *Geochem Geophys Geosystems* 17:3375–3392.  
2193 <https://doi.org/10.1002/2016GC006399>
- 2194 Janutyte I, Majdanski M, Voss PH, et al (2015) Upper mantle structure around the Trans-European  
2195 Suture Zone obtained by teleseismic tomography. *Solid Earth*
- 2196 Jauer CD, Oakey GN, Williams G, Wielens JH (2014) Saglek Basin in the Labrador Sea, east coast  
2197 Canada; stratigraphy, structure and petroleum systems. *Bull Can Pet Geol* 62:232–260
- 2198 Jefferies SP, Holdsworth RE, Abramovitz T, et al (2006) Origin and mechanical significance of foliated  
2199 cataclastic rocks in the cores of crustal-scale faults: Examples from the Median Tectonic Line,  
2200 Japan. *J Geophys Res Solid Earth* 111:. <https://doi.org/10.1029/2005JB004205>
- 2201 Johnson H, Ritchie JD, Hitchen K, et al (2005) Aspects of the Cenozoic deformational history of the  
2202 Northeast Faroe–Shetland Basin, Wyville–Thomson Ridge and Hatton Bank areas. *Geol Soc  
2203 Lond Pet Geol Conf Ser* 6:993–1007
- 2204 Jones MT, Augland LE, Shephard GE, et al (2017) Constraining shifts in North Atlantic plate motions  
2205 during the Palaeocene by U–Pb dating of Svalbard tephra layers. *Sci Rep* 7:6822
- 2206 Jongepier K, Rui JC, Grue K (1996) Triassic to Early Cretaceous stratigraphic and structural  
2207 development of the northeastern Møre Basin margin, off Mid-Norway. *Nor Geol Tidsskr*  
2208 76:199
- 2209 Kaban MK, Flóvenz ÓG, Pálmason G (2002) Nature of the crust-mantle transition zone and the  
2210 thermal state of the upper mantle beneath Iceland from gravity modelling. *Geophys J Int*  
2211 149:281–299. <https://doi.org/10.1046/j.1365-246X.2002.01622.x>
- 2212 Kalsbeek F, Higgins AK, Jepsen HF, et al (2008) Granites and granites in the East Greenland  
2213 Caledonides. *Geol Soc Am Mem* 202:227–249. [https://doi.org/10.1130/2008.1202\(09\)](https://doi.org/10.1130/2008.1202(09))
- 2214 Kandilarov A, Mjelde R, Flueh E, Pedersen RB (2015) Vp/Vs-ratios and anisotropy on the northern Jan  
2215 Mayen Ridge, North Atlantic, determined from ocean bottom seismic data. *Polar Sci* 9:293–  
2216 310
- 2217 Karabinos P, Samson SD, Hepburn JC, Stoll HM (1998) Taconian orogeny in the New England  
2218 Appalachians: Collision between Laurentia and the Shelburne Falls arc. *Geology* 26:215–218.  
2219 [https://doi.org/10.1130/0091-7613\(1998\)026<0215:TOITNE>2.3.CO;2](https://doi.org/10.1130/0091-7613(1998)026<0215:TOITNE>2.3.CO;2)
- 2220 Karson JA, Brooks CK (1999) Structural and magmatic segmentation of the Tertiary East Greenland  
2221 volcanic rifted margin. *Geol Soc Lond Spec Publ* 164:313–338
- 2222 Katz RF, Ragnarsson R, Bodenschatz E (2005) Tectonic microplates in a wax model of sea-floor  
2223 spreading. *New J Phys* 7:37
- 2224 Kay RW, Kay SM (1993) Delamination and delamination magmatism. *Tectonophysics* 219:177–189
- 2225 Keen CE, Dickie K, Dafoe LT (2018) Structural evolution of the rifted margin off northern Labrador:  
2226 The role of hyperextension and magmatism. *Tectonics* 37:1955–1972
- 2227 Keen CE, Dickie K, Dafoe LT (2017) Structural characteristics of the ocean-continent transition along  
2228 the rifted continental margin, offshore central Labrador. *Mar Pet Geol*

- 2229 Keep M, McClay KR (1997) Analogue modelling of multiphase rift systems. *Tectonophysics* 273:239–  
2230 270
- 2231 Keir D, Ebinger CJ, Stuart GW, et al (2006) Strain accommodation by magmatism and faulting as  
2232 rifting proceeds to breakup: Seismicity of the northern Ethiopian rift. *J Geophys Res Solid*  
2233 *Earth* 111:
- 2234 Kimbell GS, Ritchie JD, Johnson H, Gatliff RW (2005a) Controls on the structure and evolution of the  
2235 NE Atlantic margin revealed by regional potential field imaging and 3D modelling. *Geol Soc*  
2236 *Lond Pet Geol Conf Ser* 6:933–945. <https://doi.org/10.1144/0060933>
- 2237 Kimbell GS, Ritchie JD, Johnson H, Gatliff RW (2005b) Controls on the structure and evolution of the  
2238 NE Atlantic margin revealed by regional potential field imaging and 3D modelling. *Geol Soc*  
2239 *Lond Pet Geol Conf Ser* 6:933–945. <https://doi.org/10.1144/0060933>
- 2240 Kimbell GS, Stewart MA, Gradmann S, et al (2017) Controls on the location of compressional  
2241 deformation on the NW European margin. *Geol Soc Lond Spec Publ* 447:249–278
- 2242 King SD, Anderson DL (1998) Edge-driven convection. *Earth Planet Sci Lett* 160:289–296.  
2243 [https://doi.org/10.1016/S0012-821X\(98\)00089-2](https://doi.org/10.1016/S0012-821X(98)00089-2)
- 2244 Klausen MB, Larsen HCS (2002) East Greenland coast-parallel dike swarm and its role in continental  
2245 breakup. *Geol Soc Am Spec Pap* 362:133–158. <https://doi.org/10.1130/0-8137-2362-0.133>
- 2246 Klausen MB, Nilsson MKM (2018) The Melville Bugt Dyke Swarm across SE Greenland: A closer link to  
2247 Mesoproterozoic AMCG-complexes. *Precambrian Res.*  
2248 <https://doi.org/10.1016/j.precamres.2018.06.001>
- 2249 Klemperer SL, Hobbs RW, Freeman B (1990) Dating the source of lower crystal reflectivity using  
2250 BIRPS deep seismic profiles across the Iapetus suture. *Tectonophysics* 173:445–454.  
2251 [https://doi.org/10.1016/0040-1951\(90\)90237-3](https://doi.org/10.1016/0040-1951(90)90237-3)
- 2252 Klemperer SL, Hurich CA (1990) Lithospheric structure of the North Sea from deep seismic reflection  
2253 profiling. *Blundell DJ Gibbs AD Eds Tecton Evol North Sea Rifts Oxf Univ Press*-63
- 2254 Kley J (2018) Timing and spatial patterns of Cretaceous and Cenozoic inversion in the Southern  
2255 Permian Basin. *Geol Soc Lond Spec Publ* 469:SP469–12
- 2256 Klingelhöfer F, Edwards RA, Hobbs RW, England RW (2005) Crustal structure of the NE Rockall  
2257 Trough from wide-angle seismic data modeling. *J Geophys Res Solid Earth* 110:1–25.  
2258 <https://doi.org/10.1029/2005JB003763>
- 2259 Klitzke P, Franke D, Ehrhardt A, et al (2019) The Paleozoic evolution of the Olga Basin region,  
2260 northern Barents Sea – a link to the Timanian Orogeny. *Geochem Geophys Geosystems* 0:  
2261 <https://doi.org/10.1029/2018GC007814>
- 2262 Kodaira S, Mjelde R, Gunnarsson K, et al (1998) Structure of the Jan Mayen microcontinent and  
2263 implications for its evolution. *Geophys J Int* 132:383–400
- 2264 Köhler A, Maupin V, Balling N (2015) Surface wave tomography across the Sorgenfrei–Tornquist  
2265 Zone, SW Scandinavia, using ambient noise and earthquake data. *Geophys J Int* 203:284–  
2266 311. <https://doi.org/10.1093/gji/ggv297>

- 2267 Koopmann H, Brune S, Franke D, Breuer S (2014) Linking rift propagation barriers to excess  
2268 magmatism at volcanic rifted margins. *Geology* 42:1071–1074.  
2269 <https://doi.org/10.1130/G36085.1>
- 2270 Korenaga J (2004) Mantle mixing and continental breakup magmatism. *Earth Planet Sci Lett*  
2271 218:463–473. [https://doi.org/10.1016/S0012-821X\(03\)00674-5](https://doi.org/10.1016/S0012-821X(03)00674-5)
- 2272 Korenaga J, Holbrook WS, Kent GM, et al (2000) Crustal structure of the southeast Greenland margin  
2273 from joint refraction and reflection seismic tomography. *J Geophys Res Solid Earth*  
2274 105:21591–21614
- 2275 Krabbendam M (2001) When the Wilson Cycle breaks down: how orogens can produce strong  
2276 lithosphere and inhibit their future reworking. *Geol Soc Lond Spec Publ* 184:57–75.  
2277 <https://doi.org/10.1144/GSL.SP.2001.184.01.04>
- 2278 Krabbendam M, Barr TD (2000) Proterozoic orogens and the break-up of Gondwana: why did some  
2279 orogens not rift? *J Afr Earth Sci* 31:35–49. [https://doi.org/10.1016/S0899-5362\(00\)00071-3](https://doi.org/10.1016/S0899-5362(00)00071-3)
- 2280 Kreemer C (2009) Absolute plate motions constrained by shear wave splitting orientations with  
2281 implications for hot spot motions and mantle flow. *J Geophys Res Solid Earth* 114:
- 2282 Kristensen TB, Rotevatn A, Marvik M, et al (2018) Structural evolution of sheared margin basins: the  
2283 role of strain partitioning. Sørvestsnaget Basin, Norwegian Barents Sea. *Basin Res* 30:279–  
2284 301
- 2285 Kristoffersen Y, Talwani M (1977) Extinct triple junction south of Greenland and the Tertiary motion  
2286 of Greenland relative to North America. *Geol Soc Am Bull* 88:1037–1049
- 2287 Kroner U, Romer RL (2013) Two plates—many subduction zones: the Variscan orogeny reconsidered.  
2288 *Gondwana Res* 24:298–329
- 2289 Kuszniir NJ, Park RG (1987) The extensional strength of the continental lithosphere: its dependence  
2290 on geothermal gradient, and crustal composition and thickness. *Geol Soc Lond Spec Publ*  
2291 28:35–52
- 2292 Kuvaas B, Kodaira S (1997) Research article: The formation of the Jan Mayen microcontinent: the  
2293 missing piece in the continental puzzle between the Møre-Vøring Basins and East Greenland.  
2294 *First Break* 15:239–247. <https://doi.org/10.3997/1365-2397.1997008>
- 2295 Lamers E, Carmichael SMM (1999) The Paleocene deepwater sandstone play West of Shetland. In:  
2296 Geological Society, London, Petroleum Geology Conference series. Geological Society of  
2297 London, pp 645–659
- 2298 Larsen LM, Heaman LM, Creaser RA, et al (2009) Tectonomagmatic events during stretching and  
2299 basin formation in the Labrador Sea and the Davis Strait: evidence from age and composition  
2300 of Mesozoic to Palaeogene dyke swarms in West Greenland. *J Geol Soc* 166:999–1012
- 2301 Larsen LM, Pedersen AK, Pedersen GK, Piasecki S (1992) Timing and duration of Early Tertiary  
2302 volcanism in the North Atlantic: new evidence from West Greenland. *Geol Soc Lond Spec*  
2303 *Publ* 68:321–333. <https://doi.org/10.1144/GSL.SP.1992.068.01.20>

- 2304 Lawver LA, Gahagan LM, Norton I (2011) Chapter 5 Palaeogeographic and tectonic evolution of the  
2305 Arctic region during the Palaeozoic. *Geol Soc Lond Mem* 35:61–77.  
2306 <https://doi.org/10.1144/M35.5>
- 2307 Lepercq J-Y, Gaulier J-M (1996) Two-stage rifting in the North Viking Graben area (North Sea):  
2308 inferences from a new three-dimensional subsidence analysis. *Mar Pet Geol* 13:129–148
- 2309 Leslie AG, Smith M, Soper NJ (2008) Laurentian margin evolution and the Caledonian orogeny—A  
2310 template for Scotland and East Greenland. *Geol Soc Am Mem* 202:307–343.  
2311 [https://doi.org/10.1130/2008.1202\(13\)](https://doi.org/10.1130/2008.1202(13))
- 2312 Li Z-X, Bogdanova SV, Collins AS, et al (2008) Assembly, configuration, and break-up history of  
2313 Rodinia: a synthesis. *Precambrian Res* 160:179–210
- 2314 Lie JE, Pedersen T, Husebye ES (1990) Observations of seismic reflectors in the lower lithosphere  
2315 beneath the Skagerrak. *Nature* 346:165–168. <https://doi.org/10.1038/346165a0>
- 2316 Lister GS, Etheridge MA, Symonds PA (1986) Detachment faulting and the evolution of passive  
2317 continental margins. *Geology* 14:246. [https://doi.org/10.1130/0091-  
2318 7613\(1986\)14<246:DFATEO>2.0.CO;2](https://doi.org/10.1130/0091-7613(1986)14<246:DFATEO>2.0.CO;2)
- 2319 Liu L, Morgan JP, Xu Y, Menzies M (2018) Craton Destruction Part I: Cratonic Keel Delamination along  
2320 a weak Mid-Lithospheric Discontinuity layer. *J Geophys Res Solid Earth*
- 2321 Lorenz H, Gee DG, Larionov AN, Majka J (2012) The Grenville–Sveconorwegian orogen in the high  
2322 Arctic. *Geol Mag* 149:875–891. <https://doi.org/10.1017/S0016756811001130>
- 2323 Lowell JD (1995) Mechanics of basin inversion from worldwide examples. *Geol Soc Lond Spec Publ*  
2324 88:39–57. <https://doi.org/10.1144/GSL.SP.1995.088.01.04>
- 2325 Lundin ER, Doré AG (2005) NE Atlantic break-up: a re-examination of the Iceland mantle plume  
2326 model and the Atlantic–Arctic linkage. *Geol Soc Lond Pet Geol Conf Ser* 6:739–754.  
2327 <https://doi.org/10.1144/0060739>
- 2328 Lundin ER, Doré AG (1997) A tectonic model for the Norwegian passive margin with implications for  
2329 the NE Atlantic: Early Cretaceous to break-up. *J Geol Soc* 154:545–550.  
2330 <https://doi.org/10.1144/gsjgs.154.3.0545>
- 2331 Lundin ER, Doré AG (2018) Non-Wilsonian break-up predisposed by transforms: examples from the  
2332 North Atlantic and Arctic. *Geol Soc Lond Spec Publ* 470:SP470.6.  
2333 <https://doi.org/10.1144/SP470.6>
- 2334 Lundin ER, Doré AG (2011) Hyperextension, serpentinization, and weakening: A new paradigm for  
2335 rifted margin compressional deformation. *Geology* 39:347–350.  
2336 <https://doi.org/10.1130/G31499.1>
- 2337 Lundin ER, Doré AG, Redfield TF (2018) Magmatism and extension rates at rifted margins. *Pet Geosci*  
2338 24:379–392
- 2339 Lundin ER, Doré AG, Rønning K, Kyrkjebø R (2013) Repeated inversion and collapse in the Late  
2340 Cretaceous–Cenozoic northern Vøring Basin, offshore Norway. *Pet Geosci* 19:329–341

- 2341 Lundin ER, Redfield TF, Péron-Pindivic G, Pindell J (2014) Rifted continental margins: Geometric  
 2342 influence on crustal architecture and melting. In: 33rd Annual GCSSEPM Foundation Bob F.  
 2343 Perkins Conference. Sedimentary Basins: Origin, Depositional Histories, and Petroleum  
 2344 Systems. Gulf Coast Section SEPM, Houston, TX. p 53
- 2345 Magee C, Bastow ID, van Wyk de Vries B, et al (2017) Structure and dynamics of surface uplift  
 2346 induced by incremental sill emplacement. *Geology* 45:431–434
- 2347 Magee C, McDermott KG, Stevenson CT, Jackson CA-L (2014) Influence of crystallised igneous  
 2348 intrusions on fault nucleation and reactivation during continental extension. *J Struct Geol*  
 2349 62:183–193
- 2350 Majka J, Mazur S, Manecki M, et al (2008) Late Neoproterozoic amphibolite-facies metamorphism of  
 2351 a pre-Caledonian basement block in southwest Wedel Jarlsberg Land, Spitsbergen: new  
 2352 evidence from U–Th–Pb dating of monazite. *Geol Mag* 145:822–830.  
 2353 <https://doi.org/10.1017/S001675680800530X>
- 2354 Makris J, Ginzburg A, Shannon PM, et al (1991) A new look at the Rockall region, offshore Ireland.  
 2355 *Mar Pet Geol* 8:410–416
- 2356 Manatschal G, Lavier L, Chenin P (2015) The role of inheritance in structuring hyperextended rift  
 2357 systems: Some considerations based on observations and numerical modeling. *Gondwana*  
 2358 *Res* 27:140–164. <https://doi.org/10.1016/j.gr.2014.08.006>
- 2359 Mandler HAF, Jokat W (1998) The crustal structure of Central East Greenland: results from combined  
 2360 land–sea seismic refraction experiments. *Geophys J Int* 135:63–76.  
 2361 <https://doi.org/10.1046/j.1365-246X.1998.00586.x>
- 2362 Matte P (2001) The Variscan collage and orogeny (480–290 Ma) and the tectonic definition of the  
 2363 Armorica microplate: a review. *Terra Nova* 13:122–128
- 2364 Maupin V, Agostini A, Artemieva I, et al (2013) The deep structure of the Scandes and its relation to  
 2365 tectonic history and present-day topography. *Tectonophysics* 602:15–37.  
 2366 <https://doi.org/10.1016/j.tecto.2013.03.010>
- 2367 Maystrenko YP, Olesen O, Ebbing J, Nasuti A (2017) Deep structure of the northern North Sea and  
 2368 southwestern Norway based on 3D density and magnetic modelling. *Nor J Geol Geol Foren*  
 2369 97:
- 2370 Mazur S, Campbell S, Green C, Bouatmani R (2015) Extension across the Laptev Sea continental rifts  
 2371 constrained by gravity modeling. *Tectonics* 34:435–448.  
 2372 <https://doi.org/10.1002/2014TC003590>
- 2373 McKerrow WS, Mac Niocaill C, Dewey J (2000) The Caledonian orogeny redefined. *J Geol Soc*  
 2374 157:1149–1154
- 2375 McKerrow WS, Soper NJ (1989) The Iapetus suture in the British Isles. *Geol Mag* 126:1–8
- 2376 McWhae JRH (1981) Structure and spreading history of the northwestern Atlantic region from the  
 2377 Scotian Shelf to Baffin Bay
- 2378 Meier T, Soomro RA, Viereck L, et al (2016) Mesozoic and Cenozoic evolution of the Central  
 2379 European lithosphere. *Tectonophysics* 692:58–73

- 2380 Meissner R, Mooney W (1998) Weakness of the lower continental crust: a condition for  
2381 delamination, uplift, and escape. *Tectonophysics* 296:47–60
- 2382 Mendum JR (2012) Late Caledonian (Scandian) and Proto-Variscan (Acadian) orogenic events in  
2383 Scotland. *J Open Univ Geol Soc* 33:37–51
- 2384 Meyer R, Wijk J van, Gernigon L (2007) The North Atlantic Igneous Province: A review of models for  
2385 its formation. *Geol Soc Am Spec Pap* 430:525–552. [https://doi.org/10.1130/2007.2430\(26\)](https://doi.org/10.1130/2007.2430(26))
- 2386 Misra AA (2016) *Tectonic Inheritance in Continental Rifts and Passive*. Springer
- 2387 Mittelstaedt E, Ito G, Behn MD (2008) Mid-ocean ridge jumps associated with hotspot magmatism.  
2388 *Earth Planet Sci Lett* 266:256–270. <https://doi.org/10.1016/j.epsl.2007.10.055>
- 2389 Mjelde R, Eckhoff I, Solbakken S, et al (2007a) Gravity and S-wave modelling across the Jan Mayen  
2390 Ridge, North Atlantic; implications for crustal lithology. *Mar Geophys Res* 28:27–41.  
2391 <https://doi.org/10.1007/s11001-006-9012-3>
- 2392 Mjelde R, Faleide JJ, Breivik AJ, Raum T (2009) Lower crustal composition and crustal lineaments on  
2393 the Vøring Margin, NE Atlantic: A review. *Tectonophysics* 472:183–193.  
2394 <https://doi.org/10.1016/j.tecto.2008.04.018>
- 2395 Mjelde R, Goncharov A, Müller RD (2013) The Moho: Boundary above upper mantle peridotites or  
2396 lower crustal eclogites? A global review and new interpretations for passive margins.  
2397 *Tectonophysics* 609:636–650. <https://doi.org/10.1016/j.tecto.2012.03.001>
- 2398 Mjelde R, Raum T, Breivik A, et al (2005) Crustal structure of the Vøring Margin, NE Atlantic: a review  
2399 of geological implications based on recent OBS data. *Geol Soc Lond Pet Geol Conf Ser* 6:803–  
2400 813. <https://doi.org/10.1144/0060803>
- 2401 Mjelde R, Raum T, Breivik AJ, Faleide JJ (2008) Crustal transect across the North Atlantic. *Mar*  
2402 *Geophys Res* 29:73–87. <https://doi.org/10.1007/s11001-008-9046-9>
- 2403 Mjelde R, Raum T, Murai Y, Takanami T (2007b) Continent–ocean-transitions: Review, and a new  
2404 tectono-magmatic model of the Vøring Plateau, NE Atlantic. *J Geodyn* 43:374–392.  
2405 <https://doi.org/10.1016/j.jog.2006.09.013>
- 2406 Mogensen TE (1994) Palaeozoic structural development along the Tornquist Zone, Kattegat area,  
2407 Denmark. *Tectonophysics* 240:191–214
- 2408 Molnar NE, Cruden AR, Betts PG (2018) Unzipping continents and the birth of microcontinents.  
2409 *Geology* 46:451–454
- 2410 Molnar P, England P, Martinod J (1993) Mantle dynamics, uplift of the Tibetan Plateau, and the  
2411 Indian Monsoon. *Rev Geophys* 31:357–396. <https://doi.org/10.1029/93RG02030>
- 2412 Moore DE, Lockner DA, Tanaka H, Iwata K (2004) The coefficient of friction of chrysotile gouge at  
2413 seismogenic depths. *Int Geol Rev* 46:385–398
- 2414 Morewood NC, Mackenzie GD, Shannon PM, et al (2005) The crustal structure and regional  
2415 development of the Irish Atlantic margin region. *Pet Geol Conf Ser* 6:1023–1033

- 2416 Morley CK (2010) Stress re-orientation along zones of weak fabrics in rifts: An explanation for pure  
2417 extension in 'oblique' rift segments? *Earth Planet Sci Lett* 297:667–673
- 2418 Morley CK, Haranya C, Phoosongsee W, et al (2004) Activation of rift oblique and rift parallel pre-  
2419 existing fabrics during extension and their effect on deformation style: examples from the  
2420 rifts of Thailand. *J Struct Geol* 26:1803–1829
- 2421 Mortimer EJ, Paton DA, Scholz CA, Strecker MR (2016) Implications of structural inheritance in  
2422 oblique rift zones for basin compartmentalization: Nkhata Basin, Malawi Rift (EARS). *Mar Pet*  
2423 *Geol* 72:110–121
- 2424 Mosar J (2003) Scandinavia's North Atlantic passive margin. *J Geophys Res Solid Earth* 108:
- 2425 Moy DJ, Imber J (2009) A critical analysis of the structure and tectonic significance of rift-oblique  
2426 lineaments ('transfer zones') in the Mesozoic–Cenozoic succession of the Faroe–Shetland  
2427 Basin, NE Atlantic margin. *J Geol Soc* 166:831–844
- 2428 Müller RD, Gaina C, Roest WR, Hansen DL (2001) A recipe for microcontinent formation. *Geology*  
2429 29:203–206. [https://doi.org/10.1130/0091-7613\(2001\)029<0203:ARFMF>2.0.CO;2](https://doi.org/10.1130/0091-7613(2001)029<0203:ARFMF>2.0.CO;2)
- 2430 Murphy JB, Keppie JD (2005) The Acadian Orogeny in the Northern Appalachians. *Int Geol Rev*  
2431 47:663–687. <https://doi.org/10.2747/0020-6814.47.7.663>
- 2432 Mutter JC, Buck WR, Zehnder CM (1988) Convective partial melting: 1. A model for the formation of  
2433 thick basaltic sequences during the initiation of spreading. *J Geophys Res Solid Earth*  
2434 93:1031–1048
- 2435 Nagel TJ, Buck WR (2004) Symmetric alternative to asymmetric rifting models. *Geology* 32:937–940.  
2436 <https://doi.org/10.1130/G20785.1>
- 2437 Naliboff J, Buitter SJH (2015) Rift reactivation and migration during multiphase extension. *Earth*  
2438 *Planet Sci Lett* 421:58–67. <https://doi.org/10.1016/j.epsl.2015.03.050>
- 2439 Nasuti A, Pascal C, Ebbing J, Tønnesen JF (2011) Geophysical characterisation of two segments of the  
2440 Møre-Trøndelag Fault Complex, Mid Norway. *Solid Earth* 2:125–134
- 2441 Naylor D, Shannon PM (2005) The structural framework of the Irish Atlantic Margin. *Geol Soc Lond*  
2442 *Pet Geol Conf Ser* 6:1009–1021. <https://doi.org/10.1144/0061009>
- 2443 Nemčok M, Sinha ST, Doré AG, et al (2016) Mechanisms of microcontinent release associated with  
2444 wrenching-involved continental break-up; a review. *Geol Soc Lond Spec Publ* 431:SP431.14.  
2445 <https://doi.org/10.1144/SP431.14>
- 2446 Neumann E-R, Wilson M, Heeremans M, et al (2004) Carboniferous-Permian rifting and magmatism  
2447 in southern Scandinavia, the North Sea and northern Germany: a review. *Geol Soc Lond Spec*  
2448 *Publ* 223:11–40. <https://doi.org/10.1144/GSL.SP.2004.223.01.02>
- 2449 Neves SP, Vauchez A, Archanjo CJ (1996) Shear zone-controlled magma emplacement or magma-  
2450 assisted nucleation of shear zones? Insights from northeast Brazil. *Tectonophysics* 262:349–  
2451 364. [https://doi.org/10.1016/0040-1951\(96\)00007-8](https://doi.org/10.1016/0040-1951(96)00007-8)
- 2452 Newman R, White N (1997) Rheology of the continental lithosphere inferred from sedimentary  
2453 basins. *Nature* 385:621

- 2454 Nielsen SB, Stephenson R, Schiffer C (2014) Deep controls on intraplate basin inversion. In: Talwani P  
2455 (ed) Intraplate Earthquakes. Cambridge University Press
- 2456 Nielsen SB, Stephenson R, Thomsen E (2007) Dynamics of Mid-Palaeocene North Atlantic rifting  
2457 linked with European intra-plate deformations. *Nature* 450:1071–1074.  
2458 <https://doi.org/10.1038/nature06379>
- 2459 Nielsen SB, Thomsen E, Hansen DL, Clausen OR (2005) Plate-wide stress relaxation explains  
2460 European Palaeocene basin inversions. *Nature* 435:195–198.  
2461 <https://doi.org/10.1038/nature03599>
- 2462 Nirrengarten M, Gernigon L, Manatschal G (2014) Lower crustal bodies in the Møre volcanic rifted  
2463 margin: Geophysical determination and geological implications. *Tectonophysics* 636:143–  
2464 157. <https://doi.org/10.1016/j.tecto.2014.08.004>
- 2465 Nixon CW, Sanderson DJ, Dee SJ, et al (2014) Fault interactions and reactivation within a normal-  
2466 fault network at Milne Point, Alaska. *AAPG Bull* 98:2081–2107
- 2467 Oakey GN, Chalmers JA (2012) A new model for the Paleogene motion of Greenland relative to  
2468 North America: Plate reconstructions of the Davis Strait and Nares Strait regions between  
2469 Canada and Greenland. *J Geophys Res* 117:. <https://doi.org/10.1029/2011JB008942>
- 2470 Odinsen T, Reemst P, Van Der Beek P, et al (2000) Permo-Triassic and Jurassic extension in the  
2471 northern North Sea: results from tectonostratigraphic forward modelling. *Geol Soc Lond*  
2472 *Spec Publ* 167:83–103
- 2473 Olafsson I, Sundvor E, Eldholm O, Grue K (1992) Møre Margin: Crustal structure from analysis of  
2474 Expanded Spread Profiles. *Mar Geophys Res* 14:137–162.  
2475 <https://doi.org/10.1007/BF01204284>
- 2476 Olesen O, Ebbing J, Lundin E, et al (2007) An improved tectonic model for the Eocene opening of the  
2477 Norwegian–Greenland Sea: Use of modern magnetic data. *Mar Pet Geol* 24:53–66
- 2478 Osmundsen PT, Andersen TB (1994) Caledonian compressional and late-orogenic extensional  
2479 deformation in the Staveneset area, Sunnfjord, western Norway. *J Struct Geol* 16:1385–1401
- 2480 Osmundsen PT, Braathen A, Nordgulen Ø, et al (2003) The Devonian Nesna shear zone and adjacent  
2481 gneiss-cored culminations, North–Central Norwegian Caledonides. *J Geol Soc* 160:137–150.  
2482 <https://doi.org/10.1144/0016-764901-173>
- 2483 Parsons AJ, Whitham AG, Kelly SRA, et al (2017) Structural evolution and basin architecture of the  
2484 Traill Ø region, NE Greenland: A record of polyphase rifting of the East Greenland  
2485 continental margin. *Geosphere* 13:733–770. <https://doi.org/10.1130/GES01382.1>
- 2486 Pascal C, Cloetingh S (2002) Rifting in heterogeneous lithosphere: Inferences from numerical  
2487 modeling of the northern North Sea and the Oslo Graben. *Tectonics* 21:10–1
- 2488 Pascal C, Cloetingh SAPL (2009) Gravitational potential stresses and stress field of passive  
2489 continental margins: Insights from the south-Norway shelf. *Earth Planet Sci Lett* 277:464–  
2490 473. <https://doi.org/10.1016/j.epsl.2008.11.014>

- 2491 Paton DA, Underhill JR (2004) Role of crustal anisotropy in modifying the structural and  
 2492 sedimentological evolution of extensional basins: the Gamtoos Basin, South Africa. *Basin Res*  
 2493 16:339–359
- 2494 Peace A, McCaffrey K, Imber J, et al (2016) An evaluation of Mesozoic rift-related magmatism on the  
 2495 margins of the Labrador Sea: Implications for rifting and passive margin asymmetry.  
 2496 *Geosphere* 12:1701–1724. <https://doi.org/10.1130/GES01341.1>
- 2497 Peace AL, Dempsey E, Schiffer C, et al (2018a) Evidence for Basement Reactivation during the  
 2498 Opening of the Labrador Sea from the Makkovik Province, Labrador, Canada: Insights from  
 2499 Field Data and Numerical Models. *Geosciences* 8:308
- 2500 Peace AL, Foulger GR, Schiffer C, McCaffrey KJW (2017) Evolution of Labrador Sea–Baffin Bay: Plate  
 2501 or Plume Processes? *Geosci Can* 0:
- 2502 Peace AL, McCaffrey K, Imber J, et al (2018b) The role of pre-existing structures during rifting,  
 2503 continental breakup and transform system development, offshore West Greenland. *Basin*  
 2504 *Res* 30:373–394. <https://doi.org/10.1111/bre.12257>
- 2505 Peace AL, Phethean JJJ, Franke D, et al (this volume) A review of Pangaea dispersal and Large  
 2506 Igneous Provinces – In search of a causative mechanism. *Earth-Sci Rev*.  
 2507 <https://doi.org/10.1016/j.earscirev.2019.102902>
- 2508 Peace AL, Welford JK, Ball PJ, Nirrengarten M (2019) Deformable plate tectonic models of the  
 2509 southern North Atlantic. *J Geodyn* 128:11–37. <https://doi.org/10.1016/j.jog.2019.05.005>
- 2510 Peace AL, Welford JK, Geng M, et al (2018c) Rift-related magmatism on magma-poor margins:  
 2511 Structural and potential-field analyses of the Mesozoic Notre Dame Bay intrusions,  
 2512 Newfoundland, Canada and their link to North Atlantic Opening. *Tectonophysics* 745:24–45.  
 2513 <https://doi.org/10.1016/j.tecto.2018.07.025>
- 2514 Pease V (2011) Chapter 20 Eurasian orogens and Arctic tectonics: an overview. *Geol Soc Lond Mem*  
 2515 35:311–324. <https://doi.org/10.1144/M35.20>
- 2516 Pegrum RM (1984) The extension of the Tornquist zone in the Norwegian North Sea. *Geol Fören*  
 2517 *Stockh Förh* 106:394–395
- 2518 Peron-Pinvidic G, Gernigon L, Gaina C, Ball P (2012) Insights from the Jan Mayen system in the  
 2519 Norwegian–Greenland sea—I. Mapping of a microcontinent. *Geophys J Int* 191:385–412.  
 2520 <https://doi.org/10.1111/j.1365-246X.2012.05639.x>
- 2521 Péron-Pinvidic G, Manatschal G (2010) From microcontinents to extensional allochthons: witnesses  
 2522 of how continents rift and break apart? *Pet Geosci* 16:189–197.  
 2523 <https://doi.org/10.1144/1354-079309-903>
- 2524 Peron-Pinvidic G, Manatschal G, Osmundsen PT (2013) Structural comparison of archetypal Atlantic  
 2525 rifted margins: A review of observations and concepts. *Mar Pet Geol* 43:21–47.  
 2526 <https://doi.org/10.1016/j.marpetgeo.2013.02.002>
- 2527 Petersen KD, Schiffer C (2016) Wilson cycle passive margins: Control of orogenic inheritance on  
 2528 continental breakup. *Gondwana Res* 39:131–144. <https://doi.org/10.1016/j.gr.2016.06.012>

- 2529 Petersen KD, Schiffer C, Nagel T (2018) LIP formation and protracted lower mantle upwelling induced  
2530 by rifting and delamination. *Sci Rep* 8:16578. <https://doi.org/10.1038/s41598-018-34194-0>
- 2531 Pharaoh TC (1999) Palaeozoic terranes and their lithospheric boundaries within the Trans-European  
2532 Suture Zone (TESZ): a review. *Tectonophysics* 314:17–41. [https://doi.org/10.1016/S0040-1951\(99\)00235-8](https://doi.org/10.1016/S0040-1951(99)00235-8)  
2533
- 2534 Philippon M, Willingshofer E, Sokoutis D, et al (2015) Slip re-orientation in oblique rifts. *Geology*  
2535 43:147–150
- 2536 Phillips TB, Jackson CA, Bell RE, et al (2016) Reactivation of intrabasement structures during rifting: A  
2537 case study from offshore southern Norway. *J Struct Geol* 91:54–73
- 2538 Phillips TB, Jackson CA, Bell RE, Duffy OB (2018) Oblique reactivation of lithosphere-scale lineaments  
2539 controls rift physiography—the upper-crustal expression of the Sorgenfrei–Tornquist Zone,  
2540 offshore southern Norway. *Solid Earth* 9:403
- 2541 Phillips TB, Magee C, Jackson CA-L, Bell RE (2017) Determining the three-dimensional geometry of a  
2542 dike swarm and its impact on later rift geometry using seismic reflection data. *Geology*
- 2543 Piepjohn K, Gosen W von, Tessensohn F (2016) The Eureka deformation in the Arctic: an outline. *J*  
2544 *Geol Soc jgs2016-081*. <https://doi.org/10.1144/jgs2016-081>
- 2545 Pinet N, Lavoie D, Keating P (2013) Did the Hudson Strait in Arctic Canada record the opening of the  
2546 Labrador Sea? *Mar Pet Geol* 48:354–365
- 2547 Planke S, Alvestad E (1999) Seismic volcanostratigraphy of the extrusive breakup complexes in the  
2548 northeast Atlantic: Implications from ODP/DSDP drilling. In: *Proceedings of the Ocean*  
2549 *Drilling Program, Scientific Results*. Ocean Drilling Program College Station, Tex, pp 3–16
- 2550 Polteau S, Mazzini A, Hansen G, et al (2018) The pre-breakup stratigraphy and petroleum system of  
2551 the Southern Jan Mayen Ridge revealed by seafloor sampling. *Tectonophysics*
- 2552 Precigout J, Gueydan F, Gapais D, et al (2007) Strain localisation in the subcontinental mantle — a  
2553 ductile alternative to the brittle mantle. *Tectonophysics* 445:318–336.  
2554 <https://doi.org/10.1016/j.tecto.2007.09.002>
- 2555 Price S, Brodie J, Whitham A, Kent RAY (1997) Mid-Tertiary rifting and magmatism in the Traill Ø  
2556 region, East Greenland. *J Geol Soc* 154:419–434
- 2557 Reeve MT, Bell RE, Duffy OB, et al (2015) The growth of non-colinear normal fault systems; What can  
2558 we learn from 3D seismic reflection data? *J Struct Geol* 70:141–155
- 2559 Reilly C, Nicol A, Walsh J (2017) Importance of pre-existing fault size for the evolution of an inverted  
2560 fault system. *Geol Soc Lond Spec Publ* 439:447–463
- 2561 Ren S, Faleide JJ, Eldholm O, et al (2003) Late Cretaceous–Paleocene tectonic development of the  
2562 NW Vøring basin. *Mar Pet Geol* 20:177–206
- 2563 Ren S, Skogseid J, Eldholm O (1998) Late Cretaceous–Paleocene extension on the Vøring Volcanic  
2564 Margin. *Mar Geophys Res* 20:343–369. <https://doi.org/10.1023/A:1004554217069>

- 2565 Rey P, Vanderhaeghe O, Teyssier C (2001) Gravitational collapse of the continental crust: definition,  
2566 regimes and modes. *Tectonophysics* 342:435–449. <https://doi.org/10.1016/S0040->  
2567 1951(01)00174-3
- 2568 Ritchie JD, Johnson H, Quinn MF, Gatliff RW (2008) The effects of Cenozoic compression within the  
2569 Faroe-Shetland Basin and adjacent areas. *Geol Soc Lond Spec Publ* 306:121–136
- 2570 Ritchie JD, Ziska H, Johnson H, Evans D (2011) Geology of the Faroe-Shetland Basin and adjacent  
2571 areas
- 2572 Rivers T (2015) Tectonic Setting and Evolution of the Grenville Orogen: An Assessment of Progress  
2573 Over the Last 40 Years. *Geosci Can* 42:77–124.  
2574 <https://doi.org/10.12789/geocanj.2014.41.057>
- 2575 Roberts AM, Alvey AD, Kusznir NJ (2018) Crustal structure and heat-flow history in the UK Rockall  
2576 Basin, derived from backstripping and gravity-inversion analysis. *Pet Geosci* petgeo2017-063.  
2577 <https://doi.org/10.1144/petgeo2017-063>
- 2578 Roberts AM, Holdsworth RE (1999) Linking onshore and offshore structures: Mesozoic extension in  
2579 the Scottish Highlands. *J Geol Soc* 156:1061–1064
- 2580 Roberts AW, White RS, Christie PAF (2009) Imaging igneous rocks on the North Atlantic rifted  
2581 continental margin. *Geophys J Int* 179:1024–1038. <https://doi.org/10.1111/j.1365->  
2582 246X.2009.04306.x
- 2583 Roberts D (2003) The Scandinavian Caledonides: event chronology, palaeogeographic settings and  
2584 likely modern analogues. *Tectonophysics* 365:283–299. <https://doi.org/10.1016/S0040->  
2585 1951(03)00026-X
- 2586 Roberts D (1983) Devonian tectonic deformation in the Norwegian Caledonides and its regional  
2587 perspectives. *Nor Geol Unders* 380:85–96
- 2588 Roberts D, Siedlecka A (2002) Timanian orogenic deformation along the northeastern margin of  
2589 Baltica, Northwest Russia and Northeast Norway, and Avalonian–Cadmian connections.  
2590 *Tectonophysics* 352:169–184
- 2591 Roberts DG (1975) Marine geology of the Rockall Plateau and Trough. *Phil Trans R Soc Lond A*  
2592 278:447–509
- 2593 Roberts DG, Ginzberg A, Nunn K, McQuillin R (1988) The structure of the Rockall Trough from seismic  
2594 refraction and wide-angle reflection measurements. *Nature* 332:632–635
- 2595 Roberts DG, Thompson M, Mitchener B, et al (1999) Palaeozoic to Tertiary rift and basin dynamics:  
2596 mid-Norway to the Bay of Biscay – a new context for hydrocarbon prospectivity in the deep  
2597 water frontier. *Geol Soc Lond Pet Geol Conf Ser* 5:7–40. <https://doi.org/10.1144/0050007>
- 2598 Roberts NM, Slagstad T (2015) Continental growth and reworking on the edge of the Columbia and  
2599 Rodinia supercontinents; 1.86–0.9 Ga accretionary orogeny in southwest Fennoscandia. *Int*  
2600 *Geol Rev* 57:1582–1606
- 2601 Roest WR, Srivastava SP (1989) Sea-floor spreading in the Labrador Sea: A new reconstruction.  
2602 *Geology* 17:1000–1003. <https://doi.org/10.1130/0091->  
2603 7613(1989)017<1000:SFSITL>2.3.CO;2

- 2604 Roffeis C, Corfu F (2014) Caledonian nappes of southern Norway and their correlation with  
2605 Sveconorwegian basement domains. *Geol Soc Lond Spec Publ* 390:193–221
- 2606 Rotevatn A, Kristensen TB, Ksienzyk AK, et al (2018) Structural inheritance and rapid rift-length  
2607 establishment in a multiphase rift: the East Greenland rift system and its Caledonian  
2608 orogenic Ancestry. *Tectonics* 37:1858–1875
- 2609 Ruch J, Wang T, Xu W, et al (2016) Oblique rift opening revealed by reoccurring magma injection in  
2610 central Iceland. *Nat Commun* 7:12352
- 2611 Rumph B, Reaves CM, Orange VG, Robinson DL (1993) Structuring and transfer zones in the Faeroe  
2612 Basin in a regional tectonic context. In: Geological Society, London, Petroleum Geology  
2613 Conference series. Geological Society of London, pp 999–1009
- 2614 Salazar-Mora CA, Huismans RS, Fossen H, Egydio-Silva M (2018) The Wilson cycle and effects of  
2615 tectonic structural inheritance on rifted passive margin formation. *Tectonics*
- 2616 Schiffer C, Balling N, Ebbing J, et al (2016) Geophysical-petrological modelling of the East Greenland  
2617 Caledonides – Isostatic support from crust and upper mantle. *Tectonophysics* 692:44–57.  
2618 <https://doi.org/10.1016/j.tecto.2016.06.023>
- 2619 Schiffer C, Balling N, Jacobsen BH, et al (2014) Seismological evidence for a fossil subduction zone in  
2620 the East Greenland Caledonides. *Geology* 42:311–314. <https://doi.org/10.1130/G35244.1>
- 2621 Schiffer C, Jacobsen BH, Balling N, et al (2015a) The East Greenland Caledonides—teleseismic  
2622 signature, gravity and isostasy. *Geophys J Int* 203:1400–1418.  
2623 <https://doi.org/10.1093/gji/ggv373>
- 2624 Schiffer C, Nielsen SB (2016) Implications for anomalous mantle pressure and dynamic topography  
2625 from lithospheric stress patterns in the North Atlantic Realm. *J Geodyn* 98:53–69.  
2626 <https://doi.org/10.1016/j.jog.2016.03.014>
- 2627 Schiffer C, Peace A, Phethean J, et al (2018) The Jan Mayen Microplate Complex and the Wilson  
2628 Cycle. *Geol Soc Spec Publ* 470:
- 2629 Schiffer C, Stephenson RA (2017) Regional crustal architecture of Ellesmere Island, Arctic Canada.  
2630 *Geol Soc Lond Spec Publ*
- 2631 Schiffer C, Stephenson RA, Petersen KD, et al (2015b) A sub-crustal piercing point for North Atlantic  
2632 reconstructions and tectonic implications. *Geology* 43:1087–1090.  
2633 <https://doi.org/10.1130/G37245.1>
- 2634 Schroeder T, John BE (2004) Strain localization on an oceanic detachment fault system, Atlantis  
2635 Massif, 30 N, Mid-Atlantic Ridge. *Geochem Geophys Geosystems* 5:
- 2636 Seguret M, Seranne M, Chauvet A, Brunel A (1989) Collapse basin: A new type of extensional  
2637 sedimentary basin from the Devonian of Norway. *Geology* 17:127–130
- 2638 Seidler L, Steel R, Stemmerik L, Surlyk F (2004) North Atlantic marine rifting in the Early Triassic: new  
2639 evidence from East Greenland. *J Geol Soc* 161:583–592
- 2640 Şengör AMC, Lom N, Sağdıç NG (2018) Tectonic inheritance, structure reactivation and lithospheric  
2641 strength: the relevance of geological history. *Geol Soc Lond Spec Publ* 470:SP470–8

- 2642 Seranne M (1992) Late Palaeozoic kinematics of the Møre-Trøndelag Fault Zone and adjacent areas,  
2643 central Norway. *Nor Geol Tidsskr* 72:141–158
- 2644 Seranne M, Seguret M (1987) The Devonian basins of western Norway: tectonics and kinematics of  
2645 an extending crust. *Geol Soc Lond Spec Publ* 28:537–548
- 2646 Shannon PM (1991) The development of Irish offshore sedimentary basins. *J Geol Soc* 148:181–189
- 2647 Shannon PM, Jacob AWB, Makris J, et al (1995) Basin development and petroleum prospectivity of  
2648 the Rockall and Hatton region. *Geol Soc Lond Spec Publ* 93:435–457.  
2649 <https://doi.org/10.1144/GSL.SP.1995.093.01.35>
- 2650 Shannon PM, Jacob AWB, Makris J, et al (1994) Basin evolution in the Rockall region, North Atlantic.  
2651 *First Break* 12:515–522
- 2652 Shannon PM, Jacob AWB, O'Reilly BM, et al (1999) Structural setting, geological development and  
2653 basin modelling in the Rockall Trough. *Pet Geol Conf Ser* 5:421–431
- 2654 Shulgin A, Mjelde R, Faleide JJ, et al (2018) The crustal structure in the transition zone between the  
2655 western and eastern Barents Sea. *Geophys J Int* 214:315–330.  
2656 <https://doi.org/10.1093/gji/ggy139>
- 2657 Sibson RH (1977) Fault rocks and fault mechanisms. *J Geol Soc* 133:191–213
- 2658 Simon K, Huisman RS, Beaumont C (2009) Dynamical modelling of lithospheric extension and small-  
2659 scale convection: Implications for magmatism during the formation of volcanic rifted  
2660 margins. *Geophys J Int* 176:327–350. <https://doi.org/10.1111/j.1365-246X.2008.03891.x>
- 2661 Skogseid J, Pedersen T, Eldholm O, Larsen BT (1992) Tectonism and magmatism during NE Atlantic  
2662 continental break-up: the Vøring Margin. *Geol Soc Lond Spec Publ* 68:305–320.  
2663 <https://doi.org/10.1144/GSL.SP.1992.068.01.19>
- 2664 Skogseid J, Planke S, Faleide JJ, et al (2000) NE Atlantic continental rifting and volcanic margin  
2665 formation. *Geol Soc Lond Spec Publ* 167:295–326.  
2666 <https://doi.org/10.1144/GSL.SP.2000.167.01.12>
- 2667 Slagstad T, Kulakov E, Kirkland CL, et al (2019) Breaking the Grenville–Sveconorwegian link in Rodinia  
2668 reconstructions. *Terra Nova*
- 2669 Slagstad T, Maystrenko YP, Maupin V, Gradmann S (2018) An extinct, late Mesoproterozoic,  
2670 Sveconorwegian mantle wedge beneath SW Fennoscandia, reflected in seismic tomography  
2671 and assessed by thermal modelling. *Terra Nova* 30:72–77
- 2672 Slagstad T, Roberts NMW, Marker M, et al (2013) A non-collisional, accretionary Sveconorwegian  
2673 orogen. *Terra Nova* 25:30–37. <https://doi.org/10.1111/ter.12001>
- 2674 Sonder LJ, England PC (1989) Effects of a temperature-dependent rheology on large-scale  
2675 continental extension. *J Geophys Res Solid Earth* 94:7603–7619
- 2676 Soper NJ, England RW, Snyder DB, Ryan PD (1992) The Iapetus suture zone in England, Scotland and  
2677 eastern Ireland: a reconciliation of geological and deep seismic data. *J Geol Soc* 149:697–700

- 2678 Soper NJ, Higgins AK (1993) Basement–cover relationships in the East Greenland Caledonides:  
2679 evidence from the Eleonore Bay Supergroup at Ardencaple Fjord. *Earth Environ Sci Trans R*  
2680 *Soc Edinb* 84:103–115
- 2681 Soper NJ, Woodcock NH (1990) Silurian collision and sediment dispersal patterns in southern Britain.  
2682 *Geol Mag* 127:527–542. <https://doi.org/10.1017/S0016756800015430>
- 2683 Spencer CJ, Kirkland CL (2016) Visualizing the sedimentary response through the orogenic cycle: A  
2684 multidimensional scaling approach. *Lithosphere* 8:29–37
- 2685 Srivastava SP, Keen CE (1995) A deep seismic reflection profile across the extinct Mid-Labrador Sea  
2686 spreading center. *Tectonics* 14:372–389
- 2687 Stampfli GM, Borel GD (2002) A plate tectonic model for the Paleozoic and Mesozoic constrained by  
2688 dynamic plate boundaries and restored synthetic oceanic isochrons. *Earth Planet Sci Lett*  
2689 196:17–33
- 2690 Stampfli GM, Hochard C, V  rard C, et al (2013) The formation of Pangea. *Tectonophysics* 593:1–19.  
2691 <https://doi.org/10.1016/j.tecto.2013.02.037>
- 2692 Stemmerik L, Vigran JO, Piasecki S (1991) Dating of late Paleozoic rifting events in the North Atlantic:  
2693 New biostratigraphic data from the uppermost Devonian and Carboniferous of East  
2694 Greenland. *Geology* 19:218–221
- 2695 Stephenson R, Piepjohn K, Schiffer C, et al (2017) Integrated crustal–geological cross-section of  
2696 Ellesmere Island. *Geol Soc Lond Spec Publ* 460:SP460.12. <https://doi.org/10.1144/SP460.12>
- 2697 Stephenson RA, Jess S, Nielsen SB, et al (this volume) Late Cretaceous–Cenozoic intraplate basin  
2698 inversion and paleo -stress fields in the North Atlantic–western Alpine–Tethys realm. *Earth-*  
2699 *Sci Rev*
- 2700 Stewart M, Strachan RA, Holdsworth RE (1997) Direct field evidence for sinistral displacements along  
2701 the Great Glen Fault Zone: late Caledonian reactivation of a regional basement structure? *J*  
2702 *Geol Soc* 154:135–139. <https://doi.org/10.1144/gsjgs.154.1.0135>
- 2703 Stewart M, Strachan RA, Holdsworth RE (1999) Structure and early kinematic history of the Great  
2704 Glen Fault Zone, Scotland. *Tectonics* 18:326–342
- 2705 Stoker MS (2016) Cretaceous tectonostratigraphy of the Faroe–Shetland region. *Scott J Geol* 52:19–  
2706 41
- 2707 Stoker MS, Holford SP, Hillis RR (2018) A rift-to-drift record of vertical crustal motions in the Faroe–  
2708 Shetland Basin, NW European margin: establishing constraints on NE Atlantic evolution. *J*  
2709 *Geol Soc* 175:263–274
- 2710 Stoker MS, Hout R, Nielsen T, et al (2005) Sedimentary and oceanographic responses to early  
2711 Neogene compression on the NW European margin. *Mar Pet Geol* 22:1031–1044
- 2712 Stoker MS, Stewart MA, Shannon PM, et al (2017) An overview of the Upper Palaeozoic–Mesozoic  
2713 stratigraphy of the NE Atlantic region. *Geol Soc Lond Spec Publ* 447:11–68
- 2714   tolfov  K, Shannon PM (2009) Permo–Triassic development from Ireland to Norway: basin  
2715 architecture and regional controls. *Geol J* 44:652–676. <https://doi.org/10.1002/gj.1187>

- 2716 St-Onge MR, Gool JAMV, Garde AA, Scott DJ (2009) Correlation of Archaean and Palaeoproterozoic  
 2717 units between northeastern Canada and western Greenland: constraining the pre-collisional  
 2718 upper plate accretionary history of the Trans-Hudson orogen. *Geol Soc Lond Spec Publ*  
 2719 318:193–235. <https://doi.org/10.1144/SP318.7>
- 2720 Suckro SK, Gohl K, Funck T, et al (2013) The davis strait crust-a transform margin between two  
 2721 oceanic basins. *Geophys J Int* 193:78–97. <https://doi.org/10.1093/gji/ggs126>
- 2722 Suckro SK, Gohl K, Funck T, et al (2012) The crustal structure of southern Baffin Bay: Implications  
 2723 from a seismic refraction experiment. *Geophys J Int* 190:37–58.  
 2724 <https://doi.org/10.1111/j.1365-246X.2012.05477.x>
- 2725 Surlyk F (1990) Timing, style and sedimentary evolution of Late Palaeozoic-Mesozoic extensional  
 2726 basins of East Greenland. *Geol Soc Lond Spec Publ* 55:107–125
- 2727 Sutherland R, Davey F, Beavan J (2000) Plate boundary deformation in South Island, New Zealand, is  
 2728 related to inherited lithospheric structure. *Earth Planet Sci Lett* 177:141–151.  
 2729 [https://doi.org/10.1016/S0012-821X\(00\)00043-1](https://doi.org/10.1016/S0012-821X(00)00043-1)
- 2730 Sutton J, Watson JV (1986) Architecture of the continental lithosphere. *Phil Trans R Soc Lond A*  
 2731 317:5–12. <https://doi.org/10.1098/rsta.1986.0020>
- 2732 Svartman Dias AE, Lavier LL, Hayman NW (2015) Conjugate rifted margins width and asymmetry: The  
 2733 interplay between lithospheric strength and thermomechanical processes. *J Geophys Res*  
 2734 *Solid Earth* 120:2015JB012074. <https://doi.org/10.1002/2015JB012074>
- 2735 Svennevig K, Guarnieri P, Stemmerik L (2016) Tectonic inversion in the Wandel Sea Basin: a new  
 2736 structural model of Kilen (eastern North Greenland). *Tectonics* 2016TC004152.  
 2737 <https://doi.org/10.1002/2016TC004152>
- 2738 Tappe S, Foley SF, Stracke A, et al (2007) Craton reactivation on the Labrador Sea margins:  
 2739 <sup>40</sup>Ar/<sup>39</sup>Ar age and Sr–Nd–Hf–Pb isotope constraints from alkaline and carbonatite  
 2740 intrusives. *Earth Planet Sci Lett* 256:433–454. <https://doi.org/10.1016/j.epsl.2007.01.036>
- 2741 Tarayoun A, Mazzotti S, Craymer M, Henton J (2018) Structural Inheritance Control on Intraplate  
 2742 Present-Day Deformation: GPS Strain Rate Variations in the Saint Lawrence Valley, Eastern  
 2743 Canada. *J Geophys Res Solid Earth* 123:7004–7020
- 2744 Tegner C, Brooks CK, Duncan RA, et al (2008) <sup>40</sup>Ar–<sup>39</sup>Ar ages of intrusions in East Greenland: Rift-to-  
 2745 drift transition over the Iceland hotspot. *Lithos* 101:480–500.  
 2746 <https://doi.org/10.1016/j.lithos.2007.09.001>
- 2747 Thatcher W (1995) Microplate versus continuum descriptions of active tectonic deformation. *J*  
 2748 *Geophys Res Solid Earth* 100:3885–3894
- 2749 Theilen Fr, Meissner R (1979) A comparison of crustal and upper mantle features in fennoscandia  
 2750 and the rhenish shield, two areas of recent uplift. *Tectonophysics* 61:227–242.  
 2751 [https://doi.org/10.1016/0040-1951\(79\)90299-3](https://doi.org/10.1016/0040-1951(79)90299-3)
- 2752 Theissen-Krah S, Zastrozhnov D, Abdelmalak MM, et al (2017) Tectonic evolution and extension at  
 2753 the Møre Margin–Offshore mid-Norway. *Tectonophysics* 721:227–238

- 2754 Thomas WA (2018) Tectonic inheritance at multiple scales during more than two complete Wilson  
2755 cycles recorded in eastern North America. *Geol Soc Lond Spec Publ* 470:SP470–4
- 2756 Thybo H, Artemieva IM (2013) Moho and magmatic underplating in continental lithosphere.  
2757 *Tectonophysics* 609:605–619. <https://doi.org/10.1016/j.tecto.2013.05.032>
- 2758 Tommasi A, Knoll M, Vauchez A, et al (2009) Structural reactivation in plate tectonics controlled by  
2759 olivine crystal anisotropy. *Nat Geosci* 2:423–427. <https://doi.org/10.1038/ngeo528>
- 2760 Tommasi A, Vauchez A (2015) Heterogeneity and anisotropy in the lithospheric mantle.  
2761 *Tectonophysics* 661:11–37. <https://doi.org/10.1016/j.tecto.2015.07.026>
- 2762 Tommasi A, Vauchez A (2001) Continental rifting parallel to ancient collisional belts: an effect of the  
2763 mechanical anisotropy of the lithospheric mantle. *Earth Planet Sci Lett* 185:199–210
- 2764 Torsvik TH, Amundsen HEF, Trønnnes RG, et al (2015) Continental crust beneath southeast Iceland.  
2765 *Proc Natl Acad Sci* 201423099. <https://doi.org/10.1073/pnas.1423099112>
- 2766 Tsikalas F, Eldholm O, Faleide JJ (2005) Crustal structure of the Lofoten-Vesterålen continental  
2767 margin, off Norway. *Tectonophysics* 404:151–174.  
2768 <https://doi.org/10.1016/j.tecto.2005.04.002>
- 2769 Tsikalas F, Eldholm O, Faleide JJ (2002) Early Eocene sea floor spreading and continent-ocean  
2770 boundary between Jan Mayen and Senja fracture zones in the Norwegian-Greenland Sea.  
2771 *Mar Geophys Res* 23:247–270. <https://doi.org/10.1023/A:1023621228605>
- 2772 Tsikalas F, Faleide JJ, Eldholm O, Blaich OA (2012) The NE Atlantic conjugate margins. *Reg Geol*  
2773 *Tecton Phanerozoic Passive Margins Cratonic Basins Glob Tecton Maps* 1:140–201
- 2774 Tuitt A, Underhill JR, Ritchie JD, et al (2010) Timing, controls and consequences of compression in  
2775 the Rockall-Faroe area of the NE Atlantic Margin. *Geol Soc Lond Pet Geol Conf Ser* 7:963–  
2776 977. <https://doi.org/10.1144/0070963>
- 2777 Underhill J t, Partington MA (1993) Jurassic thermal doming and deflation in the North Sea:  
2778 implications of the sequence stratigraphic evidence. *Geol Soc Lond Pet Geol Conf Ser* 4:337–  
2779 345
- 2780 van Gool JAM, Connelly JN, Marker M, Mengel FC (2002) The Nagssugtoqidian Orogen of West  
2781 Greenland: tectonic evolution and regional correlations from a West Greenland perspective.  
2782 *Can J Earth Sci* 39:665–686. <https://doi.org/10.1139/e02-027>
- 2783 van Roermund HLM, Drury MR (1998) Ultra-high pressure ( $P > 6$  GPa) garnet peridotites in Western  
2784 Norway: exhumation of mantle rocks from  $> 185$  km depth. *Terra Nova* 10:295–301.  
2785 <https://doi.org/10.1046/j.1365-3121.1998.00213.x>
- 2786 Van Staal CR, Dewey JF, Niocail CM, McKerrow WS (1998) The Cambrian-Silurian tectonic evolution  
2787 of the northern Appalachians and British Caledonides: history of a complex, west and  
2788 southwest Pacific-type segment of Iapetus. *Geol Soc Lond Spec Publ* 143:197–242.  
2789 <https://doi.org/10.1144/GSL.SP.1998.143.01.17>
- 2790 van Staal CR, Whalen JB, Valverde-Vaquero P, et al (2009) Pre-Carboniferous, episodic accretion-  
2791 related, orogenesis along the Laurentian margin of the northern Appalachians. *Geol Soc*  
2792 *Lond Spec Publ* 327:271–316. <https://doi.org/10.1144/SP327.13>

- 2793 Van Wijk JW (2005) Role of weak zone orientation in continental lithosphere extension. *Geophys Res*  
2794 *Lett* 32:
- 2795 Van Wijk JW, Cloetingh SA (2002) Basin migration caused by slow lithospheric extension. *Earth*  
2796 *Planet Sci Lett* 198:275–288
- 2797 van Wijk JW, Huismans RS, ter Voorde M, Cloetingh S a. PL (2001) Melt generation at volcanic  
2798 continental margins: No need for a mantle plume? *Geophys Res Lett* 28:3995–3998.  
2799 <https://doi.org/10.1029/2000GL012848>
- 2800 Vauchez A, Barruol G, Tommasi A (1997) Why do continents break-up parallel to ancient orogenic  
2801 belts? *Terra Nova* 9:62–66. <https://doi.org/10.1111/j.1365-3121.1997.tb00003.x>
- 2802 Vauchez A, Nicolas A (1991) Mountain building: strike-parallel motion and mantle anisotropy.  
2803 *Tectonophysics* 185:183–201
- 2804 Vetti VV, Fossen H (2012) Origin of contrasting Devonian supradetachment basin types in the  
2805 Scandinavian Caledonides. *Geology* 40:571–574
- 2806 Vink GE (1984) A hotspot model for Iceland and the Vøring Plateau. *J Geophys Res Solid Earth*  
2807 89:9949–9959. <https://doi.org/10.1029/JB089iB12p09949>
- 2808 Vissers RL, van Hinsbergen DJ, Van Der Meer DG, Spakman W (2016) Cretaceous slab break-off in the  
2809 Pyrenees: Iberian plate kinematics in paleomagnetic and mantle reference frames.  
2810 *Gondwana Res* 34:49–59
- 2811 Voss M, Schmidt-Aursch MC, Jokat W (2009) Variations in magmatic processes along the East  
2812 Greenland volcanic margin. *Geophys J Int* 177:755–782. <https://doi.org/10.1111/j.1365-246X.2009.04077.x>
- 2814 Walsh JJ, Nicol A, Childs C (2002) An alternative model for the growth of faults. *J Struct Geol*  
2815 24:1669–1675
- 2816 Wang W, Becker TW (2019) Upper mantle seismic anisotropy as a constraint for mantle flow and  
2817 continental dynamics of the North American plate. *Earth Planet Sci Lett* 514:143–155.  
2818 <https://doi.org/10.1016/j.epsl.2019.03.019>
- 2819 Wang Z, Kusky TM, Capitanio FA (2018) On the Role of Lower Crust and Midlithosphere Discontinuity  
2820 for Cratonic Lithosphere Delamination and Recycling. *Geophys Res Lett*
- 2821 Wangen M, Mjelde R, Faleide JJ (2011) The extension of the Vøring margin (NE Atlantic) in case of  
2822 different degrees of magmatic underplating. *Basin Res* 23:83–100.  
2823 <https://doi.org/10.1111/j.1365-2117.2010.00467.x>
- 2824 Watt WS (1969) The coast-parallel dike swarm of southwest Greenland in relation to the opening of  
2825 the Labrador Sea. *Can J Earth Sci* 6:1320–1321
- 2826 Weigel W, Flüh ER, Miller H, et al (1995) Investigations of the East Greenland continental margin  
2827 between 70° and 72° N by deep seismic sounding and gravity studies. *Mar Geophys Res*  
2828 17:167–199. <https://doi.org/10.1007/BF01203425>
- 2829 Welford JK, Hall J (2013) Lithospheric structure of the Labrador Sea from constrained 3-D gravity  
2830 inversion. *Geophys J Int* 195:767–784

- 2831 Welford JK, Peace AL, Geng M, et al (2018) Crustal structure of Baffin Bay from constrained three-  
 2832 dimensional gravity inversion and deformable plate tectonic models. *Geophys J Int*  
 2833 214:1281–1300. <https://doi.org/10.1093/gji/ggy193>
- 2834 Whalen L, Gazel E, Vidito C, et al (2015) Supercontinental inheritance and its influence on  
 2835 supercontinental breakup: The Central Atlantic Magmatic Province and the breakup of  
 2836 Pangea. *Geochem Geophys Geosystems* 16:3532–3554.  
 2837 <https://doi.org/10.1002/2015GC005885>
- 2838 Whipp PS, Jackson CA-L, Gawthorpe RL, et al (2014) Normal fault array evolution above a reactivated  
 2839 rift fabric; a subsurface example from the northern Horda Platform, Norwegian North Sea.  
 2840 *Basin Res* 26:523–549
- 2841 White AP, Hodges KV (2002) Multistage extensional evolution of the central East Greenland  
 2842 Caledonides. *Tectonics* 21:12–1
- 2843 White R, McKenzie D (1989) Magmatism at rift zones: The generation of volcanic continental  
 2844 margins and flood basalts. *J Geophys Res Solid Earth* 94:7685–7729.  
 2845 <https://doi.org/10.1029/JB094iB06p07685>
- 2846 White RS (1992) Crustal structure and magmatism of North Atlantic continental margins. *J Geol Soc*  
 2847 149:841–854
- 2848 White RS, Smith LK, Roberts AW, et al (2008) Lower-crustal intrusion on the North Atlantic  
 2849 continental margin. *Nature* 452:460–464. <https://doi.org/10.1038/nature06687>
- 2850 Wilson JT (1966) Did the Atlantic Close and then Re-Open? *Nature* 211:676–681.  
 2851 <https://doi.org/10.1038/211676a0>
- 2852 Wilson M, Neumann E-R, Davies GR, et al (2004) Permo-Carboniferous magmatism and rifting in  
 2853 Europe: introduction. *Geol Soc Lond Spec Publ* 223:1–10.  
 2854 <https://doi.org/10.1144/GSL.SP.2004.223.01.01>
- 2855 Wilson PI, McCaffrey KJ, Wilson RW, et al (2016) Deformation structures associated with the  
 2856 Trachyte Mesa intrusion, Henry Mountains, Utah: Implications for sill and laccolith  
 2857 emplacement mechanisms. *J Struct Geol* 87:30–46
- 2858 Wilson RW, Holdsworth RE, Wild LE, et al (2010) Basement-influenced rifting and basin  
 2859 development: a reappraisal of post-Caledonian faulting patterns from the North Coast  
 2860 Transfer Zone, Scotland. *Geol Soc Lond Spec Publ* 335:795–826.  
 2861 <https://doi.org/10.1144/SP335.32>
- 2862 Wilson RW, Houseman GA, Buitter SJH, et al (2019) Fifty years of the Wilson Cycle Concept in Plate  
 2863 Tectonics: An Overview. *Geol Soc Lond Spec Publ* 470:SP470-2019–58.  
 2864 <https://doi.org/10.1144/SP470-2019-58>
- 2865 Wilson RW, Klint KES, van Gool JA, et al (2006) Faults and fractures in central West Greenland:  
 2866 onshore expression of continental break-up and sea-floor spreading in the Labrador–Baffin  
 2867 Bay Sea. *Geol Surv Den Greenl Bull* 11:185–204
- 2868 Winchester JA, Pharaoh TC, Verniers J (2002) Palaeozoic amalgamation of Central Europe: an  
 2869 introduction and synthesis of new results from recent geological and geophysical

- 2870 investigations. *Geol Soc Lond Spec Publ* 201:1–18.  
2871 <https://doi.org/10.1144/GSL.SP.2002.201.01.01>
- 2872 Winchester JA, Pharaoh TC, Verniers J, et al (2006) Palaeozoic accretion of Gondwana-derived  
2873 terranes to the East European Craton: recognition of detached terrane fragments dispersed  
2874 after collision with promontories. *Geol Soc Lond Mem* 32:323–332
- 2875 Withjack MO, Baum MS, Schlische RW (2010) Influence of preexisting fault fabric on inversion-  
2876 related deformation: A case study of the inverted Fundy rift basin, southeastern Canada.  
2877 *Tectonics* 29:
- 2878 Woodcock NH, Soper NJ, Strachan RA (2007) A Rheic cause for the Acadian deformation in Europe. *J*  
2879 *Geol Soc* 164:1023–1036
- 2880 Woodcock NH, Strachan RA (2012) *Geological History of Britain and Ireland*. John Wiley & Sons
- 2881 Woodcock NH, Underhill JR (1987) Emplacement-related fault patterns around the Northern Granite,  
2882 Arran, Scotland. *Geol Soc Am Bull* 98:515–527
- 2883 Wrona T, Magee C, Fossen H, et al (2019) 3-D seismic images of an extensive igneous sill in the lower  
2884 crust. *Geology*
- 2885 Wüstefeld A, Bokelmann G, Barruol G, Montagner J-P (2009) Identifying global seismic anisotropy  
2886 patterns by correlating shear-wave splitting and surface-wave data. *Phys Earth Planet Inter*  
2887 176:198–212
- 2888 Yamasaki T, Gernigon L (2009) Styles of lithospheric extension controlled by underplated mafic  
2889 bodies. *Tectonophysics* 468:169–184. <https://doi.org/10.1016/j.tecto.2008.04.024>
- 2890 Yamasaki T, Stephenson R (2009) Potential role of strain hardening in the cessation of rifting at  
2891 constant tectonic force. *J Geodyn* 47:47–62. <https://doi.org/10.1016/j.jog.2008.07.001>
- 2892 Yoshinobu AS, Barnes CG, Nordgulen Ø, et al (2002) Ordovician magmatism, deformation, and  
2893 exhumation in the Caledonides of central Norway: An orphan of the Taconic orogeny?  
2894 *Geology* 30:883–886. [https://doi.org/10.1130/0091-7613\(2002\)030<0883:OMDAEI>2.0.CO;2](https://doi.org/10.1130/0091-7613(2002)030<0883:OMDAEI>2.0.CO;2)
- 2895 Zastrozhnov D, Gernigon L, Gogin I, et al (2018) Cretaceous-Paleocene Evolution and Crustal  
2896 Structure of the Northern Vøring Margin (Offshore Mid-Norway): Results from Integrated  
2897 Geological and Geophysical Study. *Tectonics* 37:497–528
- 2898 Zhu H, Tromp J (2013) Mapping tectonic deformation in the crust and upper mantle beneath Europe  
2899 and the North Atlantic Ocean. *Science* 341:871–875
- 2900 Ziegler PA (1992) North Sea rift system. *Geodyn Rift* 1:55–75
- 2901 Ziegler PA (2012) *Evolution of Laurussia: A study in Late Palaeozoic plate tectonics*. Springer Science  
2902 & Business Media
- 2903 Ziegler PA (1988) *Evolution of the Arctic-North Atlantic and the Western Tethys/Book and Map*,  
2904 AAPG Memoir 43 edition. Amer Assn of Petroleum Geologists, Tulsa, Okla., U.S.A
- 2905 Ziska H, Varming T (2008) Palaeogene evolution of the Ymir and Wyville Thomson ridges, European  
2906 North Atlantic margin. *Geol Soc Lond Spec Publ* 306:153–168

